

Quantitative Studies of EGFR Autocrine Induced Cell Signaling and Migration

by

Elizabeth Jane Joslin

B.S. Biological Engineering
Cornell University, 2001

SUBMITTED TO THE DEPARTMENT OF BIOLOGICAL ENGINEERING
IN PARTIAL FULFILLMENT OF THE REQUIREMENTS FOR THE DEGREE OF

DOCTOR OF PHILOSOPHY IN BIOLOGICAL ENGINEERING

AT THE

MASSACHUSETTS INSTITUTE OF TECHNOLOGY

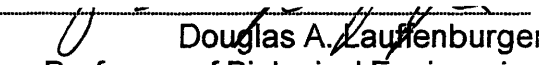
June, 2007

© 2007 Massachusetts Institute of Technology. All rights reserved.

Signature of Author: _____

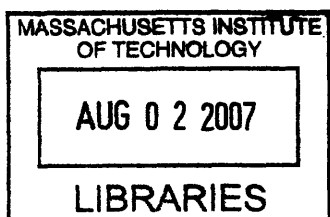

Department of Biological Engineering
May 18, 2007

Certified by: _____


Douglas A. Lauffenburger
Professor of Biological Engineering
Thesis Advisor

Accepted by: _____


Alan J. Grodzinsky
Professor of Biological Engineering
Graduate Committee Chairman



Thesis Committee:

Douglas A. Lauffenburger, Thesis Advisor, MIT

Paul Matsudaira, Committee Chair, MIT

Darrell Irvine, MIT

Alan Wells, University of Pittsburg

H. Steven Wiley, Pacific Northwest National Lab

Quantitative Studies of EGFR Autocrine Induced Cell Signaling and Migration

by

Elizabeth Jane Joslin

Submitted to the Department of Biological Engineering on May 18th, 2007
in partial fulfillment of the requirements for the degree of
Doctor of Philosophy in Biological Engineering

Abstract

Epidermal growth factor (EGF) receptor autocrine and/or paracrine signaling plays an important role in normal epithelial cell proliferation, survival, adhesion and migration. Aberrant expression of the EGF receptor and its cognate ligands have been implicated in various types of cancers, hence EGF receptor autocrine activation is thought to also be involved in tumorigenesis. EGF family ligands are synthesized as membrane-anchored proteins requiring proteolytic release to form the mature soluble, receptor-binding factor. Despite the pathophysiological importance of autocrine systems, how protease-mediated ligand release quantitatively influences receptor-mediated signaling and consequent cell behavior is poorly understood. Therefore, we explored the relationship between autocrine EGF release rate and receptor-mediated ERK activation and migration in human mammary epithelial cells. A quantitative spectrum of EGF release rates was achieved using chimeric EGF ligand precursors modulated by the addition of the metalloprotease inhibitor batimastat. We found that ERK activation increased with increasing ligand release rates despite concomitant EGF receptor downregulation. Cell migration speed depended linearly on the steady-state phospho-ERK level, but was much greater for autocrine compared to exogenous stimulation. In contrast, cell proliferation rates were constant across the various treatment conditions. In addition, we investigated an EGFR-mediated positive feedback through ERK that stimulated a 4-fold increase in release rate of our TGF α based construct. Thus, in these cells, ERK-mediated migration stimulated by EGF receptor signaling is most sensitively regulated by autocrine ligand control mechanisms.

Acknowledgements

There are many people that I must thank for making the past six years such an incredible and rewarding experience. I would first like to thank my advisor, Doug Lauffenburger. Doug, you have been such a great advisor, mentor and motivator. I had an outstanding graduate experience and I feel honored to have been in your lab. I am forever grateful for your help and your inspiration. Someone once told me that I had the *best* advisor there is... and I couldn't agree more!! I look forward to keeping in touch in the future!

I would also like to thank my collaborators Steve Wiley and Lee Opresko at PNNL. Without their experience and hard work, this project would have never been possible. I would like to thank them for all of their cell lines and reagents and their expertise. Thank you also to Alan Wells, at the University of Pittsburg, for all of his comments and insight. I would also like to thank Paul Matsudaira and Darrell Irvine for serving on my committee and for all of their useful comments and suggestions.

I would like to thank all of the past and present members of the Lauffenburger lab for making such it a great work environment. Thank you to Hyung-Do Kim for all of his help and macros. You have been a great friend and I will miss you. Thank you to Matt Lazzara for all of the helpful feedback and discussions and tissue culture sessions. I look forward to being out in Philly with you—maybe we can find a good Chinese restaurant out there. Thank you to Neil Kumar for his patience in helping me set up my migration assay. I hope we can still make it to Conan sometime soon. Thank you Pam for her help with the BioPlex assay and comments and feedback on my project. I wish you the best finding a great professorship this coming year. I would also like to thank all of the lab managers I have known, including Stacey Pawson, Christina Lewis, and Alison Kitay. You have all been awesome and great friends in the lab. I would especially like to thank Christina for her help teaching me how to count surface receptors and I am sorry her work didn't end up in a manuscript. I would like to thank previous lab members for all of the mentoring and training as well: Brian Harms, Bart Hendriks, Melissa Kemp, Catherine Cresson, Ley Richardson, and Dan Kamei. Thank you also to JoAnn for her never ending help and never empty candy dish...you are the best!

Thank you to my beh-one classmates: Sri, Ale, Nate, Maxx, Dan, Helene, Samantha, Ali, Caitlin, Sid, Alex, Jenny, Mike, and Jennifer. My first year was so much more enjoyable with all of you there and I still think we were the best graduate class in BE. Thank you to all of my friends in Boston, in the Boston Ultimate Disc Alliance, from Cornell, and from California.

And finally, I would like to thank my parents, Robin and Willy, my brother James, my sister Katy, and my brother-in-law John. I am so lucky to have such a loving family. Thank you to my grandma, Spook, for her love and support and her generosity. Thank you also to Tim Best for supporting me over the past three years.

Thank you!! I am so excited to be done and proud of this accomplishment! I couldn't have done it without you all!

Table of Contents

Abstract.....	3
Acknowledgements.....	5
Table of Contents	7
Chapter 1: Introduction and overview.....	9
1.1 Motivation: understanding cell signaling and migration as a function of EGFR ligand release	9
1.2 Chapter overview	10
1.3 References	13
Chapter 2: Background.....	15
2.1 Autocrine Growth Factor Signaling	15
2.2 Evidence For Role Of Growth Factor Autocrine Signaling In Cell Migration	18
2.2.1 <i>EGFR System</i>	18
2.2.1.1 <i>In Vitro</i>	18
2.2.1.2 <i>In Vivo</i>	23
2.2.2 <i>Examples Of Other Growth Factor Families</i>	25
2.2.2.1 <i>FGF</i>	25
2.2.2.2 <i>G-CSF/GM-CSF</i>	26
2.2.2.3 <i>HGF</i>	27
2.2.2.4 <i>VEGF</i>	28
2.3 Spatial Localization Issues	28
2.3.1 <i>Cellular Control Of Growth Factor Spatial Distribution</i>	29
2.3.2 <i>Spatial Range Of Ligand Signaling Events</i>	33
2.3.3 <i>The Mode Of Growth Factor Presentation Affects Cell Migration Behavior</i>	35
2.4 Figures	38
2.5 References	42
Chapter 3: Autocrine stimulated ERK signaling and cell motility.....	53
3.1 Introduction	54
3.2 Materials and Methods	58
3.2.1 <i>Reagents and antibodies</i>	58
3.2.2 <i>Construction of ligand chimeras and cell lines</i>	59
3.2.3 <i>EGF release rates</i>	60
3.2.4 <i>Surface receptor levels</i>	61
3.2.5 <i>EGFR and ERK phosphorylation</i>	61
3.2.6 <i>Cell counting assay</i>	62
3.2.7 <i>Sparse-labeled monolayer migration assay</i>	63
3.3 Results	64
3.3.1 <i>EGF chimeras and metalloprotease inhibition quantitatively tune autocrine ligand release rates</i>	64
3.3.2 <i>Increasing autocrine release rates downregulate surface EGFR levels but increases levels of active EGFR</i>	65
3.3.3 <i>Autocrine signaling leads to steady ERK activation</i>	66
3.3.4 <i>Autocrine presentation induces normal proliferation but enhanced migration</i>	67
3.3.5 <i>Cell migration speed is proportional to pERK1/2 as autocrine ligand release rate is varied</i>	69
3.4 Discussion	70
3.5 Figures	76

3.6	References	90
Chapter 4: Positive feedback in ligand release		97
4.1	Introduction	97
4.2	Materials and Methods	99
4.2.1	<i>Reagents and antibodies</i>	99
4.2.2	<i>Construction of ligand chimeras and cell lines</i>	99
4.2.3	<i>EGF ligand release</i>	100
4.2.4	<i>ERK phosphorylation time courses</i>	101
4.3	Results	102
4.3.1	<i>TGFα based construct release is positively regulated downstream of the EGF receptor</i>	102
4.3.2	<i>Small molecule inhibitors show release stimulated through ERK, p38 but not PKC</i> ..	104
4.3.3	<i>Mutant EGF constructs decouple ligand release from ligand capture</i>	104
4.3.4	<i>MEK inhibition completely blocks TGFα stimulated ligand release of TGFα but not EGF based construct</i>	105
4.3.5	<i>Quantitative relationship of TGFα stimulated TCT-NA release through ERK</i>	106
4.4	Discussion	106
4.5	Figures	112
4.6	References	119
Chapter 5: Investigation of ECT and TNGF cell signaling and migration on collagen IV		123
5.1	Introduction	123
5.2	Materials and Methods	127
5.2.1	<i>Cell lines and culture conditions</i>	127
5.2.2	<i>Reagents and Antibodies</i>	128
5.2.3	<i>Ligand Release Rates</i>	129
5.2.4	<i>Quantitative surface EGFR measurements</i>	129
5.2.5	<i>Western Blotting</i>	130
5.2.6	<i>Single Cell Migration Assay</i>	131
5.3	Results	132
5.3.1	<i>TNGF construct has 10-fold higher EGF release rate than ECT</i>	132
5.3.2	<i>Low and high release of EGF lead to receptor downregulation and sustained ERK phosphorylation</i>	132
5.3.3	<i>Collagen IV level dominates cell migration behavior over ligand release effects</i>	133
5.4	Discussion	135
5.5	Figures	139
5.6	References	148
Chapter 6: Conclusions and future directions		153
6.1	Figures	158
Appendix A: Computational work		161
A.1	Figures	163
A.2	References	167
A.3	Matlab Code	167

Chapter 1: Introduction and overview

1.1 Motivation: understanding cell signaling and migration as a function of EGFR ligand release

The epidermal growth factor receptor (EGFR) belongs to the ErbB family of receptor tyrosine kinases, which has several known EGF-like ligands (Yarden and Sliwkowski, 2001). Beyond its role in normal physiology, dysregulated ErbB signaling is important in disease. Altered ErbB signaling can lead to aberrant, growth and migration promoting signals that may have a major impact on tumor initiation, progression, and metastasis. ErbB signaling has received much attention in the past decade with several therapeutic interventions already in use and currently undergoing clinical trials (Arteaga, 2003; Ciardiello and Tortora, 2001; Yarden and Sliwkowski, 2001).

The ligands that bind specifically to the EGFR are synthesized as membrane integral proteins that require cleavage from the cell surface to form the mature soluble ligand (Harris et al., 2003). Traditional techniques have employed exogenous treatment of recombinant forms of the soluble ligand to study cell signaling and response to the various EGF receptor ligands. However,

it is thought that the ligands elicit spatially restricted autocrine and/or paracrine stimulation within the tissue expressing both the ligands and the receptors, which is the case for several types of tumors (Normanno et al., 2003; Normanno et al., 2006; Salomon et al., 1995). A recent study demonstrated that co-expression of an EGFR ligand, TGF α , and the cognate metalloprotease, TACE, at elevated levels is highly predictive of poor prognosis across a set of 295 primary breast tumors (Kenny and Bissell, 2007). Significantly, reversion of a malignant phenotype could be obtained by reduction of TACE activity, suggesting that quantitative control of protease-mediated autocrine EGF ligand release could be critical for governing phenotypic behavior. The motivation of this work was to develop a cell system where we could quantitatively modulate release of an EGF receptor ligand and systematically study the cell signaling and response. Instead of varying a soluble cue, we wanted to employ the cells to make the ligand and control the rate of cleavage at the cell surface with various techniques. Understanding the cue-signaling-response relationship for cells under varying degrees of autocrine stimulation would shed light on more *in vivo*-like conditions and help develop new understanding for disease signaling and response states.

1.2 Chapter overview

This thesis is composed of three chapters addressing the effects of modulating ligand release on cell signaling and behavior. The experimental cell system studied consisted of a human mammary epithelial cell line retrovirally transduced for stable expression of various EGF chimeras. Chimeras contained various

domains of ligands fused to the soluble EGF binding domain, keeping the receptor-ligand interactions constant. Changing the domain encoding protease shedding specifically modulated autocrine ligand release.

Chapter 3 describes our investigation of how the protease-mediated ligand release rate quantitatively governs receptor-mediated signaling and consequent cell proliferation and migration behavior. In addition, results compare the effects of exogenous stimulation and saturating autocrine presentation on cell migration. We found that cell migration speed was directly proportional to the steady-state phospho-ERK level stimulated by autocrine release, demonstrating a “dose-response” relationship. In addition, migration speed was faster under the “chronic” autocrine stimulation than under the “acute” exogenous EGF treatment despite the greater signaling peaks and integrals measured under exogenous conditions. Cell proliferation was found to be equivalently stimulated under exogenous and autocrine stimulation, therefore suggesting that cell migration is more sensitively controlled by the protease-mediated autocrine ligand release.

While quantifying ligand release rates within the scope of Chapter 3, we discovered that release of our TGF α based EGF chimera was positively regulated downstream of the EGF receptor. This positive feedback was unexpected and merited further investigation. Experimental results showing small molecule inhibitor affects on stimulated ligand release are described in Chapter 4. We demonstrate that positive feedback downstream of the EGF receptor contributes to a 4-fold increase in the ligand release rate of the TGF α based construct and identify ERK as the key modulator of stimulated TGF α but

not EGF cleavage. In addition, we report a quantitative dose-response relationship of stimulated ligand release as a function of ERK phosphorylation.

Finally, Chapter 5 outlines work investigating cell signaling and single cell migration under low and high ligand release. This early work utilized a TNF α anchoring domain based chimera that led to high release of EGF. In addition to modulating ligand release rate with the EGF chimeras, 2D cell migration behavior was measured on varying levels of collagen IV. This chapter summarizes the initial thesis direction that was eventually refocused due to the possibility of intracellular binding of the TNF ligand, challenges associated with measuring single cell migration, and inconclusive statistical analysis.

Overall, we believe that the greatest achievement of this thesis is a greater understanding of autocrine induced signaling, ligand release regulation, and cell migration. We have obtained a “cue-signal-response” relationship under varying autocrine presentation and we show increased cell speed under autocrine versus exogenous stimulation. Results have generated hypotheses regarding potential differences in signaling dynamics (or lack thereof) and subsequent migration behavior observed under autocrine stimulation that open areas for future research.

1.3 References

- Arteaga, C.L. 2003. ErbB-targeted therapeutic approaches in human cancer. *Exp Cell Res.* 284:122-30.
- Ciardiello, F., and G. Tortora. 2001. A novel approach in the treatment of cancer: targeting the epidermal growth factor receptor. *Clin Cancer Res.* 7:2958-70.
- Harris, R.C., E. Chung, and R.J. Coffey. 2003. EGF receptor ligands. *Exp Cell Res.* 284:2-13.
- Kenny, P.A., and M.J. Bissell. 2007. Targeting TACE-dependent EGFR ligand shedding in breast cancer. *J Clin Invest.* 117:337-45.
- Normanno, N., C. Bianco, A. De Luca, M.R. Maiello, and D.S. Salomon. 2003. Target-based agents against ErbB receptors and their ligands: a novel approach to cancer treatment. *Endocr Relat Cancer.* 10:1-21.
- Normanno, N., A. De Luca, C. Bianco, L. Strizzi, M. Mancino, M.R. Maiello, A. Carotenuto, G. De Feo, F. Caponigro, and D.S. Salomon. 2006. Epidermal growth factor receptor (EGFR) signaling in cancer. *Gene.* 366:2-16.
- Salomon, D.S., R. Brandt, F. Ciardiello, and N. Normanno. 1995. Epidermal growth factor-related peptides and their receptors in human malignancies. *Crit Rev Oncol Hematol.* 19:183-232.
- Yarden, Y., and M.X. Sliwkowski. 2001. Untangling the ErbB signalling network. *Nat Rev Mol Cell Biol.* 2:127-37.

Chapter 2: Background

2.1 *Autocrine Growth Factor Signaling*

The term autocrine signaling was first proposed by Sporn and Todaro to describe the type of self stimulation that could occur if a cell produced both a hormone-like factor and the cognate receptor (Sporn and Todaro, 1980). Normal cell growth in culture required the addition of specific growth factors, whereas malignant cells could grow autonomously without the same exogenous supplements. While growth factor autocrine amplification or dysregulation has become one of the hallmarks of cancer, autocrine signaling is also now known to be a mode of signaling involved in normal physiological processes (Hanahan and Weinberg, 2000; Sporn and Roberts, 1985; Sporn and Roberts, 1992; Sporn and Todaro, 1980). For example, growth factor autocrine signaling has been implicated in wound healing (Tokumaru et al., 2000), angiogenesis (Seghezzi et al., 1998), and tissue organization during development (Wasserman and Freeman, 1998).

A prominent example of autocrine growth factor signaling that is involved in numerous cell types and cellular responses is the Epidermal Growth Factor Receptor (EGFR) system. EGFR belongs to the ErbB family of receptor tyrosine kinases, which has several known EGF-like ligands (Yarden and Sliwkowski, 2001). ErbB signaling plays an important role in normal epithelial cell proliferation, development, survival, adhesion and migration (Caric et al., 2001; Kumar and Wang, 2002; Yarden and Sliwkowski, 2001). Beyond its role in normal physiology, dysregulated ErbB signaling is also extremely important in cancer progression (Arteaga, 2002; Holbro et al., 2003). The EGF receptor and the EGFR ligands are expressed or overexpressed in several human cancers, for example lung, breast, gastric, pancreatic, colon, head and neck, prostate, ovarian, and brain cancers (Cai et al., 1999; Damstrup et al., 1999; Hsieh et al., 2000; Kopp et al., 2003; Rubin Grandis et al., 1998; Salomon et al., 1995; Suo et al., 2002; Yamanaka et al., 1993; Zhu et al., 2000). Altered ErbB signaling can lead to aberrant, growth and migration promoting signals that may have a major impact on tumor initiation, progression, and metastasis.

EGFR ligands include EGF, TGF- α , HB-EGF, betacellulin, amphiregulin, epiregulin, and epigen (Harris et al., 2003). These ligands are produced as membrane-bound peptides and proteolytic cleavage between the ligand and the membrane-spanning region releases the ligand from the membrane, see Figure 2.4.1. The region between the receptor binding domain and the transmembrane domain, the ligand releasing cleavage site, is highly variable among the EGFR ligands, although they are key determinates of

ectodomain shedding (Arribas et al., 1997; Harris et al., 2003). The ligands have the potential to signal in an autocrine, paracrine, and/or a juxtacrine mode depending on extracellular proteolytic processing. While an autocrine-signaling mode is characterized by ligands that are released from the cell surface in an active form and bind to receptors on the same cell, paracrine signaling involves the capture of ligand released from a neighboring cell. Juxtacrine signaling involves ligand-receptor binding between a cell expressing the membrane-bound ligand and an adjacent cell that expresses the correct receptor, an event that does not involve ligand cleavage and requires direct contact between the stimulatory and target cell.

Members of the ADAM family of metalloproteases proteolytically release the EGFR ligands from the cell surface. Although TACE/ADAM 17 is known to be involved in TGF- α , HB-EGF, and AR release, the full identities and regulation of the metalloproteases involved in EGFR ligand shedding are currently under investigation (Borrell-Pages et al., 2003; Harris et al., 2003; Hinkle et al., 2003; Merlos-Suarez et al., 2001). There is evidence that TGF- α and HB-EGF shedding is stimulated by signals downstream of the EGF receptor, such as PKC and MAPK activation, creating a positive feedback mechanism that may involve metalloprotease phosphorylation, see Figure 2.4.2 (Baselga et al., 1996; Fan and Derynck, 1999; Fan et al., 2003; Gechtman et al., 1999). Activation of the ERK pathway has also been implicated in increasing the transcription of EGFR ligands, creating an additional positive feedback (Baselga et al., 1996; Schulze et al., 2001).

Due to the intrinsic and closed-loop nature of autocrine signaling systems, identification and experimental analysis of true autocrine effects on cellular behavior is a challenge (Wiley et al., 2003). While there is evidence for the role of autocrine signaling in cell proliferation, less is known about whether autocrine mechanisms may be involved in the transition to, or control of a motile cellular phenotype. To this end, several cell types and growth factor families have been studied *in vitro* using various migration assays, while fewer studies have addressed this question *in vivo*. Experimental results that provide evidence for the role of growth factor autocrine signaling specifically involved in cell motility are presented below with emphasis on the EGF receptor system as an example.

2.2 Evidence For Role Of Growth Factor Autocrine Signaling In Cell Migration

2.2.1 EGFR System

2.2.1.1 *In Vitro*

Gavrilovic et al. transfected a rat bladder carcinoma cell line (NBTII) with a gene encoding TGF-alpha that resulted in an epithelial to fibroblast-like morphological transition (Gavrilovic et al., 1990). Clones were plated on glass coverslips and cell migration was measured using videomicroscopy and cell tracking. TGF-alpha synthesizing cells and parental cells stimulated with conditioned media were able to achieve higher migration speeds compared to the parental cells stimulated with exogenous TGF-alpha. The transfected cells also acquired an increase in gelatinase synthesis.

Elevated levels of the EGF receptor and expression of its ligands have been found in human prostate carcinomas (Kim et al., 1999). The DU145 prostate carcinoma cell line expresses TGF-alpha and EGFR, which are involved in growth stimulation (Tillotson and Rose, 1991). Xie et al. investigated the involvement of this autocrine stimulation in transmigration of an *in vitro* matrix (Xie et al., 1995). The parental DU145 cells were transfected to overexpress EGFR. The EGFR overexpressing variant showed an increased migration through the matrix compared to the parentals. The increased matrix invasion of the EGFR overexpressing cells was inhibited upon addition of an anti-EGFR antibody. The EGFR overexpressors and parentals secreted similar levels of proteolytic activity and thus in this invasion assay the increase in migration was determined to be autocrine stimulated and potentially independent of matrix degradation.

TGF-alpha expression has been found in human gliomas and has been correlated with tumor grade (Ekstrand et al., 1991; Schlegel et al., 1990). El-Obeid et al. demonstrated that the expression of TGF-alpha in an EGFR expressing human malignant glioma cell line (U-1242 MG) induced cell locomotion (El-Obeid et al., 1997). ¹²⁵I-labeled EGF binding studies showed that 60% of EGF bound to cells induced to express TGF-alpha compared to the same clone that was repressed using a tetracycline regulated gene expression system. Receptor phosphorylation of derived clones was similar to repressed cells also stimulated with exogenous EGF. EGFR phosphorylation levels were also found to be independent of cell seeding density. Phagokinetic track area of individual

cells in an *in vitro* migration assay was higher for autocrine-induced cells. An EGFR blocking antibody only slightly decreased cell track area of the induced TGF-alpha expressing clones, whereas exogenously added TGF-alpha was completely neutralized by the antibody. These results showed that co-expression of EGFR and TGF-alpha enabled individual glioma cells to operate in an independent, migratory manner, where EGFR activation may have occurred in cell regions inaccessible to blocking antibodies.

Dong et al. investigated the effect of a broad-spectrum matrix metalloprotease inhibitor on EGFR ligand release and migration of a human mammary epithelial cell line (hMEC) (Dong et al., 1999). The TGF-alpha concentration in hMEC-conditioned media and the speed of individually tracked cells seeded at low density decreased in presence of the inhibitor. Exogenous EGF reversed the inhibitory effect on migration speed, suggesting that the release of the endogenous ligands, such as TGF-alpha or amphiregulin, was necessary for EGFR stimulated motility in this cell system.

The migration of sheets of corneal epithelial cells in a wounding assay, which involved lifting an agarose strip to induce a gap without cell damage, was shown to be dependent on HB-EGF signaling (Block et al., 2004). Addition of an EGFR kinase inhibitor abolished the wound closure in this *in vitro* system. Incubation with an EGFR or a HB-EGF neutralizing antibody also inhibited wound closure. Inhibition of the biological activity of HB-EGF with a non-toxic diphtheria toxin analog also reduced wound closure of the corneal epithelial cell layers.

EGFR autocrine signaling has also been found to stimulate cell motility as a result of cell signaling crosstalk. Interleukin (IL)-6 is a member of the IL-6-type cytokine family and is involved in the immune response, inflammation, and hematopoiesis (Hirano, 1998). Badache et al. investigated the mechanism by which IL-6 increased breast carcinoma cell migration in an *in vitro* transwell assay (Badache and Hynes, 2001). Activation of the MAPK and PI3K signaling pathways were required for IL-6-induced cell migration. Both the addition of an anti-EGFR antibody and an EGFR kinase inhibitor also decreased the IL-6 induced migration. Although the identity of the EGFR ligand(s) involved were not determined, these results showed that IL-6 stimulated breast carcinoma cell migration through transactivation of an EGFR autocrine pathway and downstream activation of MAPK and PI3K.

EGFR activation has also been implicated in crosstalk with G Protein-Coupled Receptors (GPCR) (Gschwind et al., 2001). Gschwind et al. examined GPCR stimulated migration of squamous cell carcinoma cells using an *in vitro* transwell assay (Gschwind et al., 2003). Lysophosphatidic acid induced activation of GPCR resulted in proteolytic cleavage of membrane bound pro-amphiregulin (proAR). RNA silencing of proAR decreased LPA-stimulated migration. Addition of an AR-neutralizing antibody inhibited LPA aggravated EGFR tyrosine phosphorylation. LPA-induced AR release and cell migration was also inhibited by RNA silencing of the membrane bound metalloprotease TACE. Although the mechanism of TACE activation was unknown, the shedding of AR

was shown to be involved in GPCR-EGFR crosstalk and cell migration in this experimental system.

EGFR and GPCR crosstalk has also been implicated in bombesin stimulated migration of prostate cancer cells *in vitro*. Bombesin is a neuropeptide that was first isolated from the skin of the frog *Bombina orientalis* and later found to have a mammalian equivalent, gastrin-releasing peptide (GRP), that binds a family of GPCRs (Anastasi et al., 1971). GRP receptor overexpression has been identified in prostate cancer and bombesin has been shown to influence prostate cancer cell migration *in vitro* (Aprikian et al., 1997; Markwalder and Reubi, 1999). Madarame et al. investigated involvement of HB-EGF shedding in bombesin-stimulated prostate cell migration (Madarame et al., 2003). The addition of a metalloprotease inhibitor decreased bombesin-induced HB-EGF shedding and EGFR tyrosine phosphorylation. Addition of either an anti-EGFR antibody or the metalloprotease inhibitor partially reduced migration of bombesin stimulated cells in an *in vitro* wound assay.

EGFR autocrine signaling has recently been implicated in the role of TNF- α induced cell motility (Chen et al., 2004). TNF- α is a cytokine that has been shown to induce cytotoxicity and apoptosis in transformed cells while it is also thought to elicit pro-survival signals in normal cells (Carswell et al., 1975; Natoli et al., 1998). Chen et al. investigated the role of EGFR crosstalk in mediating TNF induced signals in a normal hMEC cell line (Chen et al., 2004). TNF stimulated hMEC proliferation and migration in an *in vitro* transwell migration assay. The addition of TNF also stimulated shedding of TGF- α in a dose-

dependent manner. TNF stimulated cell migration was decreased in the presence of a metalloprotease inhibitor or an EGFR kinase inhibitor. A late phase of ERK activation was also inhibited in the presence of the metalloprotease inhibitor suggesting that autocrine activation of the EGFR was involved in this secondary ERK signaling peak. These results implicated a novel role for EGFR transactivation in mediating TNF induced cell responses in this hMEC system.

2.2.1.2 *In Vivo*

As discussed earlier, Xie et al. demonstrated that endogenous EGFR autocrine signaling stimulated engineered DU-145 prostate carcinoma cell migration *in vitro* (Xie et al., 1995). Subsequently, Turner et al. inoculated athymic mice with the parental cells and the EGFR-overexpressing cells to determine if the results of increased transwell migration *in vitro* corresponded to *in vivo* tumor progression (Turner et al., 1996). Both the parental and EGFR-overexpressing DU-145 cells formed tumors that metastasized to the lung when inoculated into the prostate and peritoneal cavity, although the EGFR overexpressing tumors were more invasive. Injections of a PLC-gamma inhibitor reduced tumor invasiveness, as measured by the extent of tumor cell penetration of the diaphragm, suggesting a role for EGFR-mediated cell migration in this *in vivo* tumor invasion model.

Pilcher et al. demonstrated that keratinocyte migration depended on EGFR signaling using a phagokinetic assay (Pilcher et al., 1999). Inhibition of the EGFR using either a kinase inhibitor or an anti-EGFR antibody decreased the

relative migration area and the production of collagenase-1 in a primary keratinocyte cell system shown to express EGF, TGF-alpha, amphiregulin, and HB-EGF when plated on type I collagen. These results were tested in an *in vivo* porcine burn wound-healing assay. Wound incubation with an EGFR inhibitor resulted in significant decrease in burn re-epithelialization compared to control treatments, implicating a role for EGFR autocrine signaling in burn wound closure. In another study, Tokumaru et al. used a murine punch biopsy wound model to investigate the importance of EGFR ligand shedding in *in vivo* cutaneous wound healing (Tokumaru et al., 2000). Incubation with a metalloprotease inhibitor resulted in a lack of keratin staining in excised skin wound histology in contrast to the control treatment. These inhibitory effects were reversed upon addition of recombinant HB-EGF, suggesting that the shedding of EGFR ligands may play an important role in keratinocyte migration and wound healing.

The AP-1 stress response transcription factor is composed of a heterodimer of Fos and Jun proteins and has been implicated in the normal development of the epidermis (Angel and Szabowski, 2002; Yates and Rayner, 2002). The EGFR and its ligand HB-EGF are both known AP-1 target genes (Fu et al., 1999; Johnson et al., 2000). Li et al. created a transgenic mouse lacking *c-jun* in the epidermis (Li et al., 2003). These transgenic mice were born with open eyelids, a phenotypic result also seen in mice born with gene disruption of the EGFR or TGF-alpha (Luetteke et al., 1993; Miettinen et al., 1995). The conditionally *c-jun* null mice also had decreased EGFR expression and

phosphorylation at the epidermal eyelid tip, and had slower wound closure rates of punch biopsies. Addition of exogenous HB-EGF rescued the impaired motility of *c-jun* null keratinocytes in an *in vitro* scratch assay. Together these results suggest that the activation of positive transcriptional feedback downstream of EGFR activation is involved in leading edge epidermal sheet migration (Grose, 2003).

2.2.2 Examples Of Other Growth Factor Families

2.2.2.1 FGF

Basic Fibroblast Growth Factor (bFGF, also known as FGF-2) is a member of a large family of heparin-binding growth factors and is known to have various influences on several cell types (Ornitz and Itoh, 2001). In particular, FGF signaling is known to be involved in the migration of endothelial cells and is a therapeutic target for inhibition of angiogenesis in tumor progression (Cross and Claesson-Welsh, 2001). Endogenous bFGF was shown to regulate endothelial cell movement in an *in vitro* scratch assay (Sato and Rifkin, 1988). Migration of confluent bovine aortic endothelial cells past a razor-induced wound edge was inhibited upon addition of an anti-bFGF antibody. The addition of soluble recombinant bFGF reversed the inhibitory effects of the ligand-neutralizing antibody. Although this work was the first documented evidence of autocrine activity of the bFGF ligand, it was not known how the ligand reached the extracellular space and whether the method for cell removal may have caused cytoplasmic ligand leakage from dead cells at the wound edge.

Mignatti et al. later validated that bFGF stimulated cell motility of cultured fibroblasts in an autocrine manner (Mignatti et al., 1991). NIH 3T3 cells were transfected with bFGF cDNA and single cells were plated on colloidal gold-coated coverslips. Increasing phagokinetic cell track areas were correlated with the level of endogenous bFGF. The cell clone that produced the highest amount of bFGF did not show an increase in migration upon addition of exogenous, recombinant bFGF, which suggests that the cells had reached a state of receptor saturation or a maximum migratory stimulation at this level of endogenous ligand production. Addition of anti-bFGF reduced the motility of the isolated, transfected cells. These results indicated that extracellular bFGF could stimulate cell motility of the cell producing the ligand, experimentally indicating that the bFGF ligand can act in a 'true' autocrine manner.

2.2.2.2 G-CSF/GM-CSF

Granulocyte colony-stimulating factor (G-CSF) and granulocyte macrophage colony-stimulating factor (GM-CSF) stimulate growth and differentiation in the hematopoietic system, are produced by many cell types, and have also been found to be expressed by non-hematopoietic tumor cells suggesting their involvement in tumor growth and invasion (Metcalf, 1985; Mueller et al., 2001; Tachibana et al., 1995; Uemura et al., 2004). Mueller et al. analyzed RNA and protein expression of G-CSF, GM-CSF, and their receptors in 22 human gliomas and derived cell cultures (Mueller et al., 1999). The co-expression of these ligands and their cognate receptors correlated with advanced tumor stage. Receptor and ligand expression also influenced the migration of the

glioblastoma cell lines as shown in an *in vitro* wound assay. A derived cell line expressing both ligands and receptors had an increase in both the distance traveled and number of cells moving into the wounded area compared to a similar cell line expressing only G-CSF and both receptors. The addition of either an anti G-CSF or an anti GM-CSF monoclonal antibody reduced migration of the wound edge. These results suggest that G-CSF and GM-CSF autocrine signaling may contribute to increased cell migration in late stage glioblastomas.

2.2.2.3 HGF

Hepatocyte growth factor (HGF) is secreted by cells of mesodermal and mesenchymal origin, stimulates growth and migration of epithelial and endothelial cells that express the HGF receptor (HGFR), and HGFR signaling has been shown to be involved in processes such as placental development and liver regeneration (Borowiak et al., 2004; Uehara et al., 1995). Overexpression of HGFR, also known as the *met* proto-oncogene, lead to aberrant growth formation in a mouse model and HGFR has been found to be overexpressed in several types of cancer (Humphrey et al., 1995; Takayama et al., 1997; Tuck et al., 1996). Vadnais et al. used Moloney sarcoma virus (MSV)-transformed polarized epithelial MDCK cells to determine that the autocrine activation of HGFR is associated with the pseudopodial protrusion and acquisition of a motile, invasive phenotype *in vitro* (Vadnais et al., 2002). The invasive variant derived from this cell line showed constitutive HGFR phosphorylation and increased migration distances as measured using videomicroscopy and nuclear tracking. The addition of an anti-HGF-alpha antibody decreased cell motility, increased

pseudopodial retraction and the number of cell-cell contacts of the MSV-MDCK invasive variant.

2.2.2.4 VEGF

The vascular endothelial growth factor (VEGF) is known to play an important role in angiogenesis and increased expression has been associated with cancer progression (Brown et al., 1999; Mercurio et al., 2004; Salven et al., 1999; Shweiki et al., 1992). A recent study looked at the role of VEGF and other neuropilin-1 (NP1) ligands in the regulation of breast carcinoma cell migration towards conditioned media *in vitro* (Bachelder et al., 2003). An antagonistic relationship exists between VEGF and the migratory inhibitor SEMA3A. The autocrine production ratio of these competing ligands correlated with chemotactic potential of three breast carcinoma cell lines. RNAi reduction of VEGF and expression of a mutant, constitutively active NP1 coreceptor plexin-A1 decreased migration while RNAi reduction of NP1 and SEMA3A expression increased transwell migration. This work demonstrated the involvement of VEGF autocrine signaling in breast carcinoma chemotaxis through the inhibition of an endogenous migration suppressor (Mercurio 04).

2.3 Spatial Localization Issues

Up to this point, this background section has focused on evidence in the literature for involvement of autocrine growth factor signaling in cell motility phenomena. We will now consider key aspects of mechanisms underlying these phenomena, focusing our attention on features of autocrine signaling systems

that might be of particular importance for governing cell migration behavior. These features primarily revolve around the spatial distribution of autocrine ligands, their receptors, and generated downstream signals, because the central characteristic of autocrine systems distinguishing them from paracrine and/or endocrine systems is their potential action on the producing cell or proximal neighbors.

2.3.1 Cellular Control Of Growth Factor Spatial Distribution

Autocrine signaling has typically been difficult to investigate using standard techniques since the production, release, and binding of a ligand within a cell operate in a 'closed loop' fashion (Wiley et al., 2003). Therefore, several modeling approaches have been used to gain insight about the parameters that govern the dynamics of autocrine operation complemented by a growing body of experimental work. Two modeling approaches, one that used Brownian-motion theory and computer simulations to calculate the trajectories of the released ligands, and another that used continuum reaction-diffusion equations to model the fluxes of the ligands, both suggest that EGFR autocrine loops could be highly localized on the order of less than a cell diameter (Forsten and Lauffenburger, 1992a; Shvartsman et al., 2001). Using a microphysiometer assay to measure receptor ligand binding, Lauffenburger et al. showed that anti-receptor antibodies were far more effective than anti-ligand antibodies in inhibiting autocrine signaling, suggesting experimentally that these signals may operate in a spatially-restricted, local manner (Lauffenburger et al., 1998).

In vivo work by Yoshioka et al. in cardiomyocyte hypertrophy provided additional experimental evidence of the spatially restricted nature of EGFR autocrine signaling (Yoshioka et al., 2005). Previous work had shown that HB-EGF expression was increased during hypertrophy and metalloprotease inhibition attenuated hypertrophic changes (Perrella et al., 1994; Asakura et al., 2002). HB-EGF was delivered via adenovirus to cardiomyocytes. Due to the nonuniform distribution of the gene delivery, normal cells were usually surrounded by cells expressing HB-EGF. Analysis of 3D cell morphology demonstrated that HB-EGF release led to cell hypertrophy and the loss of gap junction proteins in the cells expressing HB-EGF and immediate neighboring while cells further away were unaffected (Yoshioka et al., 2005).

The modeling work by Shvartsman et al. also implicated that altering the ligand diffusion coefficient, the density of cell surface receptors, the ligand secretion rate, and the rate constants for ligand binding and endocytic internalization could modulate the spatial range of the growth factors (Shvartsman et al., 2001). Oehrtman et al. used a tetracycline-controlled TGF- α expression system in mouse B82 L fibroblasts transfected with an EGFR gene to validate a model for the escape of autocrine ligands into the extracellular bulk media (Oehrtman et al., 1998). Their experimental results suggested that the ligand secretion rate, receptor availability, and cell density in culture controlled the rate of ligand accumulation in the media.

DeWitt et al. performed a rigorous set of experiments to show that the fraction of ligand that is captured by the producing cells is a function of ligand

secretion rate and receptor synthesis rate, using a human EGF/EGFR autocrine loop engineered into mouse fibroblasts, see Figure 2.4.3 (DeWitt et al., 2001). In this study, the ligand production rate was varied using the tet-off expression system and the ligand release rate was modulated by addition of metalloprotease inhibitors. The number of surface accessible receptors was varied using an EGFR blocking antibody. The ligand secretion rate, V_L , was measured using an EGF ELISA, and the appearance rate of the receptors, V_R , was calculated under specific antibody concentrations by solving a kinetic model describing receptor-ligand, receptor-antibody binding, and trafficking at steady state. The fraction of total and surface receptors occupied was measured by analyzing microphysiometer-based assay results using a quantitative model of ligand release and receptor dynamics (Lauffenburger et al., 1998). At V_L/V_R ratios of less than 0.3, almost no ligand was found in the conditioned medium, however, 30-40% of the receptors were occupied. At levels of ligand secretion sufficient to occupy >90% of the receptors, the fraction of ligand captured dropped to <10% and the V_L/V_R ratio increased to >1. These results suggested that a significant amount of autocrine signaling could occur even when the amount of ligand in the conditioned medium is close to the limits of experimental detection. Later work by DeWitt et al. showed that ligand-receptor affinity also regulates the spatial range of the fraction of ligand captured using an EGF mutant with a lower affinity for the EGFR (DeWitt et al., 2002). The mutant ligand was captured less efficiently, shifting the relationship between V_L/V_R and the fraction of ligand captured.

Recent computational work by Maly et al. also predicted that single cells are capable of achieving autocrine signaling on a dimension smaller than the cell diameter (Maly et al., 2004). Depending on the state of several cellular parameters, from an initial state of uniform ligand release and intracellular signaling, this dynamic model of extracellular and intracellular EGFR signaling could achieve a state of no signaling, uniform signaling, or a state of steady polarized ligand release and downstream signaling on a subcellular scale. In this model ligand shedding rate, receptor density, the strength of intracellular negative feedback, and the concentration of adaptor molecules in the EGFR signaling cascade were all sensitive parameters that determined the final signaling state.

Together these modeling and experimental results begin to describe how the spatial range of growth factor signaling is dependent on several cellular parameters. *Drosophila* oogenesis is an example of a complex process that is thought to require the production of multiple growth factors and both paracrine and autocrine signaling events for proper development of two dorsal eggshell appendages (Shvartsman et al., 2002; Wasserman and Freeman, 1998). While the spatial range and fraction of extracellular ligand that is captured by the producing cell may vary, it is important to also consider how the spatial distribution of available ligand translates to the distribution of receptor activation and intracellular signaling events and subsequent cell behavior.

2.3.2 Spatial Range Of Ligand Signaling Events

Does the spatial distribution of ligand signaling affect downstream signaling and potentially cell behavior? Since previous work had implicated that EGF-induced de-adhesion during cell motility required the activation of calpain, Glading et al. investigated the importance of intermediate ERK localization on this regulation (Glading et al., 2000; Glading et al., 2001). An internalization-deficient EGFR construct was able to activate calpain, while both membrane and cytosolic localized EGFR was shown to activate ERK. Membrane-targeted ERK was sufficient for calpain activity and cell de-adhesion, however when membrane-associated ERK was sequestered, EGFR-mediated calpain activation and de-adhesion was reduced. Results from Kempniak et al. showed that cells stimulated locally with EGF coated beads had less diffuse activated ERK when compared to cells stimulated with exogenous EGF, which suggests that active ERK may also remain somewhat localized in response to a polarized stimulus (Kempniak et al., 2003). Work by Haugh et al. revealed that PLC-gamma, another important signaling pathway downstream of the EGFR that is involved in cell motility, could be activated both at the cell membrane and by internalized receptors but its action of PIP2 hydrolysis appeared to be localized to the cell membrane (Haugh et al., 1999). Together these results suggest that ERK, calpain and PLC-gamma, all key signaling components downstream of EGFR that are involved in cell motility, may play mechanistic roles in effectively transferring localized growth factor signaling inputs into cellular outcomes (Glading et al., 2002; Wells and Grandis, 2003).

Short range activation and long range inhibition of specific signaling molecules is thought to be another mechanism by which cells are able to receive and interpret an asymmetric stimulus such as a chemotactic gradient (Iijima et al., 2002; Meinhardt, 1999). Phosphoinositide-3 Kinase (PI3K) is activated by the EGF receptor and is known to be a major player cell polarization as well as membrane protrusion and migration (Condeelis et al., 2001; Iijima et al., 2002). While PI3K may act locally downstream of active EGF receptors, PTEN, which is the primary phosphatase for the PI3K product phosphatidylinositol (3,4,5)-triphosphate, is thought to work as the global inhibitor (Sulis and Parsons, 2003). For example, PI3K activation is found localized at the cell membrane closest to the chemoattractant, while PTEN is localized to the cell rear in *Dictyostelium discoideum* amoebae chemotaxis (Iijima et al., 2002). PI3K has also been implicated in cell polarity and chemotaxis of mammalian cells (Condeelis et al., 2001; Sawyer et al., 2003; Wang et al., 2002).

It is also interesting to point out that while growth factors may obtain various spatial distributions and may be polarized at the cell membrane, and downstream signals may potentially propagate this input, the EGFR itself may also play a role in signaling distribution. Verveer et al. first proposed that ligand-independent EGFR activation could spread laterally on the cell surface when cells were stimulated locally with EGF-coated beads (Verveer et al., 2000). Work by Sawano et al. later showed that local activation of the EGFR, achieved by stimulating the edge of single cells in laminar flows containing EGF, could lead to lateral spread of downstream signaling over the entire cell, but that this process

only occurred at high receptor densities or when receptor endocytosis was inhibited (Sawano et al., 2002). More recent studies have shown that local stimulation with EGF-coated beads led to actin polymerization and membrane protrusion at the point of bead contact, suggesting that under these circumstances local signaling lead to a local response that is relevant to cell migration (Kempiak et al., 2003; Segall et al., 1996). It is still under investigation whether stimulation passes through the membrane via EGFR activation locally or ligand-independent lateral propagation of EGFR activation occurs, and this mechanism could be dependent on cellular parameters such as receptor density (Reynolds et al., 2003; Schlessinger, 2002).

2.3.3 The Mode Of Growth Factor Presentation Affects Cell Migration Behavior

Maheshwari et al. used a human mammary epithelial cell line transfected with one of two different EGF chimeras or the addition of exogenous EGF to investigate the effect ligand presentation mode (i.e. autocrine vs. intracrine vs. paracrine) on cell motility (Maheshwari et al., 2001). The first chimera, EGF-Ct, encoded for the receptor binding EGF ligand domain as well as the cytoplasmic and transmembrane domains of pro-EGF, which required proteolytic cleavage at the plasma membrane prior to receptor binding and was capable of stimulating cells in an autocrine manner. The EGF-Ct cells did not stimulate the migration of neighboring parental cells, while the addition of exogenous EGF resulted in stimulated parental cell migration. The second chimera, sEGF, encoded for the mature EGF ligand but lacked a membrane-anchoring domain and was thought

to stimulate the producing cells in an intracrine fashion. Maheshwari et al. measured the migration behavior of the parental, EGF-Ct, and sEGF hMEC cell lines *in vitro*, analyzed individual cell tracks, and found that the mode of ligand presentation affected the cell speed and migration persistence time.

Expression of membrane bound EGF (EGF-Ct) and the addition of exogenous EGF both increased hMEC cell speed in 2D, which was inhibited with an EGFR blocking antibody, see Figure 2.4.4. The sEGF-expressing cells had a basal migration speed that was decreased upon anti-EGFR antibody addition, suggesting that the surface receptor-ligand complexes governed cell migration speed. The most intriguing result from this study was that the migration persistence, or the approximate time a cell traveled before significantly changing direction, of the autocrine EGF-Ct expressing cells was dramatically increased compared to the parental cells in the presence of exogenous EGF. This increased persistence time was abolished upon addition of an EGFR blocking antibody or exogenous EGF.

The results from Maheshwari et al. suggest that the expression of membrane-bound EGF in the EGF-Ct hMEC cell line may lead to spatially restricted EGFR signaling that drives persistent migration behavior. The persistent migration may be the result of an asymmetrical distribution of EGFR signaling that stimulates further directed migration. The asymmetry could result from polarized distributions of the ligand, the receptor, or an asymmetric release of the ligand. EGFR ligand autocrine signaling spatially restricted to the front of the cell could stimulate membrane protrusion, thus producing what might be

thought of as a local “pseudo-chemotaxis” response (Condeelis et al., 2001; Segall et al., 1996). Although it was shown that the EGF-Ct chimera-expressing, autocrine cells had persistent migration behavior that was abolished under exogenous EGF/paracrine-like conditions, it is not yet known if the signaling is indeed spatially restricted or how intermediate signaling modes would alter the migration behavior of this experimental system. While previous results have shown that ligand presentation mode can affect cell behaviors such as cell organization (Wiley et al., 1998), these results conclude that the mode of ligand presentation can alter cell migration behavior.

2.4 Figures

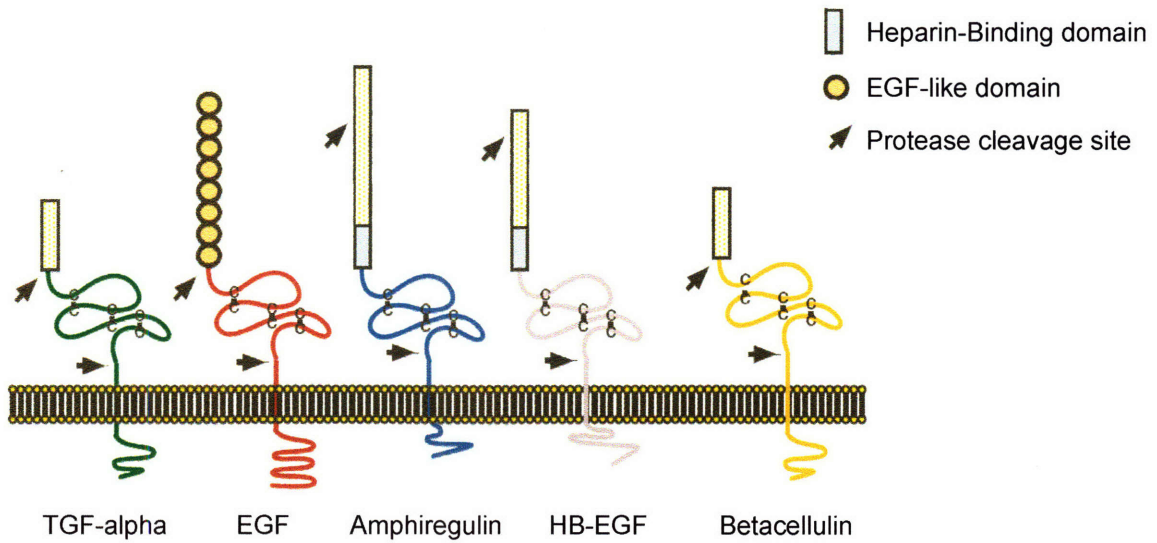


Figure 2.4.1. Schematic of EGFR ligand precursors. The EGFR receptor ligands are synthesized as membrane integral proteins that undergo proteolytic processing at the cell surface to release the mature soluble ligand. (Figure adapted from Opresko et al., 2001)

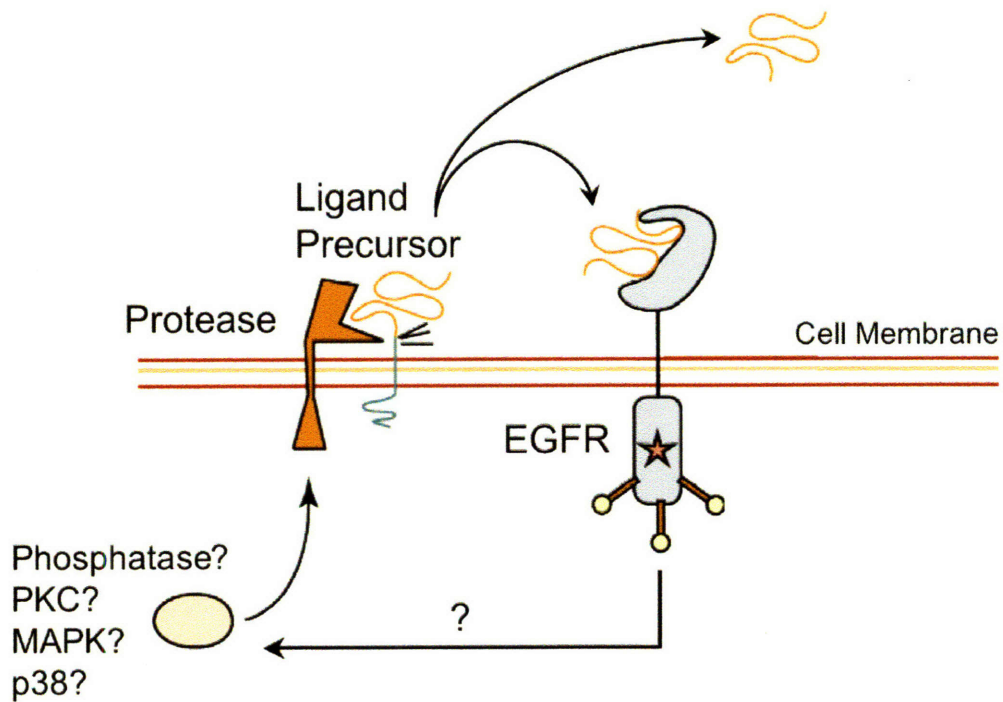


Figure 2.4.2. Schematic of ligand regulation at the cell surface.

Members of the ADAM family of metalloproteases proteolytically process the EGFR ligand precursors at the cell surface to form the mature, soluble ligand that can bind in an autocrine or paracrine manner. Some evidence suggests pathways downstream of the EGF receptor maybe regulate protease activity. (Figure adapted from Wiley et al., 2003)

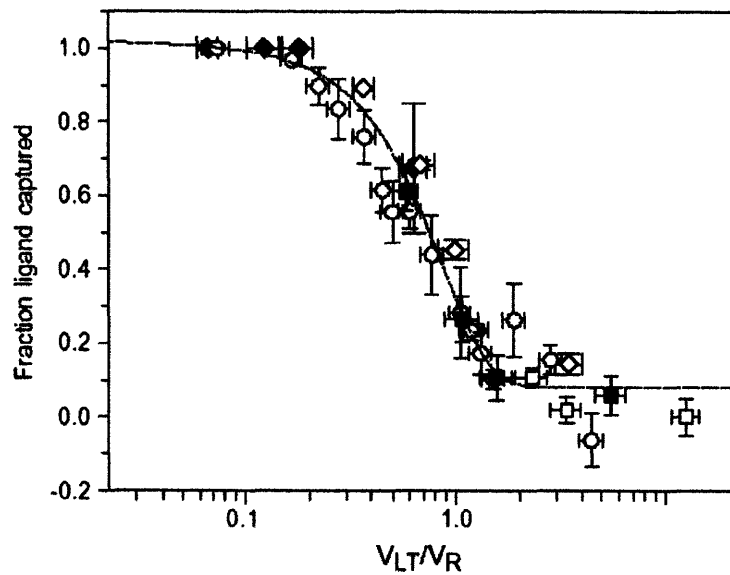


Figure 2.4.3 Ligand release rate varies the fraction of ligand captured. The relationship between the EGF secretion rate, V_L , receptor production rate, V_R , and the fraction of ligand captured for an engineered autocrine system in B82 mouse fibroblasts. (Adapted from DeWitt et al., 2001)

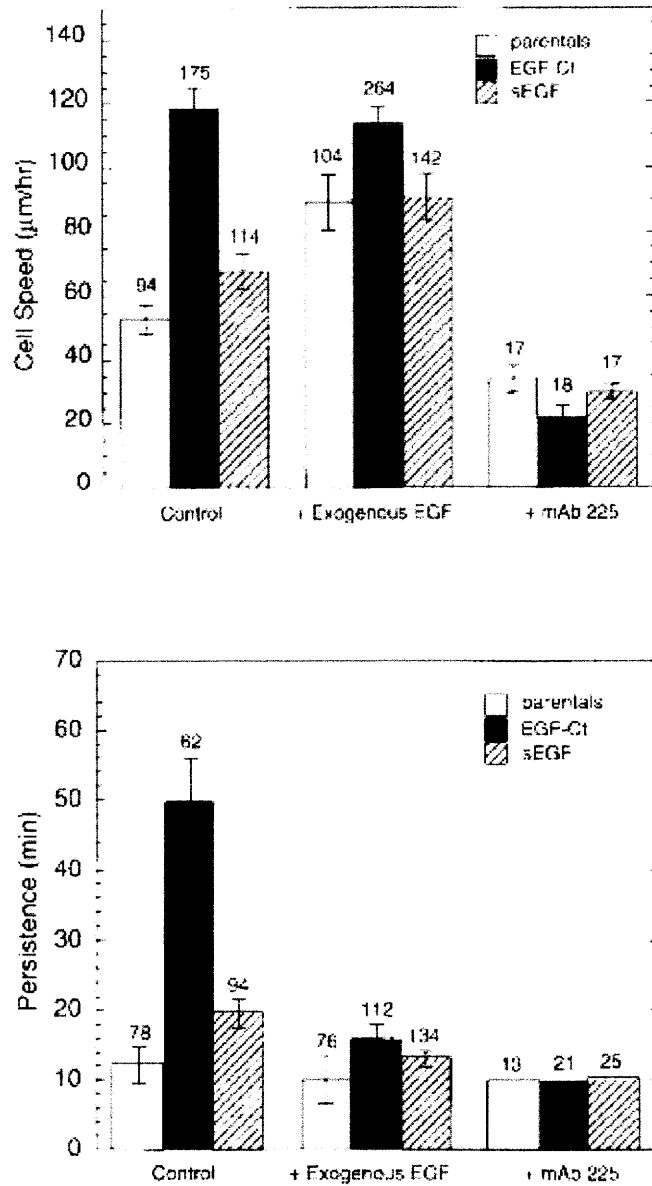


Figure 2.4.4 Autocrine presentation stimulates single cell persistence. Migration speed and persistence measurements for the EGF-Ct and sEGF cell lines, in the presence and absence of 2nM EGF and 10 µg/ml 225 mAb. (Adapted from Maheshwari et al., 2001)

2.5 References

- Anastasi, A., V. Erspamer, and M. Bucci. 1971. Isolation and structure of bombesin and alytesin, 2 analogous active peptides from the skin of the European amphibians *Bombina* and *Alytes*. *Experientia*. 27:166-7.
- Angel, P., and A. Szabowski. 2002. Function of AP-1 target genes in mesenchymal-epithelial cross-talk in skin. *Biochem Pharmacol*. 64:949-56.
- Aprikian, A.G., L. Tremblay, K. Han, and S. Chevalier. 1997. Bombesin stimulates the motility of human prostate-carcinoma cells through tyrosine phosphorylation of focal adhesion kinase and of integrin-associated proteins. *Int J Cancer*. 72:498-504.
- Arribas, J., F. Lopez-Casillas, and J. Massague. 1997. Role of the juxtamembrane domains of the transforming growth factor-alpha precursor and the beta-amyloid precursor protein in regulated ectodomain shedding. *J Biol Chem*. 272:17160-5.
- Arteaga, C.L. 2002. Epidermal growth factor receptor dependence in human tumors: more than just expression? *Oncologist*. 7 Suppl 4:31-9.
- Asakura, M., Kitakaze, M., Takashima, S., Liao, Y., Ishikura, F., Yoshinaka T., Ohmoto, H., Node, K., Yoshino, K., Ishiguro, H., Asanuma, H., Sanada, S., Matsumura, Y., Takeda, H., Beppu, S., Tada, M., Hori, M., Higashiyama, S. 2002. Cardiac hypertrophy is inhibited by antagonism of ADAM12 process of HB-EGF: metalloprotease inhibitors as a new therapy. *Nat Med*. 8:35-40.
- Bachelder, R.E., E.A. Lipscomb, X. Lin, M.A. Wendt, N.H. Chadborn, B.J. Eickholt, and A.M. Mercurio. 2003. Competing autocrine pathways involving alternative neuropilin-1 ligands regulate chemotaxis of carcinoma cells. *Cancer Res*. 63:5230-3.
- Badache, A., and N.E. Hynes. 2001. Interleukin 6 inhibits proliferation and, in cooperation with an epidermal growth factor receptor autocrine loop, increases migration of T47D breast cancer cells. *Cancer Res*. 61:383-91.
- Baselga, J., J. Mendelsohn, Y.M. Kim, and A. Pandiella. 1996. Autocrine regulation of membrane transforming growth factor-alpha cleavage. *J Biol Chem*. 271:3279-84.
- Block, E.R., A.R. Matela, N. SundarRaj, E.R. Iszkula, and J.K. Klarlund. 2004. Wounding induces motility in sheets of corneal epithelial cells through loss of spatial constraints: role of heparin-binding epidermal growth factor-like growth factor signaling. *J Biol Chem*. 279:24307-12.

- Borowiak, M., A.N. Garratt, T. Wustefeld, M. Strehle, C. Trautwein, and C. Birchmeier. 2004. Met provides essential signals for liver regeneration. *Proc Natl Acad Sci U S A.* 101:10608-13.
- Borrell-Pages, M., F. Rojo, J. Albanell, J. Baselga, and J. Arribas. 2003. TACE is required for the activation of the EGFR by TGF- α in tumors. *Embo J.* 22:1114-24.
- Brown, L.F., A.J. Guidi, S.J. Schnitt, L. Van De Water, M.L. Iruela-Arispe, T.K. Yeo, K. Tognazzi, and H.F. Dvorak. 1999. Vascular stroma formation in carcinoma in situ, invasive carcinoma, and metastatic carcinoma of the breast. *Clin Cancer Res.* 5:1041-56.
- Cai, Y.C., Z. Jiang, F. Vittemberg, X. Xu, L. Savas, B. Woda, M. Callery, and B. Banner. 1999. Expression of transforming growth factor- α and epidermal growth factor receptor in gastrointestinal stromal tumours. *Virchows Arch.* 435:112-5.
- Caric, D., H. Raphael, J. Viti, A. Feathers, D. Wancio, and L. Lillien. 2001. EGFRs mediate chemotactic migration in the developing telencephalon. *Development.* 128:4203-16.
- Carswell, E.A., L.J. Old, R.L. Kassel, S. Green, N. Fiore, and B. Williamson. 1975. An endotoxin-induced serum factor that causes necrosis of tumors. *Proc Natl Acad Sci U S A.* 72:3666-70.
- Chen, W.N., R.L. Woodbury, L.E. Kathmann, L.K. Opresko, R.C. Zangar, H.S. Wiley, and B.D. Thrall. 2004. Induced autocrine signaling through the epidermal growth factor receptor contributes to the response of mammary epithelial cells to tumor necrosis factor α . *J Biol Chem.* 279:18488-96.
- Condeelis, J.S., J.B. Wyckoff, M. Bailly, R. Pestell, D. Lawrence, J. Backer, and J.E. Segall. 2001. Lamellipodia in invasion. *Semin Cancer Biol.* 11:119-28.
- Cross, M.J., and L. Claesson-Welsh. 2001. FGF and VEGF function in angiogenesis: signalling pathways, biological responses and therapeutic inhibition. *Trends Pharmacol Sci.* 22:201-7.
- Damstrup, L., S.K. Kuwada, P.J. Dempsey, C.L. Brown, C.J. Hawkey, H.S. Poulsen, H.S. Wiley, and R.J. Coffey, Jr. 1999. Amphiregulin acts as an autocrine growth factor in two human polarizing colon cancer lines that exhibit domain selective EGF receptor mitogenesis. *Br J Cancer.* 80:1012-9.
- DeWitt, A., T. Iida, H.Y. Lam, V. Hill, H.S. Wiley, and D.A. Lauffenburger. 2002. Affinity regulates spatial range of EGF receptor autocrine ligand binding. *Dev Biol.* 250:305-16.

- DeWitt, A.E., J.Y. Dong, H.S. Wiley, and D.A. Lauffenburger. 2001. Quantitative analysis of the EGF receptor autocrine system reveals cryptic regulation of cell response by ligand capture. *J Cell Sci.* 114:2301-13.
- Dong, J., L.K. Opresko, P.J. Dempsey, D.A. Lauffenburger, R.J. Coffey, and H.S. Wiley. 1999. Metalloprotease-mediated ligand release regulates autocrine signaling through the epidermal growth factor receptor. *Proc Natl Acad Sci U S A.* 96:6235-40.
- Ekstrand, A.J., C.D. James, W.K. Cavenee, B. Seliger, R.F. Pettersson, and V.P. Collins. 1991. Genes for epidermal growth factor receptor, transforming growth factor alpha, and epidermal growth factor and their expression in human gliomas in vivo. *Cancer Res.* 51:2164-72.
- El-Obeid, A., E. Bongcam-Rudloff, M. Sorby, A. Ostman, M. Nister, and B. Westermarck. 1997. Cell scattering and migration induced by autocrine transforming growth factor alpha in human glioma cells in vitro. *Cancer Res.* 57:5598-604.
- Fan, H., and R. Derynck. 1999. Ectodomain shedding of TGF-alpha and other transmembrane proteins is induced by receptor tyrosine kinase activation and MAP kinase signaling cascades. *Embo J.* 18:6962-72.
- Fan, H., C.W. Turck, and R. Derynck. 2003. Characterization of growth factor-induced serine phosphorylation of tumor necrosis factor-alpha converting enzyme and of an alternatively translated polypeptide. *J Biol Chem.* 278:18617-27.
- Forsten, K.E., and D.A. Lauffenburger. 1992. Autocrine ligand binding to cell receptors. Mathematical analysis of competition by solution "decoys". *Biophys J.* 61:518-29.
- Fu, S., I. Bottoli, M. Goller, and P.K. Vogt. 1999. Heparin-binding epidermal growth factor-like growth factor, a v-Jun target gene, induces oncogenic transformation. *Proc Natl Acad Sci U S A.* 96:5716-21.
- Gavrilovic, J., G. Moens, J.P. Thiery, and J. Jouanneau. 1990. Expression of transfected transforming growth factor alpha induces a motile fibroblast-like phenotype with extracellular matrix-degrading potential in a rat bladder carcinoma cell line. *Cell Regul.* 1:1003-14.
- Gechtman, Z., J.L. Alonso, G. Raab, D.E. Ingber, and M. Klagsbrun. 1999. The shedding of membrane-anchored heparin-binding epidermal-like growth factor is regulated by the Raf/mitogen-activated protein kinase cascade and by cell adhesion and spreading. *J Biol Chem.* 274:28828-35.
- Glading, A., P. Chang, D.A. Lauffenburger, and A. Wells. 2000. Epidermal growth factor receptor activation of calpain is required for fibroblast motility and

- occurs via an ERK/MAP kinase signaling pathway. *J Biol Chem.* 275:2390-8.
- Glading, A., D.A. Lauffenburger, and A. Wells. 2002. Cutting to the chase: calpain proteases in cell motility. *Trends Cell Biol.* 12:46-54.
- Glading, A., F. Uberall, S.M. Keyse, D.A. Lauffenburger, and A. Wells. 2001. Membrane proximal ERK signaling is required for M-calpain activation downstream of epidermal growth factor receptor signaling. *J Biol Chem.* 276:23341-8.
- Grose, R. 2003. Epithelial migration: open your eyes to c-Jun. *Curr Biol.* 13:R678-80.
- Gschwind, A., S. Hart, O.M. Fischer, and A. Ullrich. 2003. TACE cleavage of proamphiregulin regulates GPCR-induced proliferation and motility of cancer cells. *Embo J.* 22:2411-21.
- Gschwind, A., E. Zwick, N. Prenzel, M. Leserer, and A. Ullrich. 2001. Cell communication networks: epidermal growth factor receptor transactivation as the paradigm for interreceptor signal transmission. *Oncogene.* 20:1594-600.
- Hanahan, D., and R.A. Weinberg. 2000. The hallmarks of cancer. *Cell.* 100:57-70.
- Harris, R.C., E. Chung, and R.J. Coffey. 2003. EGF receptor ligands. *Exp Cell Res.* 284:2-13.
- Haugh, J.M., K. Schooler, A. Wells, H.S. Wiley, and D.A. Lauffenburger. 1999. Effect of epidermal growth factor receptor internalization on regulation of the phospholipase C-gamma1 signaling pathway. *J Biol Chem.* 274:8958-65.
- Hinkle, C.L., M.J. Mohan, P. Lin, N. Yeung, F. Rasmussen, M.E. Milla, and M.L. Moss. 2003. Multiple metalloproteinases process protransforming growth factor-alpha (proTGF-alpha). *Biochemistry.* 42:2127-36.
- Hirano, T. 1998. Interleukin 6 and its receptor: ten years later. *Int Rev Immunol.* 16:249-84.
- Holbro, T., G. Civenni, and N.E. Hynes. 2003. The ErbB receptors and their role in cancer progression. *Exp Cell Res.* 284:99-110.
- Hsieh, E.T., F.A. Shepherd, and M.S. Tsao. 2000. Co-expression of epidermal growth factor receptor and transforming growth factor-alpha is independent of ras mutations in lung adenocarcinoma. *Lung Cancer.* 29:151-7.

- Humphrey, P.A., X. Zhu, R. Zarnegar, P.E. Swanson, T.L. Ratliff, R.T. Vollmer, and M.L. Day. 1995. Hepatocyte growth factor and its receptor (c-MET) in prostatic carcinoma. *Am J Pathol.* 147:386-96.
- Iijima, M., Y.E. Huang, and P. Devreotes. 2002. Temporal and spatial regulation of chemotaxis. *Dev Cell.* 3:469-78.
- Johnson, A.C., B.A. Murphy, C.M. Matelis, Y. Rubinstein, E.C. Piebenga, L.M. Akers, G. Neta, C. Vinson, and M. Birrer. 2000. Activator protein-1 mediates induced but not basal epidermal growth factor receptor gene expression. *Mol Med.* 6:17-27.
- Kempiak, S.J., S.C. Yip, J.M. Backer, and J.E. Segall. 2003. Local signaling by the EGF receptor. *J Cell Biol.* 162:781-7.
- Kim, H.G., J. Kassis, J.C. Souto, T. Turner, and A. Wells. 1999. EGF receptor signaling in prostate morphogenesis and tumorigenesis. *Histol Histopathol.* 14:1175-82.
- Kopp, R., E. Rothbauer, M. Ruge, H. Arnholdt, J. Spranger, M. Muders, D.G. Pfeiffer, F.W. Schildberg, and A. Pfeiffer. 2003. Clinical implications of the EGF receptor/ligand system for tumor progression and survival in gastrointestinal carcinomas: evidence for new therapeutic options. *Recent Results Cancer Res.* 162:115-32.
- Kumar, R., and R.A. Wang. 2002. Protein kinases in mammary gland development and cancer. *Microsc Res Tech.* 59:49-57.
- Lauffenburger, D.A., G.T. Oehrtman, L. Walker, and H.S. Wiley. 1998. Real-time quantitative measurement of autocrine ligand binding indicates that autocrine loops are spatially localized. *Proc Natl Acad Sci U S A.* 95:15368-73.
- Li, G., C. Gustafson-Brown, S.K. Hanks, K. Nason, J.M. Arbeit, K. Pogliano, R.M. Wisdom, and R.S. Johnson. 2003. c-Jun is essential for organization of the epidermal leading edge. *Dev Cell.* 4:865-77.
- Luetkeke, N.C., T.H. Qiu, R.L. Peiffer, P. Oliver, O. Smithies, and D.C. Lee. 1993. TGF alpha deficiency results in hair follicle and eye abnormalities in targeted and waved-1 mice. *Cell.* 73:263-78.
- Madarame, J., S. Higashiyama, H. Kiyota, A. Madachi, F. Toki, T. Shimomura, N. Tani, Y. Oishi, and N. Matsuura. 2003. Transactivation of epidermal growth factor receptor after heparin-binding epidermal growth factor-like growth factor shedding in the migration of prostate cancer cells promoted by bombesin. *Prostate.* 57:187-95.

- Maheshwari, G., H.S. Wiley, and D.A. Lauffenburger. 2001. Autocrine epidermal growth factor signaling stimulates directionally persistent mammary epithelial cell migration. *J Cell Biol.* 155:1123-8.
- Maly, I.V., H.S. Wiley, and D.A. Lauffenburger. 2004. Self-organization of polarized cell signaling via autocrine circuits: computational model analysis. *Biophys J.* 86:10-22.
- Markwalder, R., and J.C. Reubi. 1999. Gastrin-releasing peptide receptors in the human prostate: relation to neoplastic transformation. *Cancer Res.* 59:1152-9.
- Meinhardt, H. 1999. Orientation of chemotactic cells and growth cones: models and mechanisms. *J Cell Sci.* 112 (Pt 17):2867-74.
- Mercurio, A.M., R.E. Bachelder, R.C. Bates, and J. Chung. 2004. Autocrine signaling in carcinoma: VEGF and the alpha6beta4 integrin. *Semin Cancer Biol.* 14:115-22.
- Merlos-Suarez, A., S. Ruiz-Paz, J. Baselga, and J. Arribas. 2001. Metalloprotease-dependent protransforming growth factor-alpha ectodomain shedding in the absence of tumor necrosis factor-alpha-converting enzyme. *J Biol Chem.* 276:48510-7.
- Metcalf, D. 1985. The granulocyte-macrophage colony-stimulating factors. *Science.* 229:16-22.
- Miettinen, P.J., J.E. Berger, J. Meneses, Y. Phung, R.A. Pedersen, Z. Werb, and R. Derynck. 1995. Epithelial immaturity and multiorgan failure in mice lacking epidermal growth factor receptor. *Nature.* 376:337-41.
- Mignatti, P., T. Morimoto, and D.B. Rifkin. 1991. Basic fibroblast growth factor released by single, isolated cells stimulates their migration in an autocrine manner. *Proc Natl Acad Sci U S A.* 88:11007-11.
- Mueller, M.M., C.C. Herold-Mende, D. Riede, M. Lange, H.H. Steiner, and N.E. Fusenig. 1999. Autocrine growth regulation by granulocyte colony-stimulating factor and granulocyte macrophage colony-stimulating factor in human gliomas with tumor progression. *Am J Pathol.* 155:1557-67.
- Mueller, M.M., W. Peter, M. Mappes, A. Huelsen, H. Steinbauer, P. Boukamp, M. Vaccariello, J. Garlick, and N.E. Fusenig. 2001. Tumor progression of skin carcinoma cells in vivo promoted by clonal selection, mutagenesis, and autocrine growth regulation by granulocyte colony-stimulating factor and granulocyte-macrophage colony-stimulating factor. *Am J Pathol.* 159:1567-79.

- Natoli, G., A. Costanzo, F. Guido, F. Moretti, and M. Levrero. 1998. Apoptotic, non-apoptotic, and anti-apoptotic pathways of tumor necrosis factor signalling. *Biochem Pharmacol.* 56:915-20.
- Oehrtman, G.T., H.S. Wiley, and D.A. Lauffenburger. 1998. Escape of autocrine ligands into extracellular medium: experimental test of theoretical model predictions. *Biotechnol Bioeng.* 57:571-82.
- Opresko, L.K., Chrisler, W., Silva, M., Wiley, H.S. 2001. The cytoplasmic tails of epidermal growth factor receptor ligands direct their intracellular distribution and shedding kinetics in transfected cells. *poster.*
- Ornitz, D.M., and N. Itoh. 2001. Fibroblast growth factors. *Genome Biol.* 2:REVIEWS3005.
- Perrella, M.A., Maki, T., Prasad, S., Pimental, D., Singh, K., Takahashi, N., Yoshizumi, M., Alali, A., Higashiyama, S., Kelly, R.A., et al. 1994. Regulation of heparin-binding epidermal growth factor-like growth factor mRNA levels by hypertrophic stimuli in neonatal and adult rat cardiac myocytes. *J Biol Chem.* 269: 27045-50.
- Pilcher, B.K., J. Dumin, M.J. Schwartz, B.A. Mast, G.S. Schultz, W.C. Parks, and H.G. Welgus. 1999. Keratinocyte collagenase-1 expression requires an epidermal growth factor receptor autocrine mechanism. *J Biol Chem.* 274:10372-81.
- Reynolds, A.R., C. Tischer, P.J. Verveer, O. Rocks, and P.I. Bastiaens. 2003. EGFR activation coupled to inhibition of tyrosine phosphatases causes lateral signal propagation. *Nat Cell Biol.* 5:447-53.
- Rubin Grandis, J., M.F. Melhem, W.E. Gooding, R. Day, V.A. Holst, M.M. Wagener, S.D. Drenning, and D.J. Tweardy. 1998. Levels of TGF-alpha and EGFR protein in head and neck squamous cell carcinoma and patient survival. *J Natl Cancer Inst.* 90:824-32.
- Salomon, D.S., R. Brandt, F. Ciardiello, and N. Normanno. 1995. Epidermal growth factor-related peptides and their receptors in human malignancies. *Crit Rev Oncol Hematol.* 19:183-232.
- Salven, P., V. Perhoniemi, H. Tykka, H. Maenpaa, and H. Joensuu. 1999. Serum VEGF levels in women with a benign breast tumor or breast cancer. *Breast Cancer Res Treat.* 53:161-6.
- Sato, Y., and D.B. Rifkin. 1988. Autocrine activities of basic fibroblast growth factor: regulation of endothelial cell movement, plasminogen activator synthesis, and DNA synthesis. *J Cell Biol.* 107:1199-205.

- Sawano, A., S. Takayama, M. Matsuda, and A. Miyawaki. 2002. Lateral propagation of EGF signaling after local stimulation is dependent on receptor density. *Dev Cell*. 3:245-57.
- Sawyer, C., J. Sturge, D.C. Bennett, M.J. O'Hare, W.E. Allen, J. Bain, G.E. Jones, and B. Vanhaesebroeck. 2003. Regulation of breast cancer cell chemotaxis by the phosphoinositide 3-kinase p110delta. *Cancer Res*. 63:1667-75.
- Schlegel, U., P.L. Moots, M.K. Rosenblum, H.T. Thaler, and H.M. Furneaux. 1990. Expression of transforming growth factor alpha in human gliomas. *Oncogene*. 5:1839-42.
- Schlessinger, J. 2002. All signaling is local? *Mol Cell*. 10:218-9.
- Schulze, A., K. Lehmann, H.B. Jefferies, M. McMahon, and J. Downward. 2001. Analysis of the transcriptional program induced by Raf in epithelial cells. *Genes Dev*. 15:981-94.
- Segall, J.E., S. Tyerech, L. Boselli, S. Masseling, J. Helft, A. Chan, J. Jones, and J. Condeelis. 1996. EGF stimulates lamellipod extension in metastatic mammary adenocarcinoma cells by an actin-dependent mechanism. *Clin Exp Metastasis*. 14:61-72.
- Seghezzi, G., S. Patel, C.J. Ren, A. Gualandris, G. Pintucci, E.S. Robbins, R.L. Shapiro, A.C. Galloway, D.B. Rifkin, and P. Mignatti. 1998. Fibroblast growth factor-2 (FGF-2) induces vascular endothelial growth factor (VEGF) expression in the endothelial cells of forming capillaries: an autocrine mechanism contributing to angiogenesis. *J Cell Biol*. 141:1659-73.
- Shvartsman, S.Y., C.B. Muratov, and D.A. Lauffenburger. 2002. Modeling and computational analysis of EGF receptor-mediated cell communication in *Drosophila* oogenesis. *Development*. 129:2577-89.
- Shvartsman, S.Y., H.S. Wiley, W.M. Deen, and D.A. Lauffenburger. 2001. Spatial range of autocrine signaling: modeling and computational analysis. *Biophys J*. 81:1854-67.
- Shweiki, D., A. Itin, D. Soffer, and E. Keshet. 1992. Vascular endothelial growth factor induced by hypoxia may mediate hypoxia-initiated angiogenesis. *Nature*. 359:843-5.
- Sporn, M.B., and A.B. Roberts. 1985. Autocrine growth factors and cancer. *Nature*. 313:745-7.
- Sporn, M.B., and A.B. Roberts. 1992. Autocrine secretion--10 years later. *Ann Intern Med*. 117:408-14.

- Sporn, M.B., and G.J. Todaro. 1980. Autocrine secretion and malignant transformation of cells. *N Engl J Med.* 303:878-80.
- Sulis, M.L., and R. Parsons. 2003. PTEN: from pathology to biology. *Trends Cell Biol.* 13:478-83.
- Suo, Z., B. Risberg, M.G. Karlsson, K. Villman, E. Skovlund, and J.M. Nesland. 2002. The expression of EGFR family ligands in breast carcinomas. *Int J Surg Pathol.* 10:91-9.
- Tachibana, M., A. Miyakawa, H. Tazaki, K. Nakamura, A. Kubo, J. Hata, T. Nishi, and Y. Amano. 1995. Autocrine growth of transitional cell carcinoma of the bladder induced by granulocyte-colony stimulating factor. *Cancer Res.* 55:3438-43.
- Takayama, H., W.J. LaRochelle, R. Sharp, T. Otsuka, P. Kriebel, M. Anver, S.A. Aaronson, and G. Merlino. 1997. Diverse tumorigenesis associated with aberrant development in mice overexpressing hepatocyte growth factor/scatter factor. *Proc Natl Acad Sci U S A.* 94:701-6.
- Tillotson, J.K., and D.P. Rose. 1991. Endogenous secretion of epidermal growth factor peptides stimulates growth of DU145 prostate cancer cells. *Cancer Lett.* 60:109-12.
- Tokumaru, S., S. Higashiyama, T. Endo, T. Nakagawa, J.I. Miyagawa, K. Yamamori, Y. Hanakawa, H. Ohmoto, K. Yoshino, Y. Shirakata, Y. Matsuzawa, K. Hashimoto, and N. Taniguchi. 2000. Ectodomain shedding of epidermal growth factor receptor ligands is required for keratinocyte migration in cutaneous wound healing. *J Cell Biol.* 151:209-20.
- Tuck, A.B., M. Park, E.E. Sterns, A. Boag, and B.E. Elliott. 1996. Coexpression of hepatocyte growth factor and receptor (Met) in human breast carcinoma. *Am J Pathol.* 148:225-32.
- Turner, T., P. Chen, L.J. Goodly, and A. Wells. 1996. EGF receptor signaling enhances in vivo invasiveness of DU-145 human prostate carcinoma cells. *Clin Exp Metastasis.* 14:409-18.
- Uehara, Y., O. Minowa, C. Mori, K. Shiota, J. Kuno, T. Noda, and N. Kitamura. 1995. Placental defect and embryonic lethality in mice lacking hepatocyte growth factor/scatter factor. *Nature.* 373:702-5.
- Uemura, Y., M. Kobayashi, H. Nakata, R. Harada, T. Kubota, and H. Taguchi. 2004. Effect of serum deprivation on constitutive production of granulocyte-colony stimulating factor and granulocyte macrophage-colony stimulating factor in lung cancer cells. *Int J Cancer.* 109:826-32.

- Vadnais, J., G. Nault, Z. Daher, M. Amraei, Y. Dodier, I.R. Nabi, and J. Noel. 2002. Autocrine activation of the hepatocyte growth factor receptor/met tyrosine kinase induces tumor cell motility by regulating pseudopodial protrusion. *J Biol Chem.* 277:48342-50.
- Verveer, P.J., F.S. Wouters, A.R. Reynolds, and P.I. Bastiaens. 2000. Quantitative imaging of lateral ErbB1 receptor signal propagation in the plasma membrane. *Science.* 290:1567-70.
- Wang, F., P. Herzmark, O.D. Weiner, S. Srinivasan, G. Servant, and H.R. Bourne. 2002. Lipid products of PI(3)Ks maintain persistent cell polarity and directed motility in neutrophils. *Nat Cell Biol.* 4:513-8.
- Wasserman, J.D., and M. Freeman. 1998. An autoregulatory cascade of EGF receptor signaling patterns the Drosophila egg. *Cell.* 95:355-64.
- Wells, A., and J.R. Grandis. 2003. Phospholipase C-gamma1 in tumor progression. *Clin Exp Metastasis.* 20:285-90.
- Wiley, H.S., S.Y. Shvartsman, and D.A. Lauffenburger. 2003. Computational modeling of the EGF-receptor system: a paradigm for systems biology. *Trends Cell Biol.* 13:43-50.
- Wiley, H.S., M.F. Woolf, L.K. Opresko, P.M. Burke, B. Will, J.R. Morgan, and D.A. Lauffenburger. 1998. Removal of the membrane-anchoring domain of epidermal growth factor leads to intracrine signaling and disruption of mammary epithelial cell organization. *J Cell Biol.* 143:1317-28.
- Xie, H., T. Turner, M.H. Wang, R.K. Singh, G.P. Siegal, and A. Wells. 1995. In vitro invasiveness of DU-145 human prostate carcinoma cells is modulated by EGF receptor-mediated signals. *Clin Exp Metastasis.* 13:407-19.
- Yamanaka, Y., H. Friess, M.S. Kobrin, M. Buchler, H.G. Beger, and M. Korc. 1993. Coexpression of epidermal growth factor receptor and ligands in human pancreatic cancer is associated with enhanced tumor aggressiveness. *Anticancer Res.* 13:565-9.
- Yarden, Y., and M.X. Sliwkowski. 2001. Untangling the ErbB signalling network. *Nat Rev Mol Cell Biol.* 2:127-37.
- Yates, S., and T.E. Rayner. 2002. Transcription factor activation in response to cutaneous injury: role of AP-1 in reepithelialization. *Wound Repair Regen.* 10:5-15.
- Yoshioka, J., Prince, R.N., Huang, H., Perkins, S.B., Cruz, F.U., McGillivray, C., Lauffenburger, D.A., Lee, R.T. 2005. Cardiomyocyte hypertrophy and

degradation of connexin43 through spatially restricted autocrine/paracrine heparin-binding EGF. *PNAS*, 102:10622-7.

Zhu, Z., J. Kleeff, H. Friess, L. Wang, A. Zimmermann, Y. Yarden, M.W. Buchler, and M. Korc. 2000. Epiregulin is Up-regulated in pancreatic cancer and stimulates pancreatic cancer cell growth. *Biochem Biophys Res Commun*. 273:1019-24.

Chapter 3: Autocrine stimulated ERK signaling and cell motility

Aberrant expression of the epidermal growth factor (EGF) receptor has been implicated in various types of cancers. In carcinomas, the tumor cells generally both express EGF receptor and produce cognate ligands providing a potential autocrine signaling system. EGF family ligands are synthesized as membrane-anchored proteins requiring proteolytic release to form the mature soluble factor. Despite the pathophysiological importance of autocrine systems, how protease-mediated ligand release quantitatively influences receptor-mediated signaling and consequent cell behavior is poorly understood. Therefore, we explored the relationship between autocrine EGF release rates and receptor-mediated ERK activation and migration in human mammary epithelial cells. A quantitative spectrum of EGF release rates was achieved using chimeric EGF ligand precursors modulated by the addition of the metalloprotease inhibitor batimastat. We found that ERK activation increased with increasing ligand release rates despite concomitant EGF receptor downregulation. Cell migration speed depended linearly on the steady-state

phospho-ERK level, but was much greater for autocrine compared to exogenous stimulation. In contrast, cell proliferation rates were constant across the various treatment conditions. Thus, in these cells, ERK-mediated migration stimulated by EGF receptor signaling is most sensitively regulated by autocrine ligand control mechanisms.

3.1 Introduction

The EGF receptor (EGFR) tyrosine kinase family is known to play an important role in normal physiological processes including cell survival, cell proliferation, migration, and wound healing (Yarden and Sliwkowski, 2001). Aberrant expression of EGFR family ligands, as well as of the receptors themselves, is implicated in and correlated to poor prognosis in various types of cancers, including tumors of the brain, breast, lung, and prostate among others (Ishikawa et al., 2005; Normanno et al., 2003; Normanno et al., 2006; Salomon et al., 1995). The cell property most underlying this link to poor prognosis is increased cell migration to enable escape from the primary mass and initial dissemination (Condeelis et al., 2005; Wells, 2000).

The family of ligands that bind specifically to the EGFR (also known as erbB1 and HER1) includes EGF, TGF- α (TGF α), amphiregulin, heparin-binding EGF, betacellulin, epiregulin and epigen (Harris et al., 2003). These ligands are synthesized as membrane-anchored proteins containing an amino terminal extension, an EGF-like receptor binding domain, a membrane proximal region, transmembrane region and a cytoplasmic tail. Ligands such as HB-EGF

and amphiregulin may be capable of activating EGFR in a juxtacrine mode at points of cell-cell contact, while others, including EGF and TGF α , are understood to require proteolytic cleavage from the cell surface to form mature soluble growth factors that act in a local autocrine fashion or more distal paracrine manner (Borrell-Pages et al., 2003; Dong et al., 2005; Singh and Harris, 2005). While there is little sequence homology between the various ligands outside of the core EGF-like domain, the membrane proximal region is thought to be a key determinate in ectodomain shedding and protease specificity (Arribas et al., 1997; Harris et al., 2003).

The ADAM family of metalloproteases appears to be central to EGFR ligand processing. ADAM17 (also known as TACE) has been implicated in the proteolytic processing of TGF α , amphiregulin, and HB-EGF, while ADAM-10 is thought to be involved in EGF cleavage (Borrell-Pages et al., 2003; Sahin et al., 2004). Protease regulation of ligand release is under active investigation, especially because of the growing appreciation of this mechanism as underlying transactivation of EGFR family receptors by a variety of stimuli such as G protein-coupled receptor ligands and mechanical stress (Eguchi et al., 2003; Fischer et al., 2003; Ohtsu et al., 2006). Evidence exists that signaling pathway activation can stimulate autocrine ligand release (Baselga et al., 1996; Fan and Derynck, 1999; Pandiella and Massague, 1991), and that this effect can be enhanced by constitutively active pathway components (Seton-Rogers and Brugge, 2004; Seton-Rogers et al., 2004; Wilsbacher et al., 2006). A recent study has demonstrated that co-expression of TGF α and TACE at elevated

levels is highly predictive of poor prognosis across a set of 295 primary breast tumors. Significantly, reversion of a malignant phenotype could be obtained by reduction of TACE activity, suggesting that quantitative control of protease-mediated autocrine EGF ligand release could be critical for governing phenotypic behavior (Kenny and Bissell, 2007).

Autocrine ligand signaling was initially identified by the ability of transformed cells to grow in culture in the absence of exogenous growth factor supplements (Sporn and Todaro, 1980). Due to the intrinsic “closed-loop” nature of autocrine systems, however, identification and experimental analysis of autocrine effects on cellular behaviors is unusually challenging (Wiley et al., 2003). Cells expressing a form of pro-EGF that required shedding have shown increased cell migration persistence compared to exogenously stimulated cells, suggesting that autocrine presentation may stimulate distinctive cell behavior potentially due to spatial restriction of EGFR activation (Maheshwari et al., 2001). Both computational and experimental approaches have estimated that EGFR autocrine loops can operate on a scale less than a cell diameter and that several parameters, such as ligand release rate, receptor number, ligand affinity, and ligand diffusivity affect spatial localization (DeWitt et al., 2002; DeWitt et al., 2001; Forsten and Lauffenburger, 1992b; Lauffenburger et al., 1998; Maly et al., 2004; Shvartsman et al., 2001). In addition, experimental work has demonstrated that the ratio of ligand release to receptor production correlated with the fraction of ligand that was captured, suggesting that these parameters

may determine whether cells operate in an autocrine or paracrine mode (DeWitt et al., 2001).

In this current study we investigate how the protease-mediated ligand release rate quantitatively governs receptor-mediated signaling and consequent cell proliferation and migration behavior. A central issue is whether a “dose-response” relationship can be obtained across a range of ligand release rates, in manner analogous to the well-established approach used to ascertain effects of exogenous ligand/receptor interactions. A second major issue is whether there exist significant differences between cell responses to “chronic” (e.g., as in persistent autocrine ligand stimulation) as opposed to “acute” (e.g., the typical experimental method of bolus exogenous ligand addition in culture) treatment. One might imagine that cell signaling and behavioral responses to a high autocrine ligand release rate might be similar to that for exogenous ligand treatment, since both are effectively “paracrine” presentations.

To address these questions, we have designed an experimental *in vitro* cell system to test how varying ligand release alters cell signaling and cell migration. High and low release rates of EGF are achieved using chimeric transmembrane EGF ligand precursors retrovirally transfected into the 184A1 human mammary epithelial cell line. Ligand release can be “tuned” downward by the metalloprotease inhibitor batimastat, to obtain a quantitative spectrum of ligand release rates. We measured surface EGFR downregulation, ERK phosphorylation, cell proliferation, and cell migration speed under conditions of low to high ligand release. We found that cell migration speed was directly

proportional to the steady-state phospho-ERK level driven by autocrine ligand release, in a clear demonstration of a “dose-response” relationship. Surprisingly, migration speed is faster under “chronic” autocrine control than under “acute” exogenous treatment even though the latter generates greater peak and integrated levels of phosphorylated ERK as well as equivalent cell proliferation responses. Thus, cell migration -- in contrast to cell proliferation -- is more sensitively controlled by protease-mediated autocrine ligand release.

3.2 *Materials and Methods*

3.2.1 Reagents and antibodies

Batimastat (BB-94; [4-(N-hydroxyamino)-2R-isobutyl-3S-(thienylthiomethyl)succinyl]-L-phenylalanine-N-methylamide) was custom synthesized by Kimia Corporation (Santa Clara, CA). ERK phosphorylation was inhibited with the small molecule MEK inhibitor PD98059 (Calbiochem). Anti-EGFR 13A9 monoclonal antibody, which binds non-competitively to both occupied and empty EGFR (Winkler et al., 1989), was a gift from Genentech (South San Francisco, CA). The receptor blocking anti-EGFR 225 monoclonal antibody was isolated from a hybridoma cell line obtained from the American Type Culture Collection (Gill et al., 1984). Anti-EGF antibodies for EGF ELISA include 236 (R&D Systems) and a rabbit polyclonal described previously (Wiley et al., 1998). The tertiary ELISA detection antibody was an alkaline phosphatase-conjugated goat anti-rabbit antibody (Sigma). Recombinant human EGF was obtained from Peprotech. ERK antibodies used in western blots were

purchased from Cell Signaling. Luminex phospho-tyrosine EGFR and phospho-ERK1/2 BioPlex kits and lysis buffer were purchased from Bio-Rad.

3.2.2 Construction of ligand chimeras and cell lines

The Wiley lab constructed all of the EGF chimeras. The TCT ligand (EGF with the membrane-anchoring region and cytoplasmic tail of TGF α) was assembled initially in pBluescript using a construct that contained the mature coding sequence of EGF (amino acids 971 to 1023) preceded by the signal sequence of the EGFR. A Bgl II site was engineered at the 3' end of the EGF sequence followed by an Xba1 site from the original pBluescript multicloning region. Ligand specific sequences that included the juxtamembrane, transmembrane and cytoplasmic tails were amplified using PCR primers that contained a Bgl II site in the 5' primer and an Xba1 and BamH1 site in the 3' primer. The following primer sequences were used: TGF α front primer: 5' – ACT TAA GAT CTC CTG GCC GTG GTG GCT GCC AGC CAG A – 3'; TGF α back primer: 5' – CCG CTC TAG AAC TAG TGG ATC CCC TCT TCA GAC CAC TGT TTC TGA GTG – 3'. Following assembly in pBluescript the chimeric ligand was subcloned into the retroviral vector pBM-IRESpuro (Garton et al., 2002). Retroviral supernatants were collected from transfected HEK293 cells and used to transduce the parental hMEC cell line. The ECT ligand (EGF with the membrane-anchoring region of EGF) was constructed as described previously (Wiley et al., 1998). These constructs are shown schematically in Fig. 3.5.1.

The human mammary epithelial cell (hMEC) line 184A1 (Stampfer et al., 1993) was obtained from Martha Stampfer (Lawrence Berkeley National Laboratory, University of California, Berkeley, Berkeley, CA). The hMECs were retrovirally transduced with the ECT and TCT constructs and maintained in DFCI-1 medium (Band and Sager, 1989). Serum-free media consisted of DFCI-1 complete media lacking fetal bovine serum, bovine pituitary extract, or EGF supplements, with the addition of 1 mg/ml Bovine Serum Albumin (Sigma). Unless otherwise noted, cells were incubated for 16 hours in serum-free media before starting each experiment. All experiments were performed using cells within 15 passages of thawing.

3.2.3 EGF release rates

Cells were plated in DFCI-1 media in 12-well plates on day 1 at a density of 60,000-80,000 cells/well, and switched to serum-free media on day 2. After 16 hours cells were switched to 1ml of fresh serum-free media alone or containing 225 or batimastat at varying concentrations. At 2-hour time intervals media was collected from parallel plates, centrifuged at 14,000 for 10 minutes at 4°C, and the supernatant was frozen. The EGF concentration of the conditioned media, measured by ELISA, was converted to molecules of EGF and normalized to the average cell number per well measured with a Vi Cell XR. The rate of EGF release was determined from the slope of a linear fit.

3.2.4 Surface receptor levels

Anti-EGFR mAb 13A9 was labeled with ^{125}I (Perkin Elmer) using iodobeads (Pierce) as previously described (Burke and Wiley, 1999). Labeled 13A9 was used to measure surface EGFR numbers as previously described (Hendriks, 2003). Briefly, 150,000 cells were plated in 6-well plates on day 1 and switched to serum-free media with or without 10 μM Batimastat on day 2. After 19 hrs, cells were switched to fresh serum-free media containing 600 ng/ml of radiolabeled 13A9 alone or in addition to 2nM EGF and incubated at 37°C for 5 hours. In the case of metalloprotease inhibition, cells were kept under 10 μM Batimastat for an additional 5 hours (24 hours total) in the presence of radiolabeled 13A9. Surface bound antibody was removed with an acid strip solution and triplicate wells were quantified using a Gamma counter. Parallel plates were trypsinized and counted using a Vi Cell XR to determine the average number of cells per well. The experiment was repeated on a separate day to confirm results and surface receptor numbers are reported here as an average per cell measured in triplicate wells on a single day.

3.2.5 EGFR and ERK phosphorylation

Cells were plated in 6-well plates at 150,000 cells/well. Cells were starved in serum-free media for 16 hours, treated as described in figure legends, rinsed once with cold PBS, and subsequently scraped in lysis buffer, prepared as previously described (Janes et al., 2003) for western blotting or in Phosphoprotein Lysis Buffer (Bio-Rad) for the Luminex assays. Lysates were incubated on ice for 10 minutes and then centrifuged at 14,000 rpm for 10

minutes at 4°C. The supernatants were frozen at -80°C until use. Lysates were analyzed using a bicinchoninic assay (Pierce) to determine the total protein concentration. For western blotting, equal amounts of total lysate protein were diluted in lysis buffer and 4X sample buffer and run on 7.5% gels and transferred to PDVF membranes (Bio-Rad) before blocking with 5% BSA in TBS-T and incubating membranes overnight at 4°C with a primary p44/42 ERK antibody (Cell Signaling). The membranes were stripped and reprobed for total ERK (Cell Signaling). For the Luminex assays, which are quantitative immunoprecipitation bead-based assays, lysates were diluted in Bio-Rad Lysis Buffer and Bio-Rad Assay Buffer to a final protein concentration of 150 ug/ml (7.5 ug of protein per well). Linearity of the pTyrEGFR and pERK 1/2 Bio-Rad assays was checked using varying ratios of mixed lysate from EGF stimulated and unstimulated parental cells (see Figure 3.5.2) and results were used to determine the optimal loading per well. Phospho-tyrosine EGFR and phosphorylated ERK 1/2 (Thr²⁰²/Tyr²⁰⁴, Thr¹⁸⁵/Tyr¹⁸⁷) were both measured using Bio-Rad phosphoprotein single-plex kits on a Luminex as per protocol (Bio-Rad).

3.2.6 Cell counting assay

To measure the relative growth rates, cells were plated in 6-well plates at a low initial density of 50,000 cells/well in regular DFCI-1 media. On day 2, cells were counted using a Vi Cell XR, and parallel plates were switched to either regular or serum-free media. Cells from different plates were then counted in triplicate at 24-hour intervals for a total of 3 days in each media. ECT and TCT

cell growth was similar under both media conditions and data is shown comparing relative growth rates of autocrine-stimulated proliferation in serum-free media to parental cells. Growth rates were determined from an exponential fit.

3.2.7 Sparse-labeled monolayer migration assay

Single cell migration was measured from a cell monolayer using a modified high-throughput assay (Kumar et al., 2006); see Fig. 3.5.3. A confluent plate of cells was incubated with 8 mM of a fluorescent cell tracker dye, CMFDA (Invitrogen), for 25 minutes at 37°C, rinsed with PBS and then trypsinized along with a parallel plate of unlabeled cells. Cells were counted with a Vi Cell XR, mixed at a ratio of 1:10 labeled to unlabeled cells, and plated at 40,000-50,000 cells per well in a 96-well plate (Packard) in DFCI-1 complete media. The optimal cell density to obtain a non-overcrowded confluent monolayer was determined by plating increasing numbers of cells under the same conditions and visualizing cell density with a bright field microscope (data not shown). After 4 hours, cells were switched to 100 ul of serum-free media. After 15 hours, media was switched to 100 ul of serum-free media with or without stimulation. MEK inhibition involved a 30-minute pre-incubation with PD98059 (0.04, 0.2, 1, 5, and 25 μ M) prior to stimulation (see Fig. 3.5.12 legend). Fluorescent images were acquired using a Cellomics KineticScan at 15-minute intervals for 6-8 hours. Image files were exported to Imaris for cell tracking and dynamic cell coordinates were analyzed in Matlab. All cell paths lasting the duration of the experiment

were included in the analysis. We report the average cell speed and standard error of the mean for a minimum of 200 cells measured from multiple wells per condition. Cell persistence was determined from a fit to the persistent random walk equation described in Chapter 5. Cell persistence measurements were not a focus of this chapter due to the inherent cell-cell contacts in the monolayer assay.

3.3 Results

3.3.1 EGF chimeras and metalloprotease inhibition quantitatively tune autocrine ligand release rates

In this study we have chosen two EGF chimeras that encode different regulation at the cell surface to investigate the effects of ligand release on cell signaling and migration. In addition to the previously described membrane bound EGF ligand named ECT (in previous reports termed EGF-ct, EGF cytoplasmic tail), we constructed an EGF chimera that contains the transmembrane and cytoplasmic domains of TGF α , named TCT (TGF α cytoplasmic tail) (see Fig. 3.5.1). We verified TCT was correctly processed into EGF at the correct cleavage sites by mass spectrometry of immunoprecipitated ligand (data not shown). In both ECT and TCT, the core ligand arises from the physiological EGF ligand. Ligand release was measured from conditioned media at 2-hour time intervals for 8 hours and normalized to cell number. The EGF concentration was then measured using an ELISA. The slope of the accumulation estimates the rate of ligand release on a per cell per minute

basis. Minimal accumulation of EGF in ECT conditioned media was measured over 8 hours (Fig. 3.5.4). However, in the presence of 225, an EGFR blocking monoclonal antibody, the rate of EGF accumulation increased from approximately 20 to 600 molecules released per cell per minute. This suggests that the ECT cells capture most of the EGF that is cleaved from the cell surface. In contrast, the TCT cells had a 10-fold higher rate of release in serum-free media alone. Thus, the two different EGF chimeras give us “coarse-grained tuning” of autocrine ligand release rates.

Next, we added a protease inhibitor at increasing concentrations in order to “fine-tune” the ligand release rate across a quantitative spectrum. We used batimastat, an inhibitor of zinc-containing metalloproteases, because of its demonstrated efficiency in blocking the shedding of EGFR ligands from cells (Dong et al., 2005). We found that the IC₅₀ value of batimastat for the release of EGF from the TCT cells was 0.33 μ M (Fig. 3.5.4B). Adding increasing concentrations of batimastat lowered the linear rate of accumulation of EGF in the media over 8 hours (Fig. 3.5.4C). Therefore, we can use both EGF constructs as well as the addition of Batimastat to modulate the rate EGF release in quantitative manner across a spectrum of rates.

3.3.2 Increasing autocrine release rates downregulate surface EGFR levels but increases levels of active EGFR

The addition of exogenous EGF has been shown to downregulate receptor levels on the cell surface in culture (Hendriks et al., 2003). To determine the effects of the EGF release on surface receptor levels we

measured steady-state binding of ^{125}I -labeled 13A9, a non-competitive EGFR monoclonal antibody, after 5 hours in the presence or absence of 2 nM exogenous EGF in the different cell lines (Hendriks et al., 2003). We confirmed receptor downregulation of the parental cells incubated with exogenous EGF (Fig. 3.5.5A). The ECT and TCT cells displayed lower levels of surface receptors than control cells, even in the absence of exogenous ligand. The addition of soluble EGF, however, reduced the receptor level of all cells to the same final degree (Fig. 3.5.5A). The TCT cells displayed the lowest steady state levels of EGFR, which were only marginally influenced by exogenous ligand addition. TCT surface receptor levels increased when incubated in 10 μM Batimastat, suggesting that the downregulation was indeed dependent on the ligand release.

Given this substantial degree of EGFR downregulation from autocrine signaling, it could be anticipated that the level of active EGFR would be similarly decreased. To examine the net outcome of the counteracting higher ligand levels versus lower receptor levels, we measured EGFR tyrosine phosphorylation using the BioPlex quantitative immunoprecipitation bead-based assay. As shown in Fig. 3.5.5B, despite the decrease in surface EGFR the level of phosphorylated EGFR was enhanced at greater ligand levels. Thus, receptor activation increases with increasing autocrine ligand release rates.

3.3.3 Autocrine signaling leads to steady ERK activation

We next sought to determine how a key downstream signal varied with autocrine ligand release rate, in concert with the asymptotic increase in EGFR

activation. Autocrine presentation led to elevated phosphorylation levels of the main EGFR-induced MAP kinase, ERK 1/2, measured by western blot over an 8-hour time course following 16 hours of serum-starvation (see Fig. 3.5.6A). ERK1/2 phosphorylation dynamics was determined using the BioPlex assay. The medium was spiked with EGF to a final concentration of 2 nM EGF or switched to serum-free media containing 225 EGFR blocking antibody for 2 hours prior to washing and replacing with fresh serum-free media. Although the parental cells exhibit dramatic phospho-ERK dynamics after EGF stimulation, the ECT and TCT cells show phosphorylated ERK that is only briefly and mildly increased in the presence of exogenous EGF before returning to basal levels (Fig. 3.5.6B). Incubation with the receptor-blocking 225 monoclonal antibody for 2 hours abolished ERK phosphorylation in the autocrine cells. After removal of 225, several washes, and adding fresh serum-free media, ERK phosphorylation steadily increased due to autocrine presentation over a two-hour period before reaching initial levels. Phospho-ERK1/2 measured 2 hours after addition of varying batimastat concentrations was found to be an asymptotically increasing function of autocrine ligand release rate (Fig. 3.5.6C).

3.3.4 Autocrine presentation induces normal proliferation but enhanced migration

In order to determine how phenotypic cell behaviors might depend on the rate of autocrine ligand release, and whether they might differ for chronic (autocrine) versus acute (exogenous) stimulation, we measured cell proliferation and cell migration responses in our system. Cells were counted under the low

and high ligand release rates and compared to parental cells in regular DFCI-1 culture media containing 2nM EGF. The relative growth rates, calculated from an exponential fit to the growth kinetics, were found to be essentially invariant: 3.7, 3.6, and 3.2 % increase/hour for the parental, ECT, and TCT cells respectively (Fig. 3.5.7). Thus, while these cells are dependent on EGF for cell growth, the increased levels of autocrine signaling induced by the ligand chimeras did not increase this growth over the control levels.

Cell migration was measured using high-throughput imaging of multiple individual cells within a monolayer. This assay monitors the movement of a population of confluent cells while capturing cell-to-cell variation. This is likely a more physiologically relevant situation than dispersed, low-density single-cell tracking, because of the importance of cell-cell interactions in tissue. After cells were starved for 15 hours, cells were switched to fresh serum-free media with or without exogenous EGF, batimastat, or 225 antibody. After equipment set up, cells were monitored with a Cellomics KineticScan for 6 to 8 hours with images acquired every 15 minutes. EGF stimulation increased parental cell migration in a dose-dependent manner, but the ECT and TCT cells exhibited even more vigorous motility (Fig. 3.5.8A). Population averaged values of cell speed were determined from the individual cell paths under the various experimental conditions (>200 paths were analyzed in each case), and Figure 3.5.8B shows that the trends observed in Figure 3.5.8A are quantitatively valid. In addition, Figures 3.5.8B,C show that the high migration speeds induced by autocrine ligand stimulation are reduced by treatment with 10ug/ml 225 mAb and 10 μ M

batimastat, as expected. Interestingly, exogenous EGF did not significantly enhance the autocrine ligand-induced cell motility, possibly due to the relatively unaltered ERK phosphorylation under these conditions (Fig. 3.5.8B). Monitoring the migration speed values as a function of time shows that in all cases the trends explicated in Figure 3.5.8 are maintained throughout the experiment; moderate reduction occurs for all conditions most likely due to mild cytotoxic effects of the cell tracker dye (see Fig. 3.5.9).

Autocrine ligand presentation also appeared to yield increased cell persistence (see Fig. 3.5.10). However, persistence effects are difficult to interpret in the confluent monolayer assay because of the inherent continuous cell-cell interactions.

3.3.5 Cell migration speed is proportional to pERK1/2 as autocrine ligand release rate is varied

Given the concomitant increases in ERK1/2 phosphorylation levels and cell migration speed as autocrine EGF release rate is increased, we sought to ascertain the critical nature of this relationship. Figure 3.5.11A shows migration speed against phospho-ERK1/2 levels for the parental, ECT, and TCT cells. Migration speed varied in linear fashion with phospho-ERK1/2 for the autocrine (ECT, TCT) cells as well as for the parental cells, but the slope of this relationship is much greater for the autocrine-induced cells relative to exogenous-stimulated parental cells. Even though exogenous-stimulated parental cells can generate phospho-ERK1/2 levels as high as or higher than the

autocrine-induced cells, the former cannot attain nearly as great a migration speed.

In order to test whether these differential ERK-migration relationships are merely correlative or are causative, the cells were treated with a spectrum of concentrations of PD98059, a MEK inhibitor, under both exogenous and high autocrine stimulation. The quantitative dose-response relationships for both phospho-ERK and migration speed as functions of inhibitor concentration are shown in Figure 3.5.12. As shown in Figure 3.5.11B, in which the resulting migration speeds are plotted against the corresponding phospho-ERK values, the same diverse linear relationships were obtained. Therefore, cell migration speed depends critically on the phospho-ERK level in a linear manner, for both autocrine and exogenous control but with a significantly stronger dependence for the former than the latter.

3.4 Discussion

EGFR family signaling plays a key role in governing multiple cell phenotypic behaviors, including proliferation, migration, and differentiation, and is critically involved in key tissue physiological processes (Wells, 1999). Its dysregulation is associated with various pathologies including tumor progression (Condeelis et al., 2005; Wells, 2000); Normanno et al., 2006), and it is considered to be a broadly useful therapeutic target system for cancer and other diseases (Bublil and Yarden, 2007; Coffey et al., 2007; Johnston et al., 2006). The vast preponderance of basic science and clinical application studies has

focused on the receptors and downstream signaling pathways, as a locus for control of pathophysiological cell behavior. Now, however, the important but highly complex nature of ligand control in the EGFR system is beginning to be appreciated (Carpenter, 2000; Harris et al., 2003; Singh and Harris, 2005). In the realm of tumor progression, enhanced production of EGF autocrine ligands has been found to be associated with the HER2/neu oncogene expression in mammary epithelial cells (Seton-Rogers and Brugge, 2004; Seton-Rogers et al., 2004). Furthermore, high levels of co-expression of an EGFR autocrine ligand and the metalloprotease that releases it at the cell surface to enable receptor binding were found to be strongly predictive of poor prognosis across a set of primary breast tumors, with inhibition of ligand release yielding reversion of a malignant phenotype (Kenny and Bissell, 2007).

Although information has been gathered concerning regulation of autocrine ligand release by ligand structural features and metalloprotease identities (Sahin et al., 2004; Dong et al., 2005; Ohtsu et al., 2006), little is understood about how the protease-mediated ligand release rate quantitatively governs receptor-mediated signaling and consequent cell behavior. Even such a basic foundational point as the simple “dose-response” dependencies of receptor downregulation, downstream signaling, and phenotypic cell functions on autocrine ligand release rate have not been established for endogenous ligand stimulation, despite the centrality of this kind of information to subsequent analysis of underlying regulatory mechanisms. Moreover, there has been little exploration in the cell biology field of potential differences between cell

behavioral responses induced by the common but likely artifactual “acute” stimulation by exogenous ligand treatment versus those arising from the more likely physiological (but much more difficult to generate experimentally) “chronic” stimulation by endogenous ligand.

In order to begin addressing this dearth of understanding, we developed a set of EGFR ligand chimeras that vary in their transmembrane and cytosolic anchor regions (‘ECT’ and ‘TCT’; see Fig. 3.5.1) to “coarse-grain tune” EGF autocrine ligand release rate with accompanying “fine-tuning” by the metalloprotease inhibitor batimastat. The ECT construct, containing both the ligand and membrane-anchoring domain of the native EGF ligand, shows very low accumulation in the extracellular media. Blocking the EGF receptor with a monoclonal antibody leads to a significant increase (though still to a relatively low absolute level) in ligand accumulation (Fig. 3.5.4A), suggesting that the ECT cells operate in an autocrine mode where most of the ligand released by the cells is captured before diffusing into the media. While keeping the EGF receptor-binding domain of the ligand constant to ensure similar binding and receptor dynamics, we varied the membrane proximal region and cytoplasmic tail to alter protease specificity. Changing the membrane-anchoring domain and protease cleavage site to a TGF α based construct (TCT) led to a 10-fold increase in ligand release rate (Fig. 3.5.4A). Due to this dramatic difference in ligand release dynamics, we were able to further decrease the high ligand release with increasing concentrations of batimastat (see Figs 3.5.4B,C). With this system we

could rigorously investigate how varying the rate of ligand release affects receptor signaling and behavioral responses.

A first step was to examine proximal receptor downregulation and activation as a function of ligand release rate. While receptor downregulation has been previously measured in the hMEC cell line in the presence of exogenous EGF, we find here that increasing ligand release rates lead to decreasing surface receptor levels (Fig. 3.5.5A). The ECT cells have sub-saturating receptor downregulation that can be further downregulated with exogenous EGF, while the TCT cells have sustained low levels of surface receptors that are not further reduced by additional exogenous EGF treatment. These quantitative surface receptor measurements suggest that the ECT cells are not saturated with ligand while the TCT cells are producing saturating concentrations of EGF. However, we found that decreasing total numbers of cell surface receptors levels were correlated with enhanced EGFR activation (Fig. 3.5.5B). This is consistent with the idea that the occupancy-induced internalization of the EGFR, which leads to downregulation, is a mechanism to enhance ligand capture rather than attenuate signaling (Wiley et al., 2003).

Downstream of the EGF receptor, both the ECT and TCT cells have sustained ERK phosphorylation and respond only briefly to exogenous EGF stimulation (Figs 3.5.6A,B). After 1 hour the ECT and TCT cells return to their steady levels of ERK phosphorylation, while the parental cells achieved much higher levels of activation that remain above autocrine levels at 2 hours of stimulation. After blocking the autocrine activation for 2 hours with the 225

antibody, EGFR tyrosine phosphorylation (Fig. 3.5.13) and ERK phosphorylation steadily increase (Fig. 3.5.6B). Autocrine stimulation never leads to the high peaks or ephemeral dynamics characteristic of acute exogenous stimulation, even at the highest ligand release rates. It is conceivable that acute treatment with high concentrations of exogenous EGF could generate negative feedback mechanisms on EGFR signaling (Amit et al., 2007), such as Mig6 (Ferby et al., 2006) – which perhaps might not be generated by the gradual activation arising from chronic endogenous ligand release and receptor binding. Alternatively, this dynamic “overshoot” from an initial stimulus treatment toward relaxation to an ultimately “steady-state” could arise from a quantitative mis-match of receptor/ligand binding rates versus signal activation and deactivation rates (Resat et al., 2003).

Under increased autocrine presentation we found that normal cell proliferation was not altered by ligand release rate or presentation mode (Fig. 3.5.7), but in contrast we found significant effects on cell migration behavior (Fig. 3.5.8). Migration speed was shown to quantitatively depend on ligand release rate. Furthermore, we found that migration speed appears to depend in linear manner on ERK phosphorylation – whether modulated by increasing ligand release rate (Fig. 3.5.11A) or by increasing the concentration of the MEK inhibitor PD98059 (Fig. 3.5.11B). ERK is known to critically regulate key biophysical processes underlying cell migration (Brahmbhatt and Klemke, 2003; Glading et al., 2001; Huang et al., 2004). Importantly, however, the migration behavior of cells driven by autocrine, or “chronic” EGF stimulation and those driven by

exogenous, or “acute” EGF stimulation, separate clearly onto disparate curves in the speed-versus-pERK “dose-response” plot (Fig. 3.5.11). The cells driven by autocrine ligand attain much higher migration speeds than those driven by exogenous ligand for any given level of ERK phosphorylation. This finding suggests that the EGFR signaling network activity more broadly, beyond the ERK pathway, might be more effectively optimized for inducing migration when under autocrine ligand control compared to exogenous ligand treatment. A mass spectrometry study of EGFR system signaling related to migration of these same 184A1 human mammary epithelial cells indicates a large number of pathways to be significantly implicated (Wolf-Yadlin et al., 2006). Potentially, future studies could test whether key negative regulators operating within this network (Amit et al., 2007) might become more activated during the signaling “overshoots” under acute exogenous treatment compared to chronic autocrine stimulation. Perhaps lower, but steady signaling results in optimal, coordinated cell motility, while exogenous stimulation leads to transient receptor and signaling downregulation that could impede cell migration. Recall, however, that significant divergence between autocrine and exogenous ligand effects were not found for cell proliferation responses in this system; thus, different phenotypic behaviors appear to be diversely influenced by the mode of ligand presentation. In any event, the kind of rigorously quantitative dose-response capabilities that we have established here should play a vital role in examining molecular pathway regulatory mechanisms in future studies.

3.5 Figures

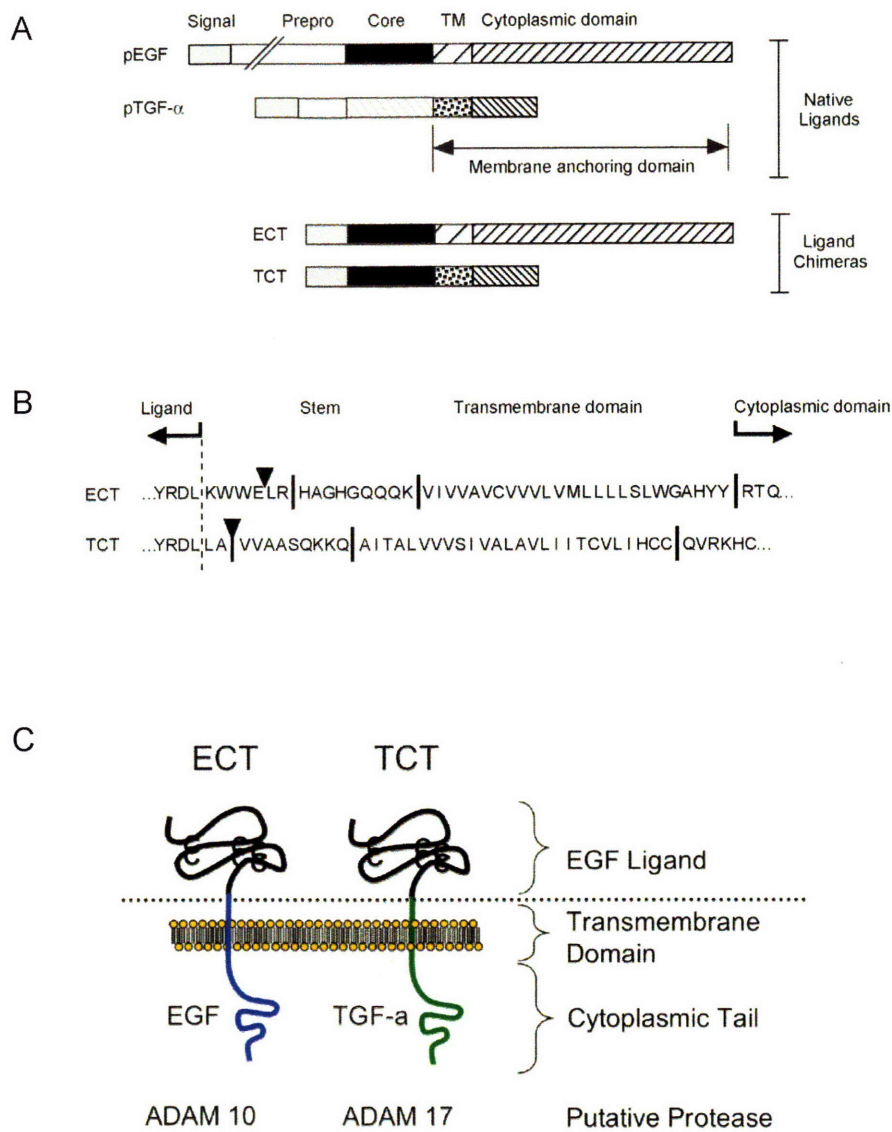


Figure 3.5.1. EGF ligand chimera constructs from the Wiley lab. (A) EGFR ligands are synthesized as integral membrane proteins that have variable membrane anchoring domains. Chimeras containing the receptor-binding domain of EGF (core) attached to the stem, transmembrane domain (TM), and cytoplasmic domain of either EGF or TGF α were constructed as shown. (B) Amino-acid sequence of each chimera showing published cleavage site (filled arrowhead). (C) Schematic of ECT and TCT constructs.

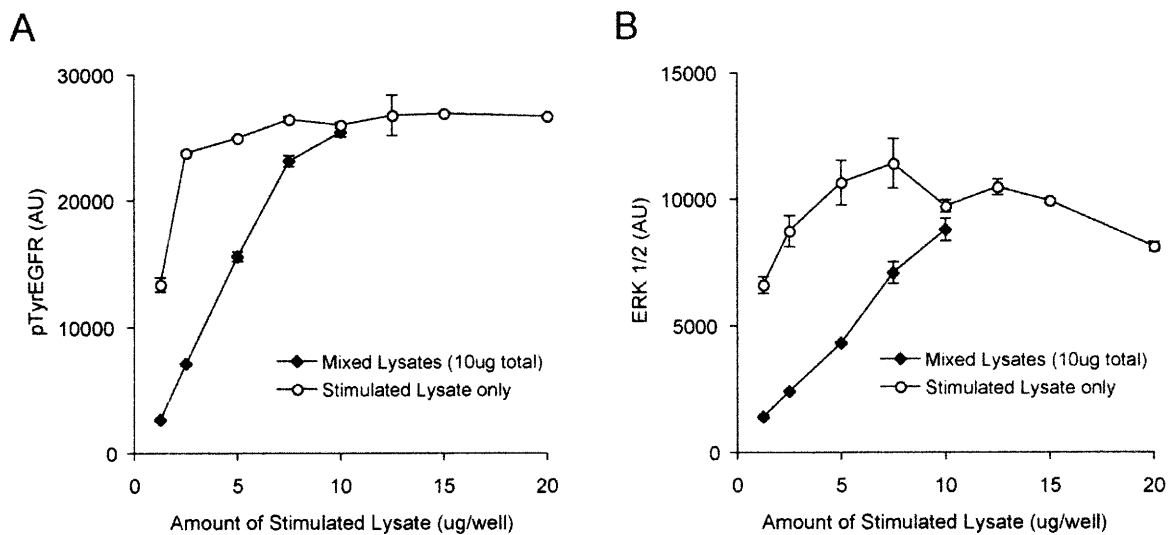


FIGURE 3.5.2. pERK1/2 and pTyrEGFR BioPlex assay development. The phospho-tyrosine EGFR and phospho-ERK 1/2 assays were checked for linearity using two approaches. First, lysate from a stimulated parental sample was loaded in increasing amounts. Second, stimulated lysate was mixed at various ratios with an unstimulated lysate, keeping the amount of total protein constant at 10 μ g per well. Varying the fraction of stimulated lysate showed linearity for both the (A) pTyrEGFR and (B) pERK 1/2 assays, indicating the extent of phosphorylation can be quantitatively determined.

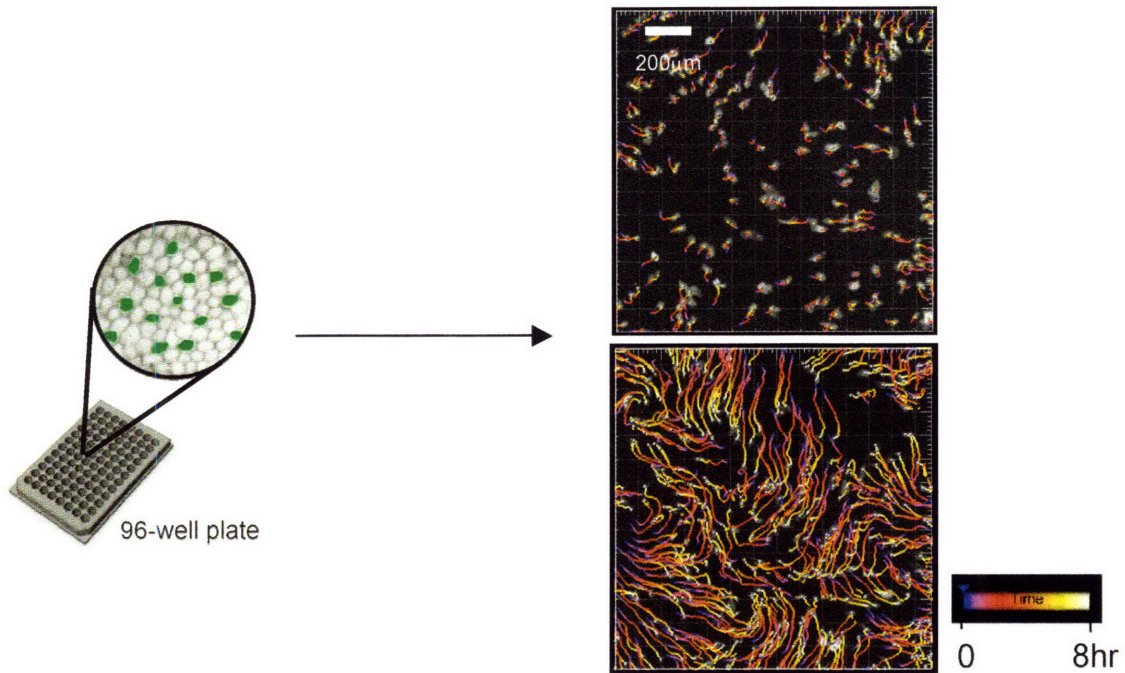


Figure 3.5.3. Sparse-labeled monolayer cell migration assay.

Fluorescently labeled cells were plated 1:10 with unlabeled cells in a 96-well plate. Images were acquired at 15-minute intervals for 6-8 hours using a Cellomics KineticScan. Labeled cells within the monolayer were tracked using Imaris. A single field is shown and individual cell paths are displayed as a function of time. The two images shown are each from a separate experimental condition; one showing non-migratory cells and the other showing stimulated motility. Scale bar: 200 μm .

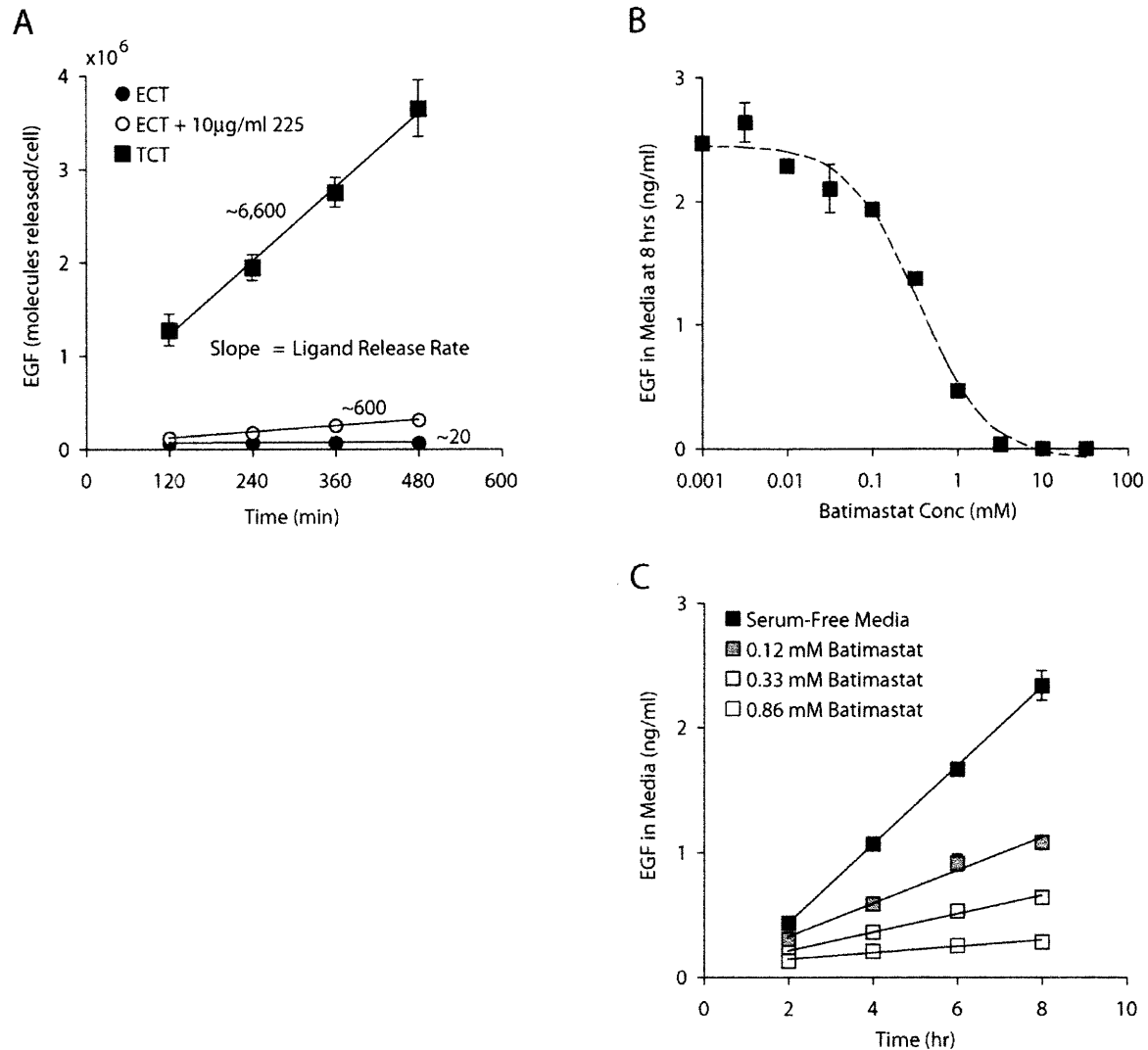


Figure 3.5.4. TCT construct has 10-fold higher release rate that is decreased with batimastat. (A) Ligand release rate is measured from the slope of EGF accumulation over time. After 16 hours in serum-free media, cells were switched to fresh serum-free media or media containing an inhibitor and samples were collected at 2-hour time intervals from triplicate wells. EGF concentration was measured using an EGF ELISA. The approximate ligand release rates (molecules of EGF released/cell/minute), verified in independent experiments, are shown next to each linear fit. (B) TCT release into the media over an 8-hour time period is inhibited using increasing concentrations of Batimastat. Fitting the conditioned EGF concentration to a dose-response curve reveals a median inhibition concentration of 0.33

μM Batimastat. (C) Adding increasing concentrations of Batimastat down modulates the linear ligand release of TCT cells. Error bars represent one s.d. from the mean of triplicate samples.

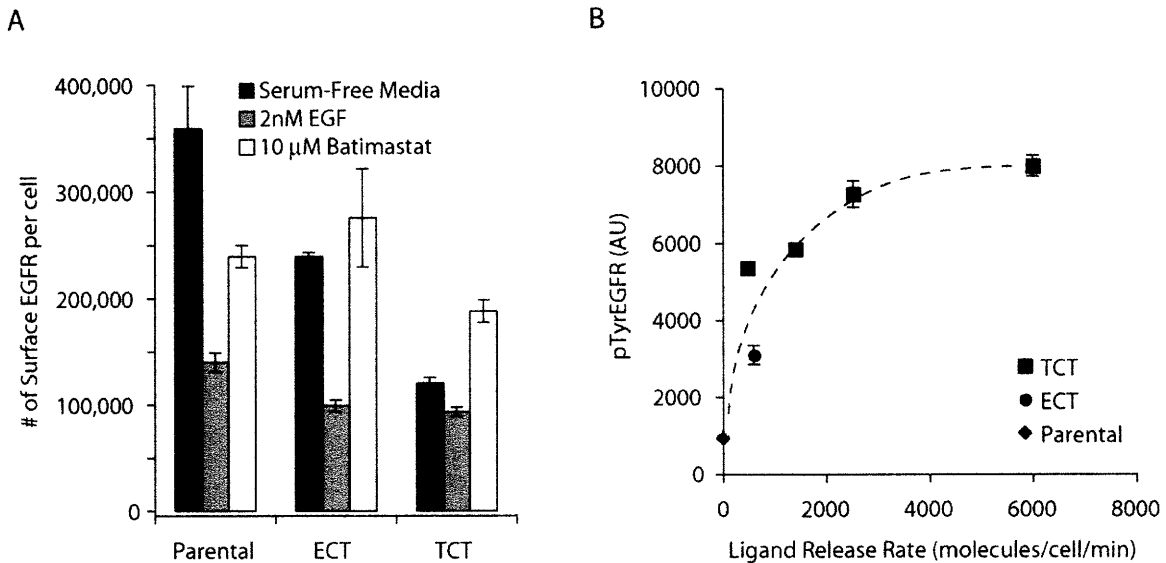


Figure 3.5.5 Autocrine signaling leads to surface EGFR downregulation and tyrosine phosphorylation in a ligand release rate dependant manner. (A) Surface receptor numbers were quantified using an equilibrium-binding assay with 125 I labeled 13A9 mAb followed by an acid strip and counting on a gamma counter. Cells were serum-starved overnight before incubating the cells in fresh serum-free media containing labeled 13A9 alone (black bars) or with 2 nM exogenous EGF (grey bars) for 5 hours, as described in “Materials and Methods”. In addition, cells were starved in the presence of 10 μ M Batimastat to block ligand shedding for 24 hours prior to receptor counting (white bars). Receptor numbers were normalized to the average cell number counted from parallel plates. Error represents one s.d. from the mean of triplicate wells. (B) Phospho-EGFR levels were measured using a quantitative immunoprecipitation bead-based Tyrosine EGFR BioRad Bio-Plex phosphoprotein detection assay. Parental, ECT, or TCT cells were switched to fresh serum-free media for 2 hours and then lysed. In addition, TCT cells were incubated with increasing concentrations of Batimastat (0.12, 0.33, and 0.86 μ M) to achieve additional release rates. Error represents one s.d. from the mean of triplicate lysates.

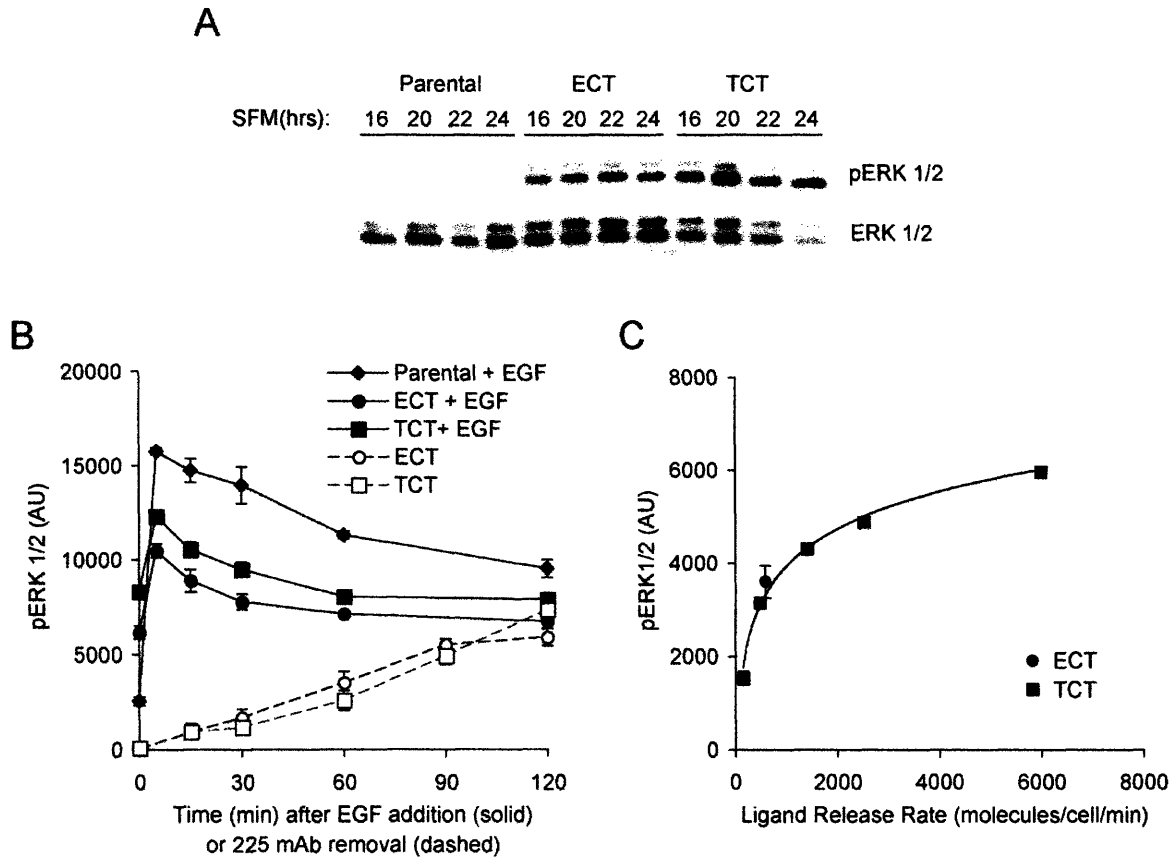


Figure 3.5.6. Autocrine stimulation leads to sustained ERK phosphorylation.

(A) Phosphorylation of ERK 1/2 measured over an 8-hour time course. Cells were incubated in serum-free media and lysed at the indicated time points. Blots were stripped and reprobbed for total ERK 1/2. (B) Phospho-ERK dynamics measured using a quantitative immunoprecipitation bead-based ERK1/2 BioRad Bio-Plex phosphoprotein detection assay. Cells were spiked with 2 nM exogenous EGF (filled circles, squares and diamonds) or blocked with 10 μ g/ml of 225 for two hours prior to 3 PBS washes and serum-free media replacement (empty circles and squares). Error represents one s.d. from the mean of triplicate lysates. (C) ERK phosphorylation was measured from triplicate lysates after two hours in serum-free media. In addition, TCT cells were incubated in Batimastat (0.12, 0.33, 0.86, and 10 μ M) to achieve additional release rates. Error represents s.d. of triplicate lysates.

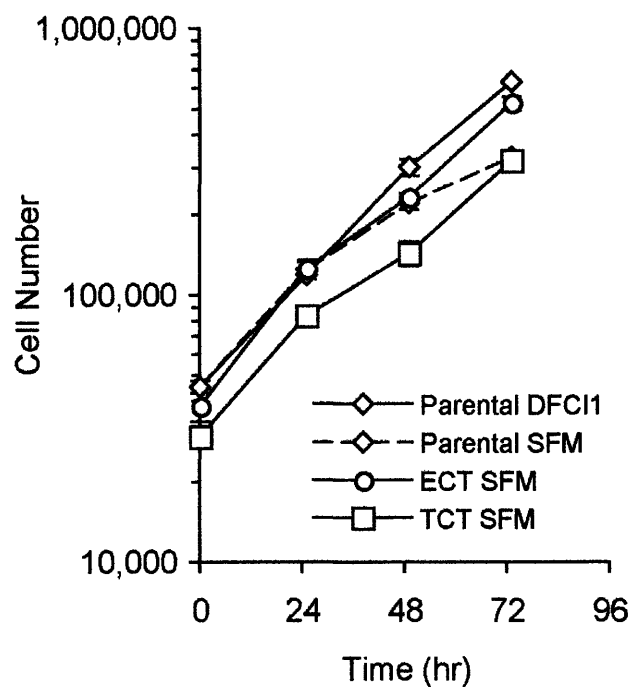


Figure 3.5.7 Autocrine presentation stimulates normal cell proliferation. Cell growth rates were measured by cell counting with a Vi Cell XR. Cell number was measured over three days in regular DFCI-1 media or Serum-Free Media (SFM). Error represents standard deviation of triplicate measurements.

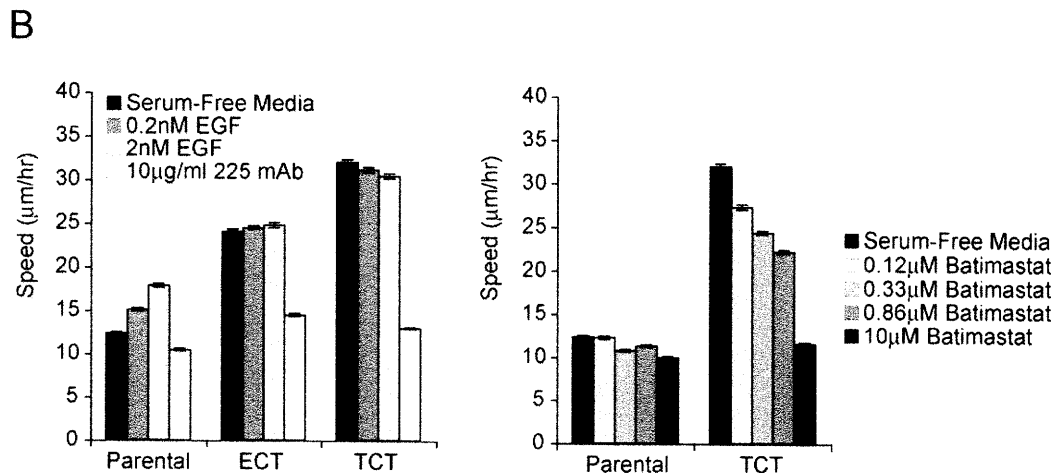
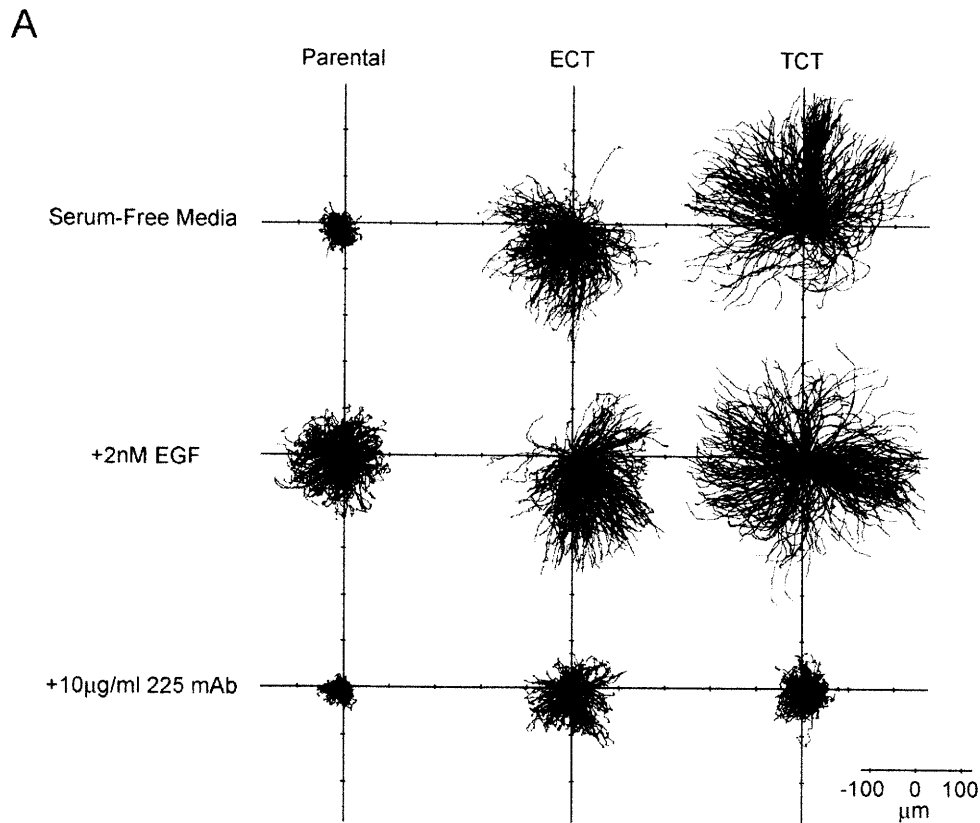


Figure 3.5.8. Autocrine stimulation leads to elevated cell migration speed. Cell migration was measured in a sparse-labeled monolayer high throughput assay. Parental, ECT, and TCT cells were starved for 15 hours and then switched to fresh serum-free media, 0.2 nM EGF, 2 nM EGF, 10 µg/ml 225 mAb, or batimastat (0.12, 0.33, 0.86, or 10 µM), approximately 1 hour before imaging. Fluorescence images were acquired at 15-minute intervals for 8 hours and imported in Imaris for single cell tracking of the labeled cells. Cell paths were analyzed in Matlab. (A) Cell paths are shown starting at each origin. (B) Average cell migration speed under each condition. Error represents s.e.m. and N >200 cells per condition.

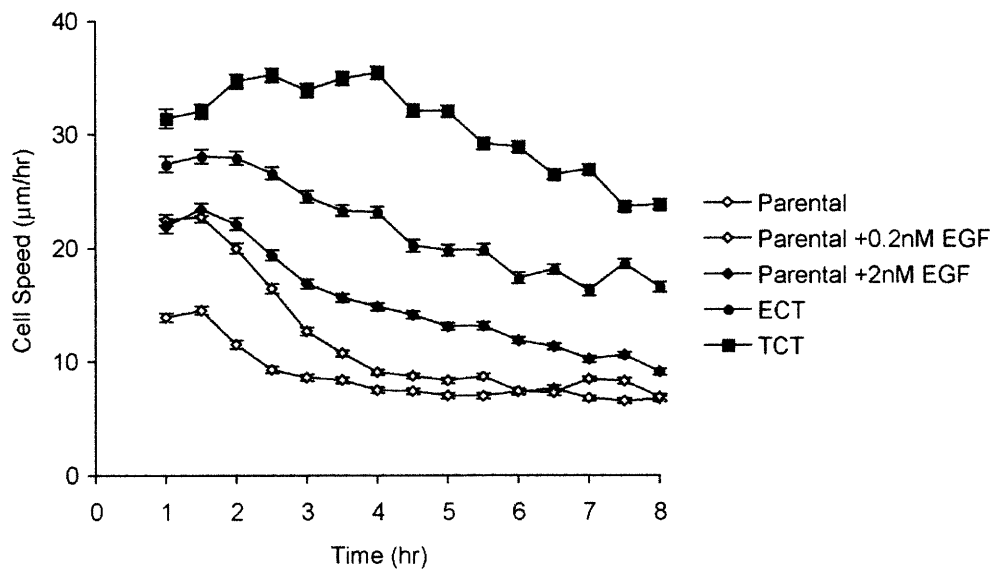


Figure 3.5.9. Cell migration speed during 30-minute intervals. Average cell speed was calculated at 30-minute time intervals. Parental, ECT, and TCT cells are shown under serum-free media conditions. In addition, the Parental cells are shown under 0.2 and 2 nM EGF stimulation. Error represents the s.e.m. of the mean calculated at each 30-minute interval and $N > 200$ for each condition.

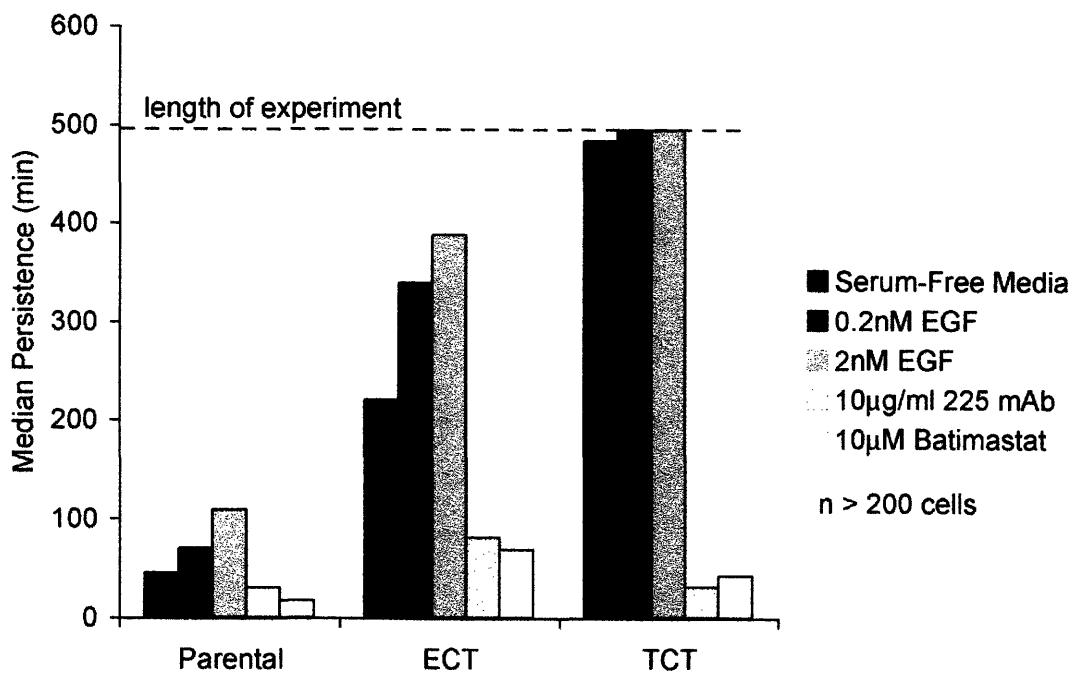


Figure 3.5.10. Cell persistence measured in the monolayer assay. Cell migration was measured in a sparse-labeled monolayer high throughput assay. Parental, ECT, and TCT cells were starved for 15 hours and then switched to fresh serum-free media, 0.2 nM EGF, 2 nM EGF, 10 µg/ml 225 mAb, or 10 µM batimastat, approximately 1 hour before imaging. Fluorescence images were acquired at 15-minute intervals for 8 hours and imported in Imaris for single cell tracking of the labeled cells. Cell paths were fit to the persistent random walk equation in Matlab. Median cell persistence under each condition (N >200 cells).

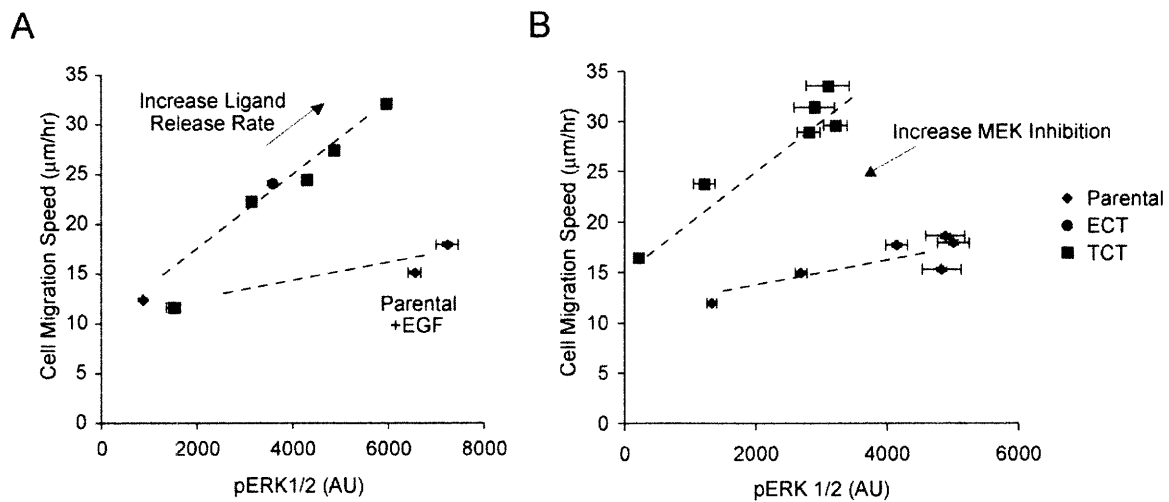


Figure 3.5.11. Cell migration speed is a function of ligand release rate and ERK phosphorylation. ERK phosphorylation was measured from triplicate lysates using a BioPlex assay. The parental cells were lysed after a 2-hour incubation with serum-free media or exogenous EGF (0.2, and 2 nM). In addition, TCT cells were lysed after a 2-hour incubation in serum-free media or increasing concentrations of batimastat (0.12, 0.33, 0.86, and 10 µM). (A) Cell migration speed (error represents s.e.m. from N >200 cells) is plotted as a function of ERK phosphorylation (error represents s.d. from triplicate lysates). (B) Parental and TCT cells were pre-incubated with multiple concentrations of the MEK inhibitor PD98059 (0.04, 0.2, 1, 5, and 25 µM) for 30 minutes. Parentals were then stimulated with 2 nM of EGF. Cell migration speed is shown as a function of ERK1/2 phosphorylation measured at 2 hours after exogenous stimulation.

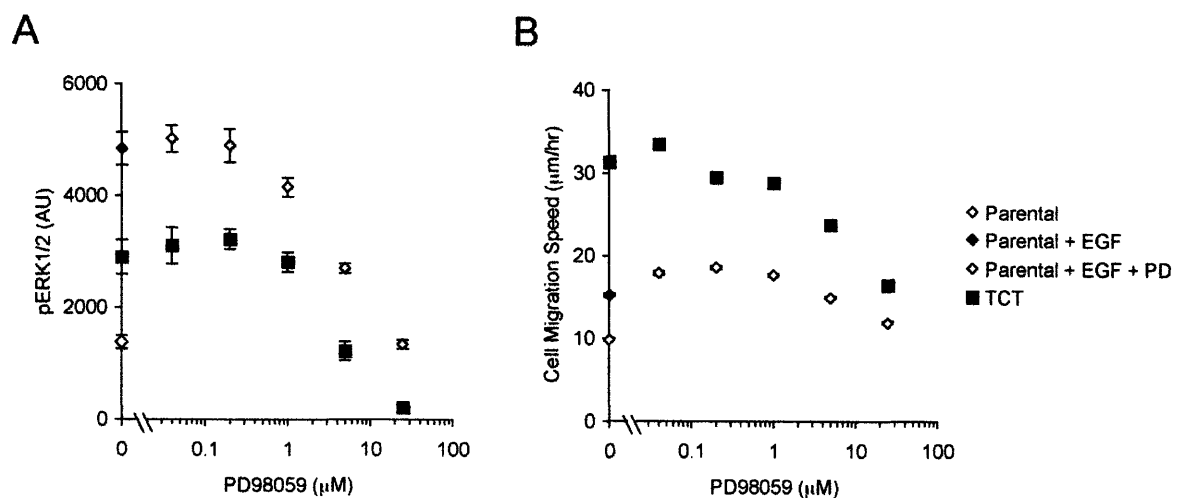


Figure 3.5.12. Quantitative dose-response relationships for phospho-ERK and migration speed as functions of inhibitor concentration. (A)

The level of ERK pathway inhibition was measured under increasing concentrations of the MEK inhibitor PD98059. Phospho-ERK 1/2 was measured in the Parental and TCT cells using the pERK 1/2 BioPlex assay. Cells were incubated with increasing concentrations of PD98059 for 30 minutes and then either switched to fresh serum-free media containing the inhibitor alone (TCT cells) or stimulated with 2 nM exogenous EGF (Parental cells). Two hours after the media change or stimulation, cells were lysed. Average of measurements from triplicate lysates are shown and error represents s.d. (B) The average cell migration speed is shown under the same levels of MEK inhibition. Error represents s.e.m and N>200 per condition.

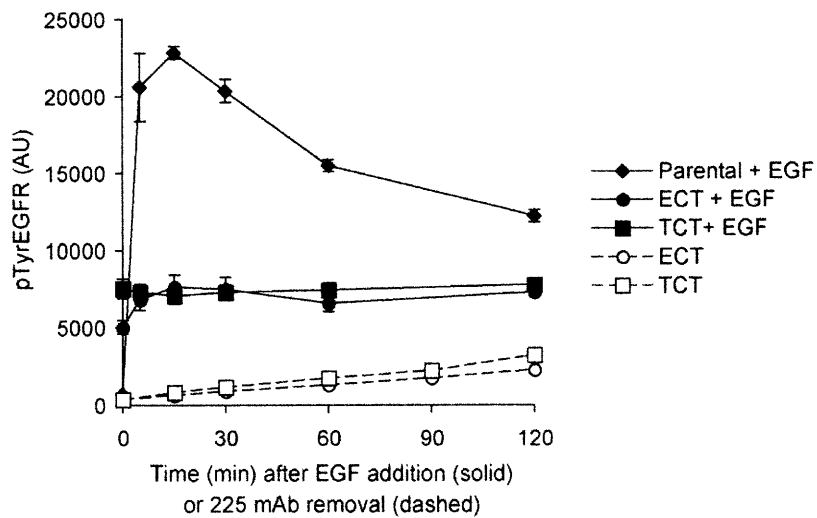


Figure 3.5.13. Phospho-tyrosine EGFR dynamics. Phospho-tyrosine EGFR dynamics measured using a quantitative immunoprecipitation bead-based pTyrEGFR BioRad Bio-Plex phosphoprotein detection assay. Cells were spiked with 2 nM exogenous EGF (filled circles, squares and diamonds) or blocked with 10 μ g/ml of 225 for two hours prior to 3 PBS washes and serum-free media replacement (empty circles and squares). Error represents one s.d. from the mean of triplicate lysates.

3.6 References

- Amit, I., A. Citri, T. Shay, Y. Lu, M. Katz, F. Zhang, G. Tarcic, D. Siwak, J. Lahad, J. Jacob-Hirsch, N. Amariglio, N. Vaisman, E. Segal, G. Rechavi, U. Alon, G.B. Mills, E. Domany, and Y. Yarden. 2007. A module of negative feedback regulators defines growth factor signaling. *Nat Genet.*
- Arribas, J., F. Lopez-Casillas, and J. Massague. 1997. Role of the juxtamembrane domains of the transforming growth factor-alpha precursor and the beta-amyloid precursor protein in regulated ectodomain shedding. *J Biol Chem.* 272:17160-5.
- Band, V., and R. Sager. 1989. Distinctive traits of normal and tumor-derived human mammary epithelial cells expressed in a medium that supports long-term growth of both cell types. *Proc Natl Acad Sci U S A.* 86:1249-53.
- Baselga, J., J. Mendelsohn, Y.M. Kim, and A. Pandiella. 1996. Autocrine regulation of membrane transforming growth factor-alpha cleavage. *J Biol Chem.* 271:3279-84.
- Borrell-Pages, M., F. Rojo, J. Albanell, J. Baselga, and J. Arribas. 2003. TACE is required for the activation of the EGFR by TGF-alpha in tumors. *Embo J.* 22:1114-24.
- Brahmbhatt, A.A., and R.L. Klemke. 2003. ERK and RhoA differentially regulate pseudopodia growth and retraction during chemotaxis. *J Biol Chem.* 278:13016-25.
- Bublil, E.M., and Y. Yarden. 2007. The EGF receptor family: spearheading a merger of signaling and therapeutics. *Curr Opin Cell Biol.* 19:124-34.
- Burke, P.M., and H.S. Wiley. 1999. Human mammary epithelial cells rapidly exchange empty EGFR between surface and intracellular pools. *J Cell Physiol.* 180:448-60.
- Carpenter, G. 2000. EGF receptor transactivation mediated by the proteolytic production of EGF-like agonists. *Sci STKE.* 2000:PE1.
- Coffey, R.J., M.K. Washington, C.L. Corless, and M.C. Heinrich. 2007. Menetrier disease and gastrointestinal stromal tumors: hyperproliferative disorders of the stomach. *J Clin Invest.* 117:70-80.
- Condeelis, J., R.H. Singer, and J.E. Segall. 2005. The great escape: when cancer cells hijack the genes for chemotaxis and motility. *Annu Rev Cell Dev Biol.* 21:695-718.

- DeWitt, A., T. Iida, H.Y. Lam, V. Hill, H.S. Wiley, and D.A. Lauffenburger. 2002. Affinity regulates spatial range of EGF receptor autocrine ligand binding. *Dev Biol.* 250:305-16.
- DeWitt, A.E., J.Y. Dong, H.S. Wiley, and D.A. Lauffenburger. 2001. Quantitative analysis of the EGF receptor autocrine system reveals cryptic regulation of cell response by ligand capture. *J Cell Sci.* 114:2301-13.
- Dong, J., L.K. Opresko, W. Chrisler, G. Orr, R.D. Quesenberry, D.A. Lauffenburger, and H.S. Wiley. 2005. The membrane-anchoring domain of epidermal growth factor receptor ligands dictates their ability to operate in juxtacrine mode. *Mol Biol Cell.* 16:2984-98.
- Eguchi, S., G.D. Frank, M. Mifune, and T. Inagami. 2003. Metalloprotease-dependent ErbB ligand shedding in mediating EGFR transactivation and vascular remodelling. *Biochem Soc Trans.* 31:1198-202.
- Fan, H., and R. Derynck. 1999. Ectodomain shedding of TGF- α and other transmembrane proteins is induced by receptor tyrosine kinase activation and MAP kinase signaling cascades. *Embo J.* 18:6962-72.
- Ferby, I., M. Reschke, O. Kudlacek, P. Knyazev, G. Pante, K. Amann, W. Sommergruber, N. Kraut, A. Ullrich, R. Fassler, and R. Klein. 2006. Mig6 is a negative regulator of EGF receptor-mediated skin morphogenesis and tumor formation. *Nat Med.* 12:568-73.
- Fischer, O.M., S. Hart, A. Gschwind, and A. Ullrich. 2003. EGFR signal transactivation in cancer cells. *Biochem Soc Trans.* 31:1203-8.
- Forsten, K.E., and D.A. Lauffenburger. 1992. Interrupting autocrine ligand-receptor binding: comparison between receptor blockers and ligand decoys. *Biophys J.* 63:857-61.
- Garton, K.J., N. Ferri, and E.W. Raines. 2002. Efficient expression of exogenous genes in primary vascular cells using IRES-based retroviral vectors. *Biotechniques.* 32:830, 832, 834 passim.
- Gill, G.N., T. Kawamoto, C. Cochet, A. Le, J.D. Sato, H. Masui, C. McLeod, and J. Mendelsohn. 1984. Monoclonal anti-epidermal growth factor receptor antibodies which are inhibitors of epidermal growth factor binding and antagonists of epidermal growth factor binding and antagonists of epidermal growth factor-stimulated tyrosine protein kinase activity. *J Biol Chem.* 259:7755-60.
- Glading, A., F. Uberall, S.M. Keyse, D.A. Lauffenburger, and A. Wells. 2001. Membrane proximal ERK signaling is required for M-calpain activation downstream of epidermal growth factor receptor signaling. *J Biol Chem.* 276:23341-8.

- Harris, R.C., E. Chung, and R.J. Coffey. 2003. EGF receptor ligands. *Exp Cell Res.* 284:2-13.
- Hendriks, B.S., L.K. Opresko, H.S. Wiley, and D. Lauffenburger. 2003. Coregulation of epidermal growth factor receptor/human epidermal growth factor receptor 2 (HER2) levels and locations: quantitative analysis of HER2 overexpression effects. *Cancer Res.* 63:1130-7.
- Huang, C., K. Jacobson, and M.D. Schaller. 2004. MAP kinases and cell migration. *J Cell Sci.* 117:4619-28.
- Ishikawa, N., Y. Daigo, A. Takano, M. Taniwaki, T. Kato, S. Hayama, H. Murakami, Y. Takeshima, K. Inai, H. Nishimura, E. Tsuchiya, N. Kohno, and Y. Nakamura. 2005. Increases of amphiregulin and transforming growth factor-alpha in serum as predictors of poor response to gefitinib among patients with advanced non-small cell lung cancers. *Cancer Res.* 65:9176-84.
- Janes, K.A., J.G. Albeck, L.X. Peng, P.K. Sorger, D.A. Lauffenburger, and M.B. Yaffe. 2003. A high-throughput quantitative multiplex kinase assay for monitoring information flow in signaling networks: application to sepsis-apoptosis. *Mol Cell Proteomics.* 2:463-73.
- Johnston, J.B., S. Navaratnam, M.W. Pitz, J.M. Maniate, E. Wiechec, H. Baust, J. Gingerich, G.P. Skliris, L.C. Murphy, and M. Los. 2006. Targeting the EGFR pathway for cancer therapy. *Curr Med Chem.* 13:3483-92.
- Kenny, P.A., and M.J. Bissell. 2007. Targeting TACE-dependent EGFR ligand shedding in breast cancer. *J Clin Invest.* 117:337-45.
- Kumar, N., M.H. Zaman, H.D. Kim, and D.A. Lauffenburger. 2006. A high-throughput migration assay reveals HER2-mediated cell migration arising from increased directional persistence. *Biophys J.* 91:L32-4.
- Lauffenburger, D.A., G.T. Oehrtman, L. Walker, and H.S. Wiley. 1998. Real-time quantitative measurement of autocrine ligand binding indicates that autocrine loops are spatially localized. *Proc Natl Acad Sci U S A.* 95:15368-73.
- Maheshwari, G., H.S. Wiley, and D.A. Lauffenburger. 2001. Autocrine epidermal growth factor signaling stimulates directionally persistent mammary epithelial cell migration. *J Cell Biol.* 155:1123-8.
- Maly, I.V., H.S. Wiley, and D.A. Lauffenburger. 2004. Self-organization of polarized cell signaling via autocrine circuits: computational model analysis. *Biophys J.* 86:10-22.

- Normanno, N., C. Bianco, A. De Luca, M.R. Maiello, and D.S. Salomon. 2003. Target-based agents against ErbB receptors and their ligands: a novel approach to cancer treatment. *Endocr Relat Cancer*. 10:1-21.
- Normanno, N., A. De Luca, C. Bianco, L. Strizzi, M. Mancino, M.R. Maiello, A. Carotenuto, G. De Feo, F. Caponigro, and D.S. Salomon. 2006. Epidermal growth factor receptor (EGFR) signaling in cancer. *Gene*. 366:2-16.
- Ohtsu, H., P.J. Dempsey, and S. Eguchi. 2006. ADAMs as mediators of EGF receptor transactivation by G protein-coupled receptors. *Am J Physiol Cell Physiol*. 291:C1-10.
- Pandiella, A., and J. Massague. 1991. Multiple signals activate cleavage of the membrane transforming growth factor-alpha precursor. *J Biol Chem*. 266:5769-73.
- Resat, H., J.A. Ewald, D.A. Dixon, and H.S. Wiley. 2003. An integrated model of epidermal growth factor receptor trafficking and signal transduction. *Biophys J*. 85:730-43.
- Sahin, U., G. Weskamp, K. Kelly, H.M. Zhou, S. Higashiyama, J. Peschon, D. Hartmann, P. Saftig, and C.P. Blobel. 2004. Distinct roles for ADAM10 and ADAM17 in ectodomain shedding of six EGFR ligands. *J Cell Biol*. 164:769-79.
- Salomon, D.S., R. Brandt, F. Ciardiello, and N. Normanno. 1995. Epidermal growth factor-related peptides and their receptors in human malignancies. *Crit Rev Oncol Hematol*. 19:183-232.
- Seton-Rogers, S.E., and J.S. Brugge. 2004. ErbB2 and TGF-beta: a cooperative role in mammary tumor progression? *Cell Cycle*. 3:597-600.
- Seton-Rogers, S.E., Y. Lu, L.M. Hines, M. Koundinya, J. LaBaer, S.K. Muthuswamy, and J.S. Brugge. 2004. Cooperation of the ErbB2 receptor and transforming growth factor beta in induction of migration and invasion in mammary epithelial cells. *Proc Natl Acad Sci U S A*. 101:1257-62.
- Shvartsman, S.Y., H.S. Wiley, W.M. Deen, and D.A. Lauffenburger. 2001. Spatial range of autocrine signaling: modeling and computational analysis. *Biophys J*. 81:1854-67.
- Singh, A.B., and R.C. Harris. 2005. Autocrine, paracrine and juxtacrine signaling by EGFR ligands. *Cell Signal*. 17:1183-93.
- Sporn, M.B., and G.J. Todaro. 1980. Autocrine secretion and malignant transformation of cells. *N Engl J Med*. 303:878-80.

- Stampfer, M.R., C.H. Pan, J. Hosoda, J. Bartholomew, J. Mendelsohn, and P. Yaswen. 1993. Blockage of EGF receptor signal transduction causes reversible arrest of normal and immortal human mammary epithelial cells with synchronous reentry into the cell cycle. *Exp Cell Res.* 208:175-88.
- Wells, A. 1999. EGF receptor. *Int J Biochem Cell Biol.* 31:637-43.
- Wells, A. 2000. Tumor invasion: role of growth factor-induced cell motility. *Adv Cancer Res.* 78:31-101.
- Wiley, H.S., S.Y. Shvartsman, and D.A. Lauffenburger. 2003. Computational modeling of the EGF-receptor system: a paradigm for systems biology. *Trends Cell Biol.* 13:43-50.
- Wiley, H.S., M.F. Woolf, L.K. Opresko, P.M. Burke, B. Will, J.R. Morgan, and D.A. Lauffenburger. 1998. Removal of the membrane-anchoring domain of epidermal growth factor leads to intracrine signaling and disruption of mammary epithelial cell organization. *J Cell Biol.* 143:1317-28.
- Wilsbacher, J.L., S.L. Moores, and J.S. Brugge. 2006. An active form of Vav1 induces migration of mammary epithelial cells by stimulating secretion of an epidermal growth factor receptor ligand. *Cell Commun Signal.* 4:5.
- Winkler, M.E., L. O'Connor, M. Winget, and B. Fendly. 1989. Epidermal growth factor and transforming growth factor alpha bind differently to the epidermal growth factor receptor. *Biochemistry.* 28:6373-8.
- Wolf-Yadlin, A., N. Kumar, Y. Zhang, S. Hautaniemi, M. Zaman, H.D. Kim, V. Grantcharova, D.A. Lauffenburger, and F.M. White. 2006. Effects of HER2 overexpression on cell signaling networks governing proliferation and migration. *Mol Syst Biol.* 2:54.
- Yarden, Y., and M.X. Sliwkowski. 2001. Untangling the ErbB signalling network. *Nat Rev Mol Cell Biol.* 2:127-37.

Chapter 4: Positive feedback in ligand release

4.1 Introduction

As introduced in Chapter 2, the family of ADAM metalloproteases are involved in proteolytic cleavage of the EGFR ligands. TACE/ADAM 17 is known to be involved in TGF- α , HB-EGF, and AR release, while ADAM 10 is thought to be involved in EGF cleavage (Borrell-Pages et al., 2003; Harris et al., 2003; Hinkle et al., 2004; Merlos-Suarez et al., 2001; Sahin et al., 2004). There is evidence that TGF- α and HB-EGF shedding is stimulated by signals downstream of the EGF receptor, such as PKC and MAPK activation, creating a positive feedback mechanism that may involve metalloprotease phosphorylation (Baselga et al., 1996; Fan and Derynck, 1999; Fan et al., 2003; Gechtman et al., 1999). Ligand shedding in response to intracellular signaling is an active area of research due to the increasing examples of EGF receptor transactivation. Various forms of stimuli, such as gastrin-releasing peptide, carbachol, TNF α , and prostaglandin E2, lead to EGFR receptor activation through a triple membrane-passing signaling mechanism of EGFR transactivation and suggest important

interreceptor communications (Chen et al., 2004; Gschwind et al., 2001; Lui et al., 2003; McCole et al., 2002; Pai et al., 2002).

Previous work looking at EGF cleavage has shown that blocking the EGF receptor produces increased ligand accumulation in the extracellular media and allows estimation of the fraction of ligand that is captured at the cell surface (DeWitt et al, 01). To study the cleavage of the various EGFR ligands, chimeras were constructed in the Wiley lab with the same EGF receptor-binding domain attached to different membrane anchoring domains. The chimeras were used to parse out the differences in ligand shedding while constraining receptor binding and activation to EGF stimulation. As mentioned in Chapter 3, the ECT (EGF with the native membrane anchoring domain of EGF) and TCT (EGF fused to the membrane-anchoring domain of TGF α) chimeras were constructed and retrovirally transduced into the 184A1 human mammary epithelial cell line. Our initial work with the ECT release showed an increase in release in the presence of a receptor-blocking antibody (see section 3.3.1). However, we show here that in the presence of 10 ug/ml 225 receptor blocking antibody, the linear rate of ligand release of the TCT ligand decreased four fold compared to incubation in serum-free media alone. These results suggest the existence of positive feedback within the TCT autocrine loop. We also demonstrate the involvement of p38 and ERK in the constitutive and stimulated release of the EGF and TGF α based constructs and disparities in the ligand shedding specific to the membrane anchoring domains.

4.2 Materials and Methods

4.2.1 Reagents and antibodies

Batimastat (BB-94; [4-(N-hydroxyamino)-2R-isobutyl-3S-(thienylthiomethyl)succinyl]-L-phenylalanine-N-methylamide) was custom synthesized by Kimia Corporation (Santa Clara, CA). Cells were also inhibited with PD98059 (Calbiochem), SB203580 (Calbiochem), bisindolylmaleimide I (BIM; Calbiochem), and gefitinib (WuXi PharmaTech, Shanghai, China) dissolved in DMSO. The receptor blocking anti-EGFR 225 monoclonal antibody was isolated from a hybridoma cell line obtained from the American Type Culture Collection (Gill et al., 1984). Anti-EGF antibodies for the EGF ELISA include 236 (R&D Systems) and a rabbit polyclonal described previously (Wiley et al., 1998). The tertiary ELISA detection antibody was an alkaline phosphatase-conjugated goat anti-rabbit antibody (Sigma). Cells were stimulated exogenously with recombinant human EGF (Peprotech), TGF α , and HGF (both R&D Systems).

4.2.2 Construction of ligand chimeras and cell lines

The TCT construct was made in the Wiley lab as previously described, see section 3.3.2. The TCT-NA, and ECT-NA constructs were also made in the Wiley lab, and are similar to the TCT and ECT ligands with the exception to one point mutation in the EGF ligand domain of Leucine 15 to Glutamate (L15E). This mutation creates a non-binding EGF ligand when cleaved from the cell surface (termed NA for no affinity) (Nandagopal et al., 1996).

The human mammary epithelial cell (hMEC) line 184A1 (Stampfer et al., 1993) was obtained from Martha Stampfer (Lawrence Berkeley National Laboratory, University of California, Berkeley, Berkeley, CA). The hMECs were retrovirally transduced with the TCT, TCT-NA, and ECT-NA constructs and maintained in DFCI-1 medium (Band and Sager, 1989) containing 2ug/ml puromycin for selection. Serum-free media consisted of DFCI-1 complete media lacking fetal bovine serum, bovine pituitary extract, or EGF supplements, with the addition of 1 mg/ml Bovine Serum Albumin (Sigma). Unless otherwise noted, cells were incubated for 16 hours in serum-free media before starting each experiment. All experiments were performed using cells within 15 passages of thawing.

4.2.3 EGF ligand release

Cells were plated in DFCI-1 media in 12-well plates on day 1 at a density of 60,000-80,000 cells/well, and switched to serum-free media on day 2. After 16 hours cells were switched to 1ml of fresh serum-free media alone or containing 10 ug/ml 225 mAb, 10uM batimastat and 10 ug/ml 225 mAb, 40 ng/ml HGF, or 40 ng/ml HGF and 10 ug/ml 225 mAb. In the case that specific cell signaling pathways were inhibited, cells were preincubated for 30 minutes with 0.25% DMSO as a carrier control, 10uM batimastat, 10uM bisindolylmaleimide I (BIM), 10uM SB203580, 1uM gefitinib, or PD98059 (at the concentration shown in the figure legends) prior to replacement with fresh inhibitor containing media with or without exogenous TGF α stimulation at t=0. For time course experiments media

was collected at 2-hour time intervals from parallel plates, centrifuged at 14,000 for 10 minutes at 4°C, and the supernatant was frozen. For single time point measurements, conditioned media was only collected after 8 hours. The EGF concentration of the conditioned media, measured by ELISA, was converted to molecules of EGF and normalized to the average cell number per well measured with a Vi Cell XR.

4.2.4 ERK phosphorylation time courses

ERK phosphorylation time courses were measured using the in-cell western blot with the Odyssey system (LI-COR), which quantifies relative ERK phosphorylation levels under multiple conditions in a high-throughput assay. On day 1, cells were plated in 96-well plates (Nunc) at a density of 20,000 cells/well. Cells were switched to 100ul of serum-free media on day 2, and starved for at least 16 hours. On day 3, cells were pretreated with PD98059 (0.2 to 25 uM) for 30-minutes (when cells were inhibited), stimulated with exogenous TGF α (varying from 0.6 to 20ng/ml) at different time points, and fixed simultaneously with formaldehyde (4% in PBS) for 20 minutes at room temperature. Cells were permeabilized in 0.1% triton in PBS and blocked with Odyssey Blocking Buffer (LI-COR) 1:1 in PBS (OBB). Cells were stained for ERK 1/2 phosphorylation on Thr²⁰² and Tyr²⁰⁴ (Cell Signaling; 1:100 in OBB) overnight at 4°C. IRDye 800 anti-rabbit IgG (Rockland; 1:800 in OBB) was used as the secondary antibody. Plates were washed 3X with 0.1% Tween 20 in PBS between each antibody incubation and prior to scanning. Plates were scanned using the Odyssey

system (LI-COR). The integrated intensity of each well was normalized to untreated wells on the same plate to show normalized fold ERK phosphorylation at each time point under each condition. Several metrics can be abstracted from time course measurements, including the peak and integral of the fold phosphorylation. EGF release is shown as a function of fold ERK phosphorylation at the final 2-hour time point; however, similar relationships are found with the other metrics.

4.3 Results

4.3.1 TGF α based construct release is positively regulated downstream of the EGF receptor

To study the regulation of the various EGFR ligands, chimeras were constructed with the same EGF receptor-binding domain attached to different membrane anchoring domains. The chimeras are used to parse out the differences in ligand shedding while constraining receptor binding and activation to EGF stimulation only. The TCT chimera, EGF fused to the membrane-anchoring domain of TGF α , was constructed and retrovirally transduced into the 184A1 human mammary epithelial cell line by the Wiley lab, as previously described (see section 3.2.2). Previous work with EGF cleavage has shown that blocking the EGF receptors produces increased ligand accumulation in the extracellular media and allows estimation of the fraction of ligand that is captured at the cell surface (DeWitt et al, 2001). However, we show here that in the presence of 10 μ g/ml 225 receptor blocking antibody, the linear rate of ligand release of the TCT cells decreased four fold compared to incubation in serum-

free media alone, see Figure 4.5.1. This suggests that receptor activation is influencing ligand release of the TGF α based construct, which is in contrast to previous work studying EGF cleavage. Incubation with 10 μ M batimastat and 10 μ g/ml 225 antibody led to almost complete reduction of the TCT cleavage (decreased to 2% of release rate in serum-free media alone). Therefore, TCT release involves positive feedback and constitutive, EGFR independent, contributions.

In addition, we thought it would be interesting to add an exogenous ligand and explore whether stimulation of similar pathways through a different receptor could activate the same degree of stimulated ligand release. HGF activation of the c-Met/HGF tyrosine kinase receptor activates downstream pathways including ERK and PKC (Kermorgant et al., 2004; Paumelle et al., 2002). We added exogenous HGF to the TCT cells in the presence of receptor blocking 225 antibody to see if stimulation of pathways activated by the HGF receptor would restore the stimulated TCT ligand release. Interestingly, HGF stimulation did increase the rate of TCT release when added in addition to 225 EGFR blocking antibody, see Figure 4.5.2. However, HGF also decreased the stimulated release of TCT in the absence of 225, suggesting that the exogenous stimulation may disrupt the TCT signaling and lower the degree of stimulated ligand release. HGF stimulation had no effect on ECT release with or without 225 present.

4.3.2 Small molecule inhibitors show release stimulated through ERK, p38 but not PKC

To begin investigating the pathways involved in TCT release we used several small molecule inhibitors and measured EGF accumulation over an 8-hour time course, see Figure 4.5.3. While the DMSO carrier control and PKC inhibitor (BIM) showed no effect on TCT release, the SB203580 p38 inhibitor decreased TCT cleavage to a small degree. However, p38 inhibition in combination with blocking the EGF receptor with 225 antibody had synergistic effects on decreasing ligand release. The small molecule EGFR kinase inhibitor, gefitinib, showed a similar decrease in ligand release to 225 although slightly more effective under these concentrations. This could be due to the absence of ligand competition in the case of the direct kinase inhibition or it could be due to ligand capture that is not present under receptor blocking conditions. Interestingly, MEK inhibition alone completely abolished ligand shedding.

4.3.3 Mutant EGF constructs decouple ligand release from ligand capture

The closed loop nature of this feedback system makes it difficult to parse out the contributions of constitutive and induced ligand shedding. Measuring ligand accumulation in the media under various conditions is obscured by ligand capture at the cell surface. To decouple ligand shedding from receptor binding and stimulation, the Wiley Lab developed constructs with a single amino acid substitution in the EGF ligand (L15E), which abolishes receptor-binding affinity (termed "NA" for no affinity). To explore the differences in positive feedback between EGF and TGF α release, both ECT-NA and TCT-NA constructs were

retrovirally transduced into the 184A1 cell line. The basal accumulation of these ligands in the media is not affected by the presence of receptor blocking antibody, which confirms that the mutant ligand is not being captured or stimulating release (see Figure 4.5.4).

4.3.4 MEK inhibition completely blocks TGF α stimulated ligand release of TGF α but not EGF based construct

Constitutive release of the non-binding EGF ligand was observed for both the ECT-NA and TCT-NA cells in serum-free medium, see Figure 4.5.5. This basal shedding was decreased upon inhibition of p38 and MEK in both cell lines, which suggests that these signaling pathways are involved proteolytic release when cells are in an unstimulated state. To look at stimulated release and use EGF release as a metric for the degree of ligand shedding, we stimulated the cells with exogenous TGF α , which does not interfere with the EGF ELISA used to measure the conditioned media. Both constructs had an increased level of ligand release in the presence of exogenous TGF α . However, the TCT-NA cells responded with a large burst of ligand shedding over the first four hours that was not seen in the ECT-NA cells. In addition, the effects of p38 and MEK inhibition on the stimulated ligand release were different between the two cell lines. While the ECT-NA stimulated release was decreased similarly in the presence of both p38 and MEK inhibitors, the TCT-NA stimulated release was completely abolished by MEK inhibition and seemed unaffected by p38 inhibition. This suggests that p38 plays a role in basal shedding of both the EGF and TGF α

based constructs while MEK is only partially involved in stimulated EGF release while it seems to be exclusively implicated in stimulated release of TGF α .

4.3.5 Quantitative relationship of TGF α stimulated TCT-NA release through ERK

To further investigate stimulated release of the TCT-NA construct we measured ERK phosphorylation and EGF release under increasing levels of exogenous stimulation. ERK phosphorylation increased in both the peak and phosphorylation level at each time point measured under increasing concentrations of TGF α (see Figure 4.5.6). Ligand released also increased monotonically with increasing concentrations of TGF α . The same behaviors were seen in reverse when the TCT-NA cells were co-treated with increasing concentrations of the MEK inhibitor, PD98059. Together, these results show a quantitative, linear relationship between the amounts of ligand released as a function of fold ERK phosphorylation measured at 2 hours, see Figure 4.5.7. ERK stimulation and inhibition show similar behavior on ligand shedding, hence, we conclude that ERK is a key modulator of TGF α release.

4.4 Discussion

Evidence suggests that pathways downstream of the EGF receptor might be involved in ligand shedding (Baselga et al., 1996; Fan and Derynck, 1999; Gechtman et al., 1999). Still, we were surprised to find that our engineered EGF chimera was positively regulated. In previous autocrine studies the receptors

were blocked to determine the fraction of ligand captured by the cells (DeWitt et al., 2001). Rather than seeing an increase in ligand release related to the fraction of ligand captured at the cell surface, in the presence of 225 EGF receptor blocking antibody we saw a 4-fold decrease in TCT ligand release, see Figure 4.5.1. This suggested that ligand binding, receptor activation and potentially signaling downstream of the EGF receptor were involved in the release of the TGF α based construct in serum-free media alone; a result not seen with the EGF anchoring domain in the ECT construct (see section 3.3.1).

The decreased release rate of TCT cells observed in the presence of receptor blocking antibody was partially restored with exogenous HGF stimulation, see Figure 4.5.2. Interestingly, the stimulated TCT rate of release in serum-free media was decreased under HGF exogenous stimulation without blocking the EGF receptors. Together these results suggest that under exogenous HGF stimulation, the release of the TCT ligand is independent of autocrine EGFR signaling, and the resulting rate of ligand release is lower than that observed under autocrine stimulation. The overall decrease in release rate suggests something intrinsic in the autocrine stimulation that leads to the maximal release. Therefore, the TCT ligand is an autocrine loop with a four-fold increase in ligand release that is positively regulated specifically by autocrine stimulation.

Using small molecule inhibitors we investigated the role of specific pathways in the stimulated release of the TCT ligand. MEK, p38, and EGFR inhibitors decreased the ligand release, while PKC inhibition showed no effect

(see Figure 4.5.3). In addition, the combination of the EGF receptor blocking antibody 225 and the p38 inhibitor (SB203580) lead to a synergistic decrease in ligand release, suggesting that the stimulated release downstream of the EGF receptor operates independently of p38 effects. While PKC has been shown to be important in ligand shedding, these previous studies involved stimulation with a phorbol ester (PMA or TPA) that activates PKC (Izumi et al., 1998; Le Gall et al., 2003). Therefore, the stimulation of ligand release through a positive feedback downstream of EGFR may not elicit or require the same PKC stimulation.

To further investigate the positive feedback it was necessary to decouple ligand release from ligand capture. The L15E mutation in the EGF ligand domain conferred non-binding ligands that should not be captured at the cell surface (termed NA for “no affinity”). Incubation in serum-free media alone or containing receptor blocking antibody resulted in similar levels of EGF in the conditioned media, verifying that ligand is not being captured or influencing ligand release in the ECT-NA and TCT-NA cells (see Figure 4.5.4). These results and EGF accumulation over an 8-hour time course showed that both the EGF and TGF α based non-binding constructs had constitutive release in serum-free media (see Figure 4.5.5). Both p38 and MEK inhibition decreased the constitutive release of both ligands, suggesting that some basal level of signaling existed under resting conditions that was contributing ligand cleavage.

The ECT-NA and TCT-NA were both released at a higher rate in the presence of exogenous TGF α ; however, they were stimulated to different

degrees. The TGF α based construct was shed initially at a high rate of 9,600 molecules of EGF released/cell/min in response to exogenous stimulation but that rate of release tapered off after about 4 hours, to 2,000 molecules of EGF released/cell/min. This decrease in stimulated ligand shedding could be due to a depletion of available surface pro-ligand, with the rate of ligand release becoming limited to the rate of ligand synthesis. Alternatively, if the surface ligand is in excess, it could be a result of exogenously stimulated signaling dynamics that start off with a peak and trend downwards after about 2 hours, suggesting that ligand release is directly proportional to the level of ERK activity. In contrast, the ECT-NA stimulated ligand release is simply a small, 2-fold increase, mirroring the constitutive shedding. Therefore, the rate of ECT release and fraction of ligand captured, both measured in the presence of receptor blocking 225 antibody as discussed in Chapter 3, underestimate the true values because both are measured while inhibiting the small amount of stimulated EGF release demonstrated here. Interestingly, neither p38 nor MEK inhibition affect the ECT-NA stimulated release. The stimulated TCT-NA release is unaffected by p38 inhibition and completely abolished during MEK inhibition, suggesting disparate mechanisms of stimulated release are involved with the two different ligands.

To further investigate the role of ERK signaling in TCT-NA release, ligand release and ERK phosphorylation were measured under increasing exogenous stimulation or increasing MEK inhibition, see Figure 4.5.6. Ligand release as a function of ERK phosphorylation (measured at 2 hours) shows a quantitative, linear relationship under increasing exogenous stimulation and increasing MEK

inhibition (see Figure 4.5.7). These results implicate ERK as a key player in TGF α but not EGF shedding and while the exact mechanism is unknown, previous work has shown that ERK can phosphorylate a serine residue on ADAM17 in response to EGF stimulation (Fan et al., 2003).

It is interesting to speculate that TGF α , and not EGF, is the most prominent EGFR ligand thought to be involved in autocrine growth receptor activation in cancer progression and has been implicated as a potential biomarker for patient prognosis and response to therapy (Hsieh et al., 2000; Ishikawa et al., 2005; Seth et al., 1999; Yarden and Sliwkowski, 2001). The positive feedback associated with TGF α and not EGF shedding may enable cells to sustain an autocrine loop during cancer development and progression as the cells become autonomous.

The decrease in TCT release in the presence of exogenous stimulation through the HGF receptor suggests negative regulation that is not present under autocrine presentation alone. This result corroborates with the increased cell migration speed seen under autocrine but not exogenous stimulation shown in Chapter 3. Future work could investigate the signaling downstream of HGF stimulation that leads to this decrease in stimulated release and perhaps discover a similar increase in the level of negative regulation following exogenous stimulation to that which may be involved in the decrease in overall cell speed. In addition, a mathematical model of ligand release rate and EGF receptor activation could employ the ligand release kinetics measured here. Future work could computationally investigate whether the decrease following the

initial steep slope of stimulated TCT-NA ligand release (see Figure 4.5.5, bottom right) is indeed due to decreasing pro-ligand availability or ERK activity. In addition, mutant EGF constructs could be constructed to investigate the involvement of similar feedback on the release of the remaining EGF receptor ligands.

4.5 Figures

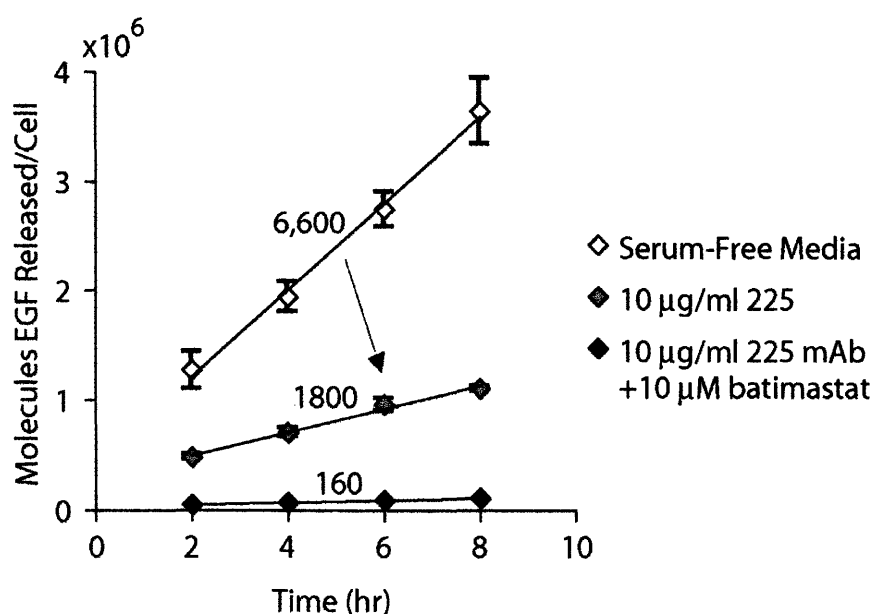


Figure 4.5.1. Blocking the EGF receptor decreases TCT release rate by 4-fold.

The EGF release rate of TCT cells was measured in the presence and absence of the 225 receptor-blocking antibody and a broad-spectrum metalloprotease inhibitor, batimastat. After 16 hours in serum-free media, cells were switched to fresh serum-free media alone or containing 10 $\mu\text{g/ml}$ 225 or 225 in addition to 10 μM batimastat. Media from triplicate wells was collected from parallel plates at 2-hour intervals, assayed for the amount of EGF with an ELISA, and normalized to the cell number determined with a ViCell XR. The rate of ligand release was determined from the slope of each linear fit (molecules of EGF released per cell per min) and error at each time interval represents the standard deviation from triplicate wells. The arrow points to the 4-fold decrease in TCT release rate in the presence of 225.

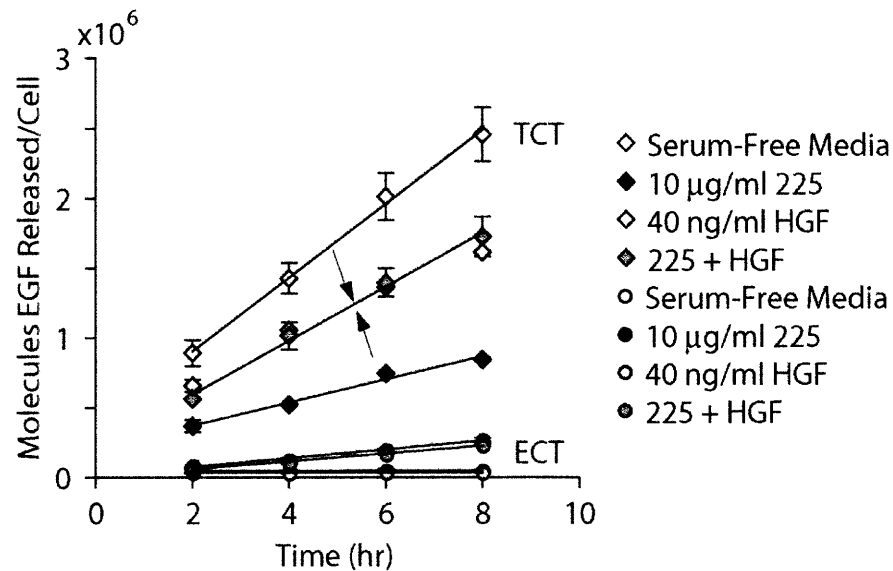


Figure 4.5.2. HGF stimulation increases release of TCT in the presence of 225. The EGF release rate of TCT (diamonds) and ECT (circles) cells was measured in the presence and absence of the 225 receptor-blocking antibody and exogenous stimulation with HGF. After 16 hours in serum-free media, cells were switched to fresh serum-free media alone or containing 40 ng/ml HGF, 10 $\mu\text{g/ml}$ 225, or 225 in addition to 40 ng/ml HGF. Media from triplicate wells was collected from parallel plates at 2-hour intervals, assayed for the amount of EGF with an ELISA, and normalized to the cell number determined with a ViCell XR. Error represents standard deviation from triplicate wells. Arrows point to increase in TCT release rate in the presence of 225 and HGF and also the decrease in the stimulated release of TCT in the presence of HGF alone.

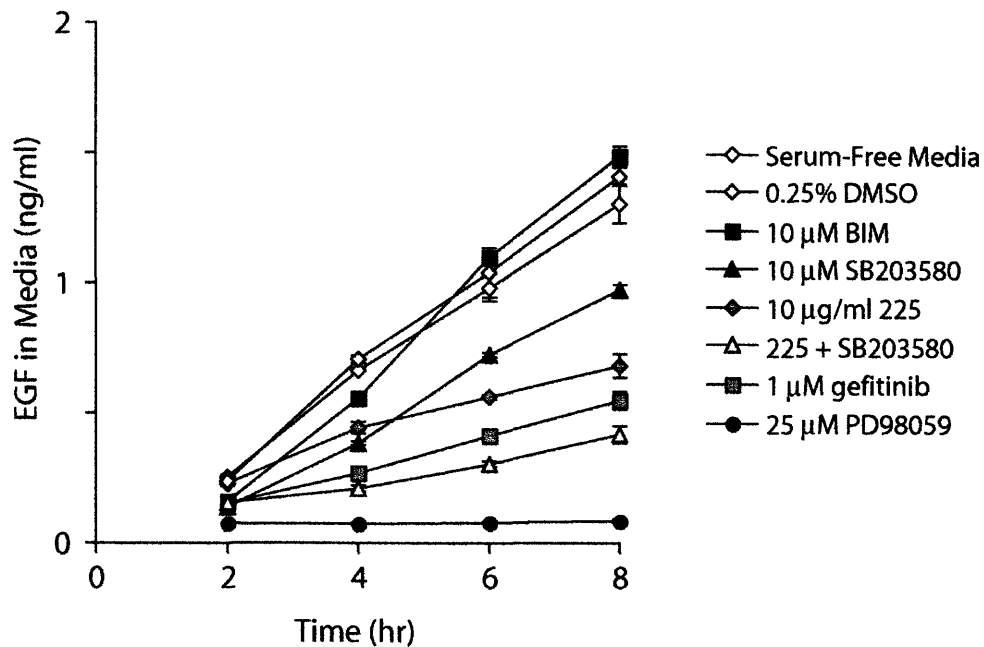
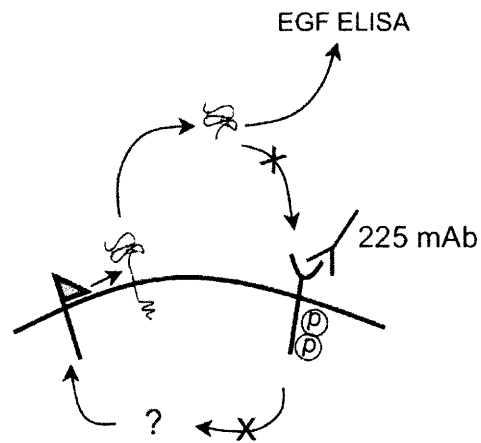


Figure 4.5.3. Small molecule inhibition shows TCT release stimulated through ERK and p38 but not PKC. After 16 hours in serum-free media, TCT cells were pre-incubated with inhibitor for 30 minutes. At t=0 cells were switched to fresh serum-free media alone, 0.25% DMSO as a carrier control, 10 uM bisindolylmaleimide I (BIM), 10 uM SB203580, 10 ug/ml 225, 10 ug/ml 225 and 10 uM SB203580, 1 uM gefitinib, or 25 uM PD98059. Media was collected from parallel plates at 2-hour intervals and EGF concentration was measured with an ELISA. Error represents standard deviation from triplicate wells.

A



B

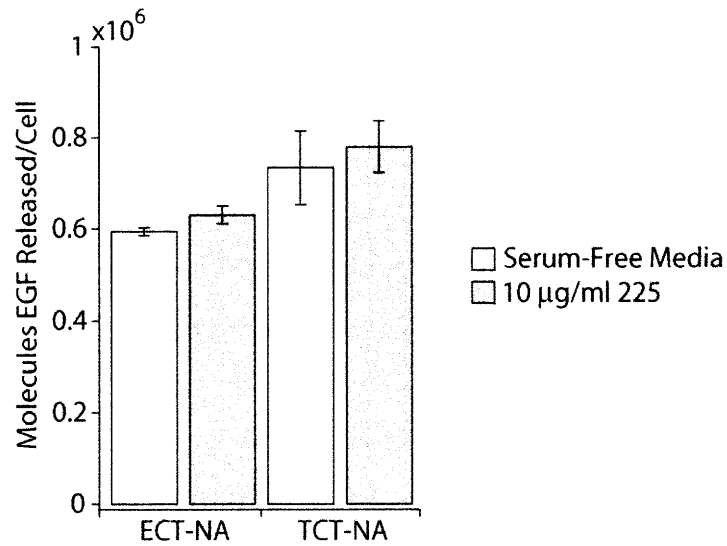


Figure 4.5.4. Blocking the EGF receptor does not alter accumulation of EGF in the media for ECT-NA or TCT-NA cells. (A) Schematic of blocking the EGF receptor and measuring EGF(L15E) release. Since the mutant EGF should have no affinity for the EGF receptor, this experiment is a control to show that ligand is not being captured by the cells. (B) EGF released in the to the extracellular media was measured after an 8-hour incubation in serum-free media alone or containing 10 ug/ml 225 mAb. The concentration of EGF in the conditioned media was measured with an ELISA and normalized to the cell number. Error bars represent the standard deviation from triplicate wells.

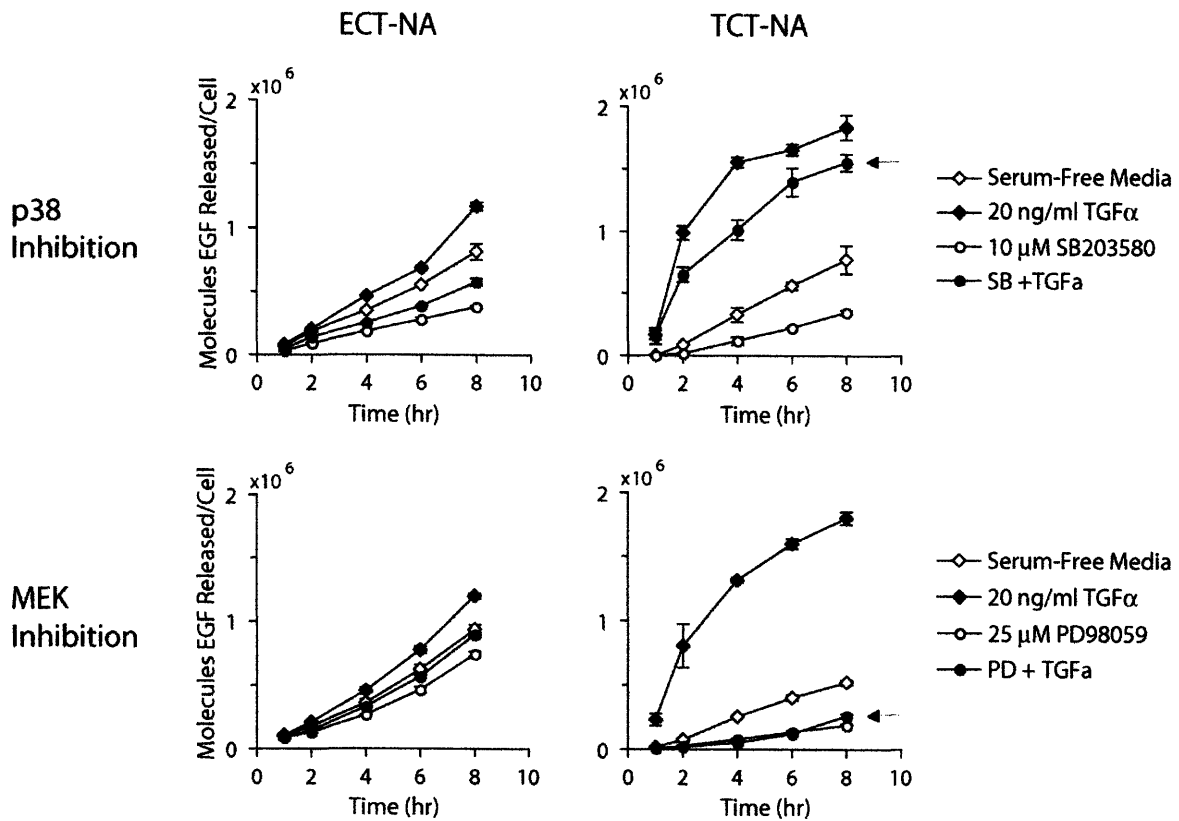


Figure 4.5.5. Differential regulation of ECT-NA and TCT-NA constitutive and stimulated release by p38 and ERK. Constitutive and TGF α stimulated release was measured for the ECT-NA and TCT-NA cells in serum-free media alone or under p38 or MEK inhibition. After 16 hours in serum-free media, cells were pre-incubated with inhibitor and at t=0 cells were switched to fresh serum-free media alone or stimulated exogenously with 20 ng/ml TGF α in the presence or absence of 10 μ M SB203580 (top) or 25 μ M PD98059 (bottom). Media was collected from parallel plates at 2-hour intervals and EGF was measured by ELISA and normalized to cell number. Error represents standard deviation from triplicate wells. Arrows show difference between p38 and MEK inhibition on the TGF α stimulated release of TCT-NA.

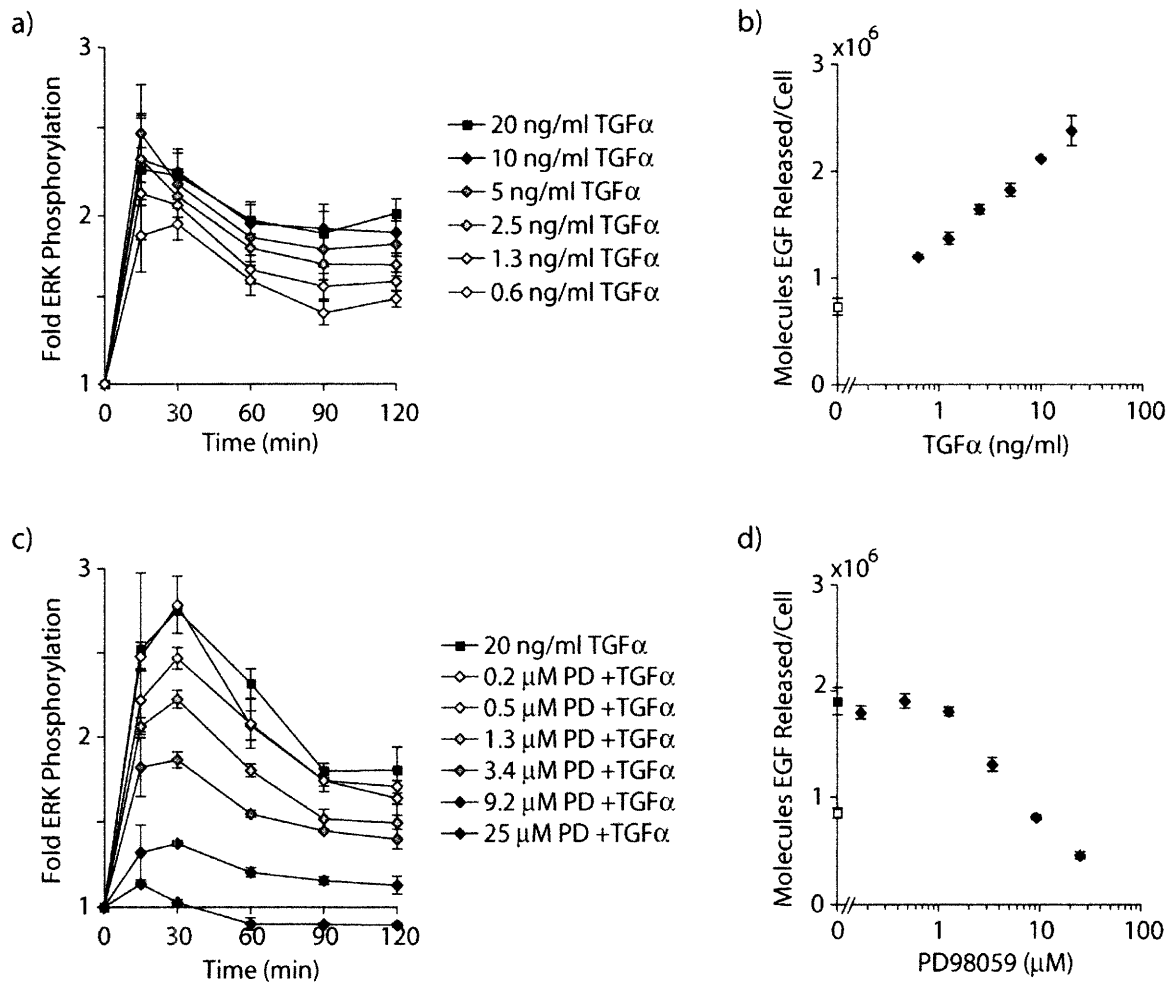


Figure 4.5.6. TGFα stimulates and MEK inhibition diminishes TCT-NA release in a dose-dependent manner.

ERK phosphorylation time courses and EGF release was measured under increasing TGFα stimulation and MEK inhibition. Fold ERK phosphorylation was measured over a 2-hour time course by in-cell western under a) increasing TGFα concentrations and c) 20 ng/ml of TGFα in addition to increasing concentrations of PD98059. EGF release was measured after an 8-hour incubation in serum-free media alone (open squares) or (b) increasing levels of TGFα stimulation (filled diamonds) and (d) 20 ng/ml TGFα stimulation (filled square) and increasing concentrations of PD98059 (filled diamonds). The concentration of EGF in the conditioned media was measured with an ELISA and normalized to cell number. Under inhibitory conditions, cells were pre-incubated with inhibitor for 30-minutes prior to TGFα stimulation. Error represents standard deviation measured from triplicate wells.

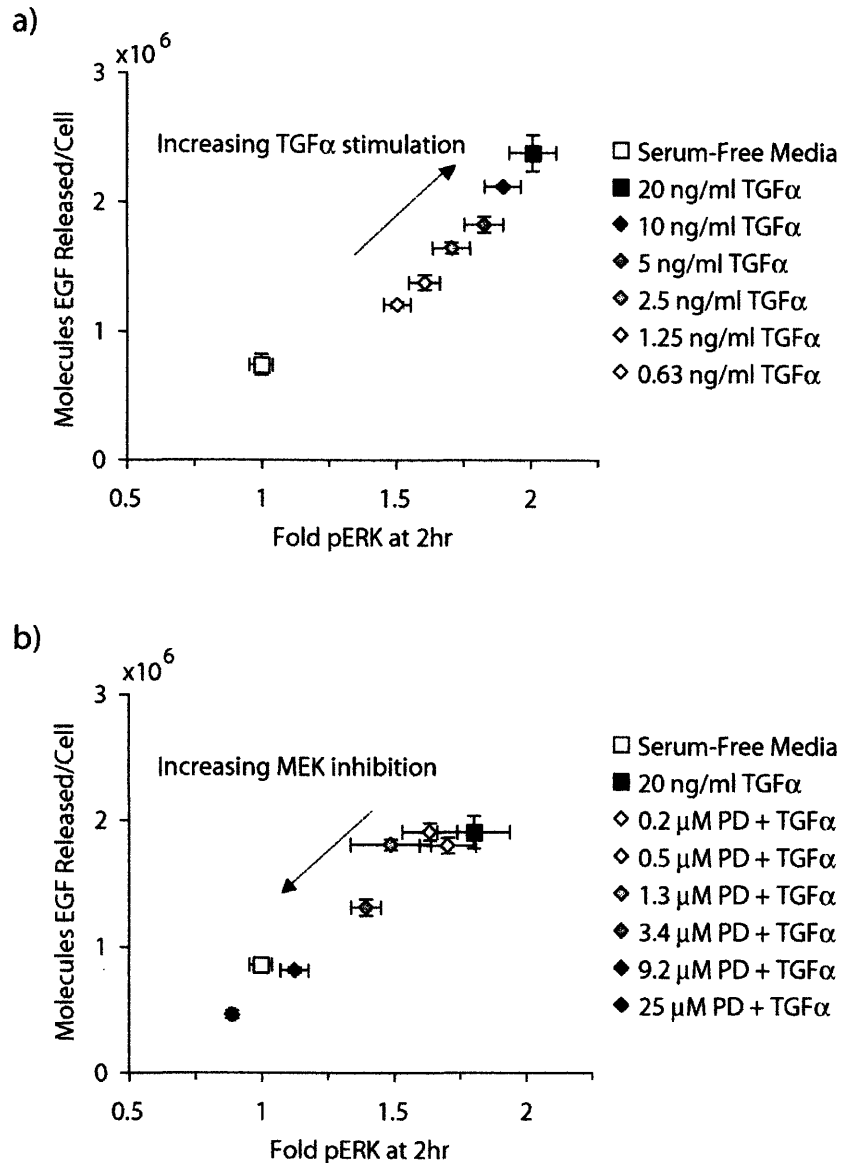


Figure 4.5.7. TGF α stimulates TCT-NA release through ERK. EGF release over 8 hours is shown as a function of ERK phosphorylation measured 2 hours after TGF α stimulation and in the presence or absence of varying levels of MEK inhibition. After 16 hours in serum-free media, TCT-NA cells were stimulated with a) varying amounts of TGF α or b) pre-incubated with varying PD98059 concentrations for 30-minutes before stimulation with 20 ng/ml of TGF α . Media was collected after 8 hours and EGF was measured by ELISA and normalized to cell number. Fold ERK phosphorylation over unstimulated cells is shown for the 2-hour time point, measured by in-cell western. Full ERK phosphorylation time courses are shown in Supplementary Fig. S2. Error represents standard deviation from triplicate wells.

4.6 References

- Band, V., and R. Sager. 1989. Distinctive traits of normal and tumor-derived human mammary epithelial cells expressed in a medium that supports long-term growth of both cell types. *Proc Natl Acad Sci U S A*. 86:1249-53.
- Baselga, J., J. Mendelsohn, Y.M. Kim, and A. Pandiella. 1996. Autocrine regulation of membrane transforming growth factor-alpha cleavage. *J Biol Chem*. 271:3279-84.
- Borrell-Pages, M., F. Rojo, J. Albanell, J. Baselga, and J. Arribas. 2003. TACE is required for the activation of the EGFR by TGF-alpha in tumors. *Embo J*. 22:1114-24.
- Chen, W.N., R.L. Woodbury, L.E. Kathmann, L.K. Opresko, R.C. Zangar, H.S. Wiley, and B.D. Thrall. 2004. Induced autocrine signaling through the epidermal growth factor receptor contributes to the response of mammary epithelial cells to tumor necrosis factor alpha. *J Biol Chem*. 279:18488-96.
- DeWitt, A.E., J.Y. Dong, H.S. Wiley, and D.A. Lauffenburger. 2001. Quantitative analysis of the EGF receptor autocrine system reveals cryptic regulation of cell response by ligand capture. *J Cell Sci*. 114:2301-13.
- Fan, H., and R. Derynck. 1999. Ectodomain shedding of TGF-alpha and other transmembrane proteins is induced by receptor tyrosine kinase activation and MAP kinase signaling cascades. *Embo J*. 18:6962-72.
- Fan, H., C.W. Turck, and R. Derynck. 2003. Characterization of growth factor-induced serine phosphorylation of tumor necrosis factor-alpha converting enzyme and of an alternatively translated polypeptide. *J Biol Chem*. 278:18617-27.
- Gechtman, Z., J.L. Alonso, G. Raab, D.E. Ingber, and M. Klagsbrun. 1999. The shedding of membrane-anchored heparin-binding epidermal-like growth factor is regulated by the Raf/mitogen-activated protein kinase cascade and by cell adhesion and spreading. *J Biol Chem*. 274:28828-35.
- Gill, G.N., T. Kawamoto, C. Cochet, A. Le, J.D. Sato, H. Masui, C. McLeod, and J. Mendelsohn. 1984. Monoclonal anti-epidermal growth factor receptor antibodies which are inhibitors of epidermal growth factor binding and antagonists of epidermal growth factor binding and antagonists of epidermal growth factor-stimulated tyrosine protein kinase activity. *J Biol Chem*. 259:7755-60.
- Gschwind, A., E. Zwick, N. Prenzel, M. Leserer, and A. Ullrich. 2001. Cell communication networks: epidermal growth factor receptor transactivation

- as the paradigm for interreceptor signal transmission. *Oncogene*. 20:1594-600.
- Harris, R.C., E. Chung, and R.J. Coffey. 2003. EGF receptor ligands. *Exp Cell Res*. 284:2-13.
- Hinkle, C.L., S.W. Sunnarborg, D. Loiselle, C.E. Parker, M. Stevenson, W.E. Russell, and D.C. Lee. 2004. Selective roles for tumor necrosis factor alpha-converting enzyme/ADAM17 in the shedding of the epidermal growth factor receptor ligand family: the juxtamembrane stalk determines cleavage efficiency. *J Biol Chem*. 279:24179-88.
- Hsieh, E.T., F.A. Shepherd, and M.S. Tsao. 2000. Co-expression of epidermal growth factor receptor and transforming growth factor-alpha is independent of ras mutations in lung adenocarcinoma. *Lung Cancer*. 29:151-7.
- Ishikawa, N., Y. Daigo, A. Takano, M. Taniwaki, T. Kato, S. Hayama, H. Murakami, Y. Takeshima, K. Inai, H. Nishimura, E. Tsuchiya, N. Kohno, and Y. Nakamura. 2005. Increases of amphiregulin and transforming growth factor-alpha in serum as predictors of poor response to gefitinib among patients with advanced non-small cell lung cancers. *Cancer Res*. 65:9176-84.
- Izumi, Y., M. Hirata, H. Hasuwa, R. Iwamoto, T. Umata, K. Miyado, Y. Tamai, T. Kurisaki, A. Sehara-Fujisawa, S. Ohno, and E. Mekada. 1998. A metalloprotease-disintegrin, MDC9/meltrin-gamma/ADAM9 and PKCdelta are involved in TPA-induced ectodomain shedding of membrane-anchored heparin-binding EGF-like growth factor. *Embo J*. 17:7260-72.
- Kermorgant, S., D. Zicha, and P.J. Parker. 2004. PKC controls HGF-dependent c-Met traffic, signalling and cell migration. *Embo J*. 23:3721-34.
- Le Gall, S.M., R. Auger, C. Dreux, and P. Mauduit. 2003. Regulated cell surface pro-EGF ectodomain shedding is a zinc metalloprotease-dependent process. *J Biol Chem*. 278:45255-68.
- Lui, V.W., S.M. Thomas, Q. Zhang, A.L. Wentzel, J.M. Siegfried, J.Y. Li, and J.R. Grandis. 2003. Mitogenic effects of gastrin-releasing peptide in head and neck squamous cancer cells are mediated by activation of the epidermal growth factor receptor. *Oncogene*. 22:6183-93.
- McCole, D.F., S.J. Keely, R.J. Coffey, and K.E. Barrett. 2002. Transactivation of the epidermal growth factor receptor in colonic epithelial cells by carbachol requires extracellular release of transforming growth factor-alpha. *J Biol Chem*. 277:42603-12.

- Merlos-Suarez, A., S. Ruiz-Paz, J. Baselga, and J. Arribas. 2001. Metalloprotease-dependent protransforming growth factor-alpha ectodomain shedding in the absence of tumor necrosis factor-alpha-converting enzyme. *J Biol Chem.* 276:48510-7.
- Nandagopal, K., D.K. Tadaki, J.A. Lamerdin, E.H. Serpersu, and S.K. Niyogi. 1996. The functional importance of Leu15 of human epidermal growth factor in receptor binding and activation. *Protein Eng.* 9:781-8.
- Pai, R., B. Soreghan, I.L. Szabo, M. Pavelka, D. Baatar, and A.S. Tarnawski. 2002. Prostaglandin E2 transactivates EGF receptor: a novel mechanism for promoting colon cancer growth and gastrointestinal hypertrophy. *Nat Med.* 8:289-93.
- Paumelle, R., D. Tulasne, Z. Kherrouche, S. Plaza, C. Leroy, S. Reveneau, B. Vandebunder, and V. Fafeur. 2002. Hepatocyte growth factor/scatter factor activates the ETS1 transcription factor by a RAS-RAF-MEK-ERK signaling pathway. *Oncogene.* 21:2309-19.
- Sahin, U., G. Weskamp, K. Kelly, H.M. Zhou, S. Higashiyama, J. Peschon, D. Hartmann, P. Saftig, and C.P. Blobel. 2004. Distinct roles for ADAM10 and ADAM17 in ectodomain shedding of six EGFR ligands. *J Cell Biol.* 164:769-79.
- Seth, D., K. Shaw, J. Jazayeri, and P.J. Leedman. 1999. Complex post-transcriptional regulation of EGF-receptor expression by EGF and TGF-alpha in human prostate cancer cells. *Br J Cancer.* 80:657-69.
- Stampfer, M.R., C.H. Pan, J. Hosoda, J. Bartholomew, J. Mendelsohn, and P. Yaswen. 1993. Blockage of EGF receptor signal transduction causes reversible arrest of normal and immortal human mammary epithelial cells with synchronous reentry into the cell cycle. *Exp Cell Res.* 208:175-88.
- Wiley, H.S., M.F. Woolf, L.K. Opresko, P.M. Burke, B. Will, J.R. Morgan, and D.A. Lauffenburger. 1998. Removal of the membrane-anchoring domain of epidermal growth factor leads to intracrine signaling and disruption of mammary epithelial cell organization. *J Cell Biol.* 143:1317-28.
- Yarden, Y., and M.X. Sliwkowski. 2001. Untangling the ErbB signalling network. *Nat Rev Mol Cell Biol.* 2:127-37.

Chapter 5: Investigation of ECT and TNGF cell signaling and migration on collagen IV

This chapter outlines efforts towards the initial aims of this thesis based off of previous work in our lab. Several experimental results led us to change the focus of this thesis and explore alternative migration assays. While unsuccessful aims are rarely published, the work is presented below to document the initial efforts and may serve as a reference for future work in cell migration or single cell analysis.

5.1 *Introduction*

The membrane anchoring domains of the EGFR ligands may determine the cellular distribution as well as the potential for proteolytic release from the cell surface. A recent study set out to explore how the presence of the membrane anchoring domain of EGF affects normal autocrine ligand presentation and cell behavior (Wiley et al., 1998). Wiley et al. expressed two EGF chimeras, EGF-ct and sEGF, in human mammary epithelial cells (hMEC) and looked at cell growth

and the ability for the cells to organize on Matrigel compared to the parental hMECs. Parental hMECs had a maximal growth rate and formed well-defined complex structures in the presence of exogenous EGF. The hMECs transduced with the membrane bound EGF-Ct chimera (see Figure 5.5.1, referred to as ECT in this work) grew at a maximal rate that did not increase in the presence of additional exogenous EGF, although the growth rate could be decreased in the presence of monoclonal antibody 225, an antibody that blocks EGF-EGFR binding. The ECT cells also formed complex structures on Matrigel; a process that was abrogated in the presence of 225. HMECs that were transduced with the artificial secreted form of human EGF, the sEGF chimera, grew at a maximal rate that was unaffected by additional exogenous EGF or the EGFR antibody, and did not form organized structures on Matrigel. The sEGF colocalized with the EGFR within small cytoplasmic vesicles and the sEGF hMECs had a decreased receptor density suggesting that the secreted EGF was intercepting the receptors prior to reaching the cell surface leading to receptor downregulation and was signaling in an 'intracrine' mode (Wiley et al., 1998). These results suggested that removal of the membrane-anchoring domain changed the signaling from an EGF autocrine to an intracrine mode, and the spatial restriction of EGF access to the receptors is important for hMEC organization in vitro.

Maheshwari et al. measured the migration behavior of the parental, ECT, and sEGF hMEC cell lines in a subsequent study and found that the mode of ligand presentation (autocrine versus exogenous EGF) affected the migration persistence time (Maheshwari et al., 2001). Single cells migrating on tissue

culture plastic, under serum-free conditions, with and without exogenous EGF and the 225 EGFR blocking antibody, were tracked every ten minutes for up to six hours. The cell migration speed was calculated from the total cell displacement over time while the persistence was measured by fitting the mean-squared displacement over time to a random walk model. The parental hMECs had a basal mean migration speed of 50 $\mu\text{m/hr}$ in the absence of EGF (see Figure 2.4.4). The ECT-expressing cells had a much higher speed of 120 $\mu\text{m/hr}$ while the sEGF-expressing cells showed a small increase over the parentals at 65 $\mu\text{m/hr}$. Upon addition of 2nM exogenous EGF the migration speed of the parentals and sEGF cell lines increased to 90 $\mu\text{m/hr}$, while the ECT cell speed seemed unaffected. The cell speed was decreased in all cases to the range of 25-35 $\mu\text{m/hr}$ in the presence of 225 EGFR blocking antibody. Since it had already been shown that EGF effects migration speed and persistence measurements in fibroblasts, the surprising result from this study was that the ECT cells had a high persistence value that was abolished upon addition of 2nM exogenous EGF and also in the presence of the 225 mAb (Ware et al., 1998).

The persistent migration behavior under autocrine signaling conditions observed by Maheshwari et al. is the foundation from which the hypotheses of this chapter are based. The results from Maheshwari et al. suggest that the expression of membrane-bound EGF in the ECT hMEC cell line may lead to spatially restricted EGFR signaling that drives persistent migration behavior. The sEGF-expressing cells have a basal migration speed that is decreased upon 225 mAb addition, suggesting that the surface receptor-ligand complexes govern cell

migration speed. The persistent measurement results may be the result of an asymmetrical distribution of ligand-receptor complexes that stimulates further directed migration. The asymmetry could result from polarized distributions of the ligand, the receptor, or an asymmetric release of the ligand. EGFR ligand autocrine signaling spatially restricted to the front of the cell would stimulate membrane protrusion, thus producing a type of chemotactic response, with key downstream signaling pathways including PLC-gamma and PI3 kinase (Chung et al., 2001; Condeelis et al., 2001; Feldner and Brandt, 2002; Firtel and Chung, 2000; Haugh et al., 1999; Hill et al., 2000; Iijima et al., 2002; Levchenko and Iglesias, 2002; Maheshwari and Lauffenburger, 1998; Piccolo et al., 2002; Sawyer et al., 2003; Segall et al., 1996; Wells et al., 1999; Wyckoff et al., 1998; Xie et al., 1998). Although it was shown that the ECT chimera-expressing autocrine cells showed persistent migration behavior that was abolished under exogenous EGF conditions, which could also be considered a paracrine signaling mode, it is not yet known if the signaling is indeed spatially restricted or how intermediate signaling modes would alter the migration behavior.

It has also previously been shown by DeWitt et al. that the ligand secretion rate governs the fraction of ligand captured, and hence the spatial restriction of ligand, see Fig. 5.5.2 (DeWitt et al., 2001). The overall objective of this work will be to understand the role and mechanism of spatially restricted EGFR autocrine ligand signaling in governing cell migration. The hypothesis is that cell migration speed, S , and directional persistence, P , regulated by EGFR autocrine ligands are governed by both the ligand secretion rate. We hypothesize that S will be

greatest under conditions of maximal ligand/receptor binding (i.e., increasing ligand release rate) whereas P will be greatest under conditions of spatially-restricted ligand capture. Ligand secretion rates will be varied using chimeric ligands developed in the Wiley lab, and by addition of a metalloprotease inhibitor. The ligand release rate and fraction of ligand captured will be measured for the varying secretion rates using an EGF ELISA assay. The migration S and P will be measured for cells exhibiting varying ligand release rates using single cell tracking.

5.2 *Materials and Methods*

5.2.1 Cell lines and culture conditions

We used the same parental non-transformed human mammary epithelial cell (hMEC) line 184A1-1. This cell line has several characteristics that provided a desirable background for the autocrine and migration studies. First, this cell line expresses normal levels of p53 and has genetic stability (Stampfer et al., 1997). Second, this cell line is dependent on EGFR activation for growth and migration (Stampfer et al., 1993). The cells produce low levels of TGF- α and amphiregulin and therefore they should possess the endogenous mechanisms necessary for ligand maturation and release (Bates et al., 1990; Li et al., 1992; Stampfer et al., 1993). In this chapter, results using the ECT and TNGF chimeras are presented. The ECT construct has been described previously (Wiley et al., 1998). The TNGF construct is a fusion between the soluble EGF

domain and the transmembrane and cytoplasmic tail of the TNF-alpha cytokine (see Figure 5.5.1).

HMECs are grown under normal culture conditions in DFCI-1 complete medium that has previously been described (Band and Sager, 1989). Since the medium has many undefined additives that may contain growth factors and other stimuli, the medium composition was optimized to obtain serum-free conditions (serum-free media consists of DFCI-1 Complete containing 1mg/ml BSA (Sigma) to block non-specific binding and lacking EGF, bovine pituitary extract, and FBS). The sodium bicarbonate in the media is replaced with additional HEPES (final concentration 25nM) for pH buffering during experimental conditions that lack CO₂ incubation.

5.2.2 Reagents and Antibodies

Gardin was purchased from CalBioChem. The EGFR tyrosine kinase was inhibited with the small molecule MEK inhibitor PD153035, purchased from Calbiochem. Anti-EGFR 13A9 monoclonal antibody, which binds to both occupied and empty EGFR (Winkler et al., 1989), was a gift from Genentech (South San Francisco, CA). Anti-EGFR mAb 13A9 was labeled with ¹²⁵I (Perkin Elmer) using iodobeads (Pierce) as previously described (Burke and Wiley, 1999). Anti-EGFR 225 monoclonal antibody was isolated from a hybridoma cell line obtained from the American Type Culture Collection (Gill et al., 1984). Anti-EGF antibodies for EGF ELISA include 236 (R&D Systems) and a rabbit polyclonal described previously (Wiley et al., 1998). The tertiary ELISA detection

antibody was an alkaline phosphatase-conjugated goat anti-rabbit antibody (Sigma). Recombinant human EGF was obtained from Peprtech. ERK and EGFR antibodies used in western blots were purchased from Cell Signaling. The p1173 EGFR antibody was purchased from Santa Cruz Biotechnology. The beta-actin antibody was purchased from Sigma. Mouse collagen type IV was purchased from B&D Biosciences and diluted in PBS to achieve the final coating concentration. Glass bottomed Delta T migration dishes were purchased from Biopetechs.

5.2.3 Ligand Release Rates

Cells were plated in DFCI-1 media in 12-well plates on day 1 at a density of 60,000-80,000 cells/well, and switched to serum-free media on day 2. After 16 hrs cells were switched to 1ml of fresh serum-free media alone or containing 225, a DMSO carrier control, or Galardin. Media was collected from parallel plates at various time intervals, centrifuged at 14,000 for 10 min at 4°C, and the supernatant was frozen at 2-hour time intervals. The EGF concentration of the conditioned media, measured by ELISA, was converted to molecules of EGF and normalized to the average cell number per well measured with a Coulter Counter. The rate of EGF release was determined from the slope of a linear fit.

5.2.4 Quantitative surface EGFR measurements

Radioactively labeled 13A9 was used to measure surface EGFR numbers as previously described (Hendriks, 2003). Briefly, 150,000 cells were plated in 6-

well plates on day 1 and switched to serum-free media on day 2. After 19 hrs, cells were switched to fresh serum-free media containing increasing concentrations of ^{125}I labeled 13A9 mAb and incubated at 37°C for 5 hrs. Surface bound antibody was removed with an acid strip solution and duplicate wells were quantified using a Gamma counter. Parallel plates were trypsinized and counted using a Coulter Counter to determine the average number of cells per well. Surface receptor number and the K_D were determined from a fit to the binding equation shown in Figure 5.5.4 using Matlab. The experiment was repeated on either one or two additional days and results were reported as the average fit R_s plus the standard deviation.

5.2.5 Western Blotting

Cells were plated in 10cm plates at 500,000 cells/dish. Cells were starved in serum-free media overnight, treated as described in figure legends, rinsed once in cold PBS, and subsequently scraped in lysis buffer as previously described (Janes et al., 2003) for western blotting. Lysates were incubated on ice for 10 min and then centrifuged at 14,000 rpm for 10 min at 4°C. The supernatants were frozen at -80°C until use. Lysates were analyzed using a bicinchoninic assay (Pierce) to determine the total protein concentration. For western blotting, equal amounts of total lysate protein were diluted in lysis buffer and 4X sample buffer and run on 7.5% gels and transferred to PDVF membranes (Bio-Rad) before blocking with 5% BSA in TBS-T or Blotto (5% w/v non-fat dry milk powder in TBS-T) and incubating membranes overnight at 4°C with the

primary antibody. The membranes were striped and reprobed for total ERK or EGFR.

5.2.6 Single Cell Migration Assay

Single cell migration behavior was measured using time-lapse video microscopy of cells sparsely plated on multiple concentrations of collagen IV. Prior to cell plating, BiopTechs dishes were sterilized with UV radiation for 20 minutes, incubated with 1ml of a given collagen IV concentration for 1hr at 37C, and then blocked with 1% BSA in PBS for 1hr at 37C. Plates were rinsed with PBS and 4,000 cells were plated in serum-free media. Cells were plated sparsely to maintain obstacle free cell paths. Cells were starved overnight and subsequently switched to fresh serum-free media alone, or containing exogenous EGF or 225, and sealed with a BiopTechs lid and transferred to the heated stage of the microscope. Images from up to 19 specified fields were acquired at 10 min intervals for 6-8 hours using a custom automation designed in Improvison Openlab software. Images were turned into Quicktime movies and DIAS software was used for single cell tracking to obtain cell paths and centroid positions over time. Cells that collided during the course of the experiment were not included in the analysis after the point of contact. Data was then exported into matlab for analysis.

5.3 Results

5.3.1 TNGF construct has 10-fold higher EGF release rate than ECT

The ligand release rate of the EGF construct, ECT (see figure 5.5.1), had a very low rate of accumulation in the extracellular media, approximately 20 molecules of EGF per cell per min (see Figure 5.5.2). However, when the receptors were blocked with 225, a competitive monoclonal antibody, approximately 600 molecules per cell per minute were accumulating in the media. In contrast, by attaching the TNF-alpha transmembrane and cytoplasmic tail to EGF, the TNGF construct had a 10-fold higher rate of accumulation in the media. Blocking the TNGF cell receptors with 225 had no significant affect on EGF accumulation. However, the high TNGF rate of EGF release was decreased to 75% and 50% of the maximum rate with increasing concentrations of Galardin, a commercially available broad-spectrum metalloprotease inhibitor (see Figure 5.5.3).

5.3.2 Low and high release of EGF lead to receptor downregulation and sustained ERK phosphorylation

Under both the low and high ligand release rate conditions, western blot analysis showed EGFR downregulation (see Figure 5.5.4). Parental levels increased from 12 to 24 hours most likely due to the withdrawal of EGF from the culture media. However, the ECT and TNGF lysates showed lower levels of total EGFR that did not increase to parental levels after 24 hours in serum-free media. This observation was further investigated by a quantitative surface receptor counting assay. Cells were incubated with several concentrations of ¹²⁵I labeled

13A9, a non-competitive EGFR antibody. After 5 hrs at 37C, cells were striped in an acid wash and counted using a gamma counter. A binding equation was fit to the experimental measurements to determine the surface receptor number (see Figure 5.5.5 a). Receptor downregulation at the cell surface was verified with these quantitative measurements, although day-to-day variability of receptor counts was high (see Figure 5.5.5 b).

The low and high ligand release also lead to sustained ERK phosphorylation up to 24 hours measured by western blot (see Figure 5.5.4). Interestingly, when stimulated with exogenous EGF, the ECT but not the TNGF cells showed an increase in receptor phosphorylation (see Figure 5.5.6). This increase was much lower than that of the parental cells, which could be due to receptor availability at the cell surface. When the ECT and TNGF cells were incubated with receptor blocking 225 mAb, ERK phosphorylation was only decreased in the ECT cells. However, when incubated with an EGFR small molecule kinase inhibitor, both cell types showed decreased ERK signaling. Under both cases ERK phosphorylation resumed after washes and removal of the inhibitor.

5.3.3 Collagen IV level dominates cell migration behavior over ligand release effects

Single cell migration was measured on three collagen IV conditions under low and high ligand release. Plates were incubated for 1hr at 37C with 1, 10, and 100 ug/ml of Collagen IV prior to cell plating. Cells were traced using DIAS and cell paths were exported to Matlab. The average cell speed was measured as

the total cell displacement over the total time. Median persistence values were determined from a fit of mean squared displacement over time to the persistent random walk model (Dunn and Brown, 1987; Gail and Boone, 1970):

$$\langle (\Delta x)^2 \rangle = 2S^2P[\Delta t - P(1 - \exp\{-\Delta t/P\})]$$

The persistent random walk model describes the migration of a single cell in the absence of directional bias. The basic assumption is that each cell moves randomly over large time intervals, but over shorter time scales cells can show persistent behavior. This model breaks down when a cell does not migrate in a random fashion, i.e. if it moves continuously in a circle or if it migrates in a straight line. Cell speed and persistence values measured for varying collagen IV conditions are shown in Figure 5.5.8. While cell speed seems to stay constant under varying collagen conditions, the persistence measurements seem to have more of a biphasic relationship, increasing at the intermediate level of collagen. Cell migration speed is decreased in the presence of the 225 EGFR blocking antibody.

Statistical analysis was used to determine whether the high and low ligand release led to differences in cell persistence. Due to the distributions of individual cell data, shown in Figure 5.5.9 a, the average and standard deviation are not descriptive of the underlying dataset. This exponential decay is typical of persistence values and still these types of experiments are summarized with an average persistence value. Here, the persistence data was log transformed to obtain a normal distribution and then experiments performed on separate days

were analyzed in Matlab using an ANOVA plot (see Figure 5.5.9 b and 5.5.10). Comparison of the ECT and TNGF migration behavior did not reveal statistically significant effects of ligand release rate on cell persistence.

5.4 Discussion

While there is an abundance of literature that suggests the importance of EGFR signaling in both physiological and pathological processes, little is known about how EGFR ligand dynamics control cell signaling and behavior (Yarden, 2001). EGF chimeric ligands were used to vary the rate of ligand release while keeping the soluble, receptor binding domain constant. In this study, two chimeras were used, including the ECT construct, containing a truncated form of the native ligand, and TNGF, a fusion of the soluble EGF ligand to the membrane anchoring domain and cytoplasmic tail of TNF-alpha. The short, extracellular juxtamembrane domain is thought to regulate protease specificity, therefore it was hypothesized that ADAM10 would cleave the ECT ligand, while ADAM17 (TACE) would cleave the TNGF chimera (Arribas et al., 1997; Black et al., 1997; Harris et al., 2003; Sahin et al., 2004). The overall objective was to determine if increasing ligand release would alter the persistent migration behavior observed previously with the ECT cells on tissue culture plastic (Maheshwari et al., 2001) and study the effects of varying matrix-coating conditions.

EGF release rates were measured with an ELISA and normalized to cell number. The TNGF construct had a 10-fold higher release rate than the ECT. Incubation with receptor blocking 225 monoclonal antibody did not influence the

rate of accumulation, suggesting that a very small fraction was being captured by the EGF receptors. This could be due to the level of surface receptor downregulation that was demonstrated by both western blot and a quantitative receptor counting protocol (see Figures 5.5.4 and 5.5.5). In addition, exogenous EGF did not stimulate TNGF receptor phosphorylation, which suggests that the high release of the TNGF lead to surface receptor saturation (see Figure 5.5.6). The 225 effects on TNGF release rate also suggest that signaling downstream of the EGF receptor did not affect the proteolytic cleavage of the TNGF construct.

Interestingly, incubation with the receptor blocking 225 antibody did not reduce ERK phosphorylation of the TNGF cells. This result suggested that receptor activation was occurring at inaccessible sites. Perhaps the TNGF construct could activate receptor internally, before reaching the surface. In addition, metalloprotease inhibition only decreased TNGF release to 50% of the maximum release rate. Together these results suggested that the TNGF construct was potentially being released internally and/or activating receptors prematurely. In retrospect, we may be able to explain these results. It was later brought to our attention that the TNGF chimera was designed similar to the native TNF α ligand, which is a Type II membrane protein, and the ligand is inserted upside down relative to the native EGF ligand (Type I). This difference in protein synthesis may have changed the requirement for proteolytic processing to bind and activate the receptor, and the presence of TNGF intracrine stimulation could explain why ERK phosphorylation was not reduced when blocking the EGFR with 225.

Meanwhile, cell migration experiments were underway on three collagen-IV coating conditions. Several aspects of the initial migration data needed to be addressed. First, cells within each the population showed a high degree of variability. The ECT cells had a population of cells within each experiment that were very persistent while the majority of the cells were not. It was not clear why there was this discrepancy in behavior or how to analyze the results. One data analysis technique used here was transformation of the persistence data to enable normal statistical analysis of non-normal distributions. Second, the cells migrated differently on different days. Figure 5.5.10 shows day-to-day variations of cell speed and persistence measurements. If cells behaved very different on a single day, it could be argued that there may have been experimental error or variance within the setup. However, the variation measured showed statistically significant differences on multiple days. Third, the overall behaviors were not similar to those previously reported for the ECT cells measured on tissue culture plastic (Maheshwari et al., 2001). Maheshwari et al. previously showed that ECT persistence was abolished in the presence of both the EGFR blocking antibody and exogenous EGF, suggesting the autocrine presentation led to the interesting cell behavior. In this work we did not see the same response under multiple collagen coating conditions. The collagen IV substratum may alter cell signaling and response and overall mask the effects of the EGF autocrine stimulation in these cells. It is understandable that persistence may vary with adhesion strength and therefore we expected to see an affect of collagen conditions. However, the interesting behaviors shown in the foundation of this

work were not observed under any collagen condition. In addition, our signaling results suggested that we could not be sure that the TNGF construct was only controlling EGFR signaling on the cell surface and therefore we did not believe that our results of varying ligand release with the TNGF construct and the single cell migration results were conclusive.

5.5 Figures

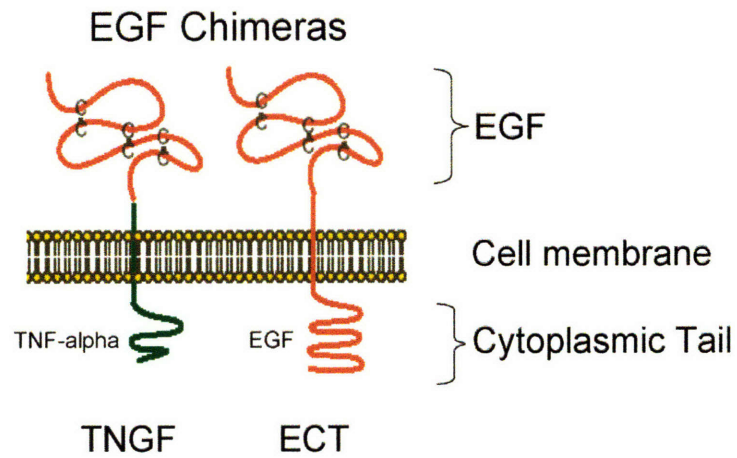


Figure 5.5.1. Schematic of TNGF and ECT chimeras. The TNGF chimera has the soluble EGF domain fused to the transmembrane and cytoplasmic domains of TNF-alpha. ECT is a truncated form of the native EGF ligand, missing only the amino-terminal variable region.

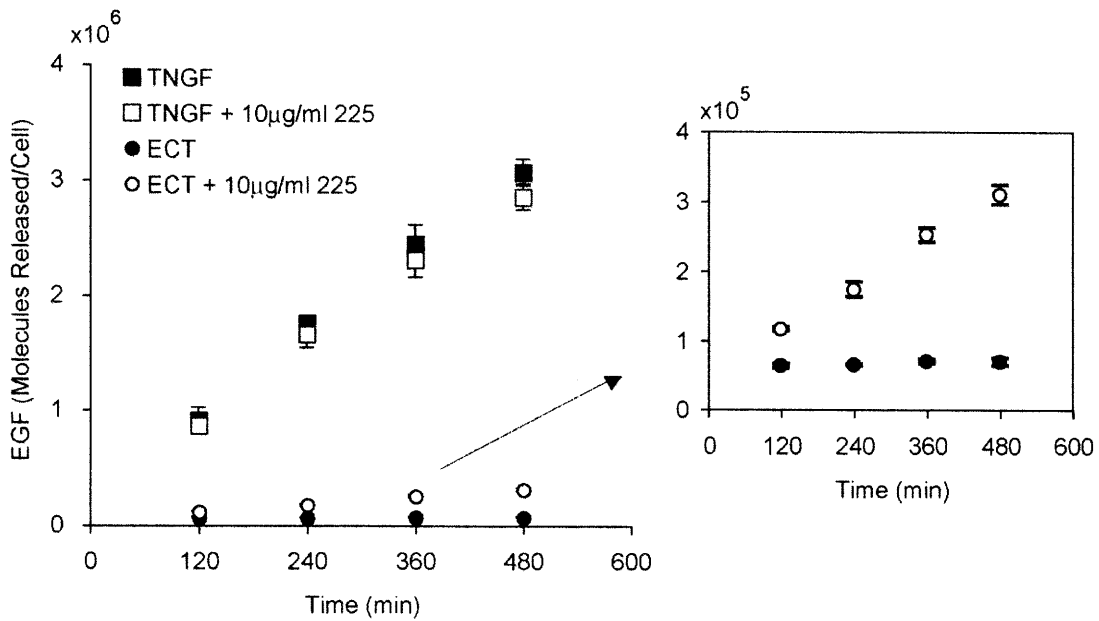


Figure 5.5.2. TNGF and ECT EGF release into culture media. EGF in conditioned media measured by ELISA. EGF concentrations are converted to molecules of EGF and normalized to the average cell number. The slope of a linear fit estimates the ligand release rate. Inset shows detail of ECT release. EGF release rates of TNGF, ECT, and ECT in the presence of 225 mAb are 6,000, 20, and 600 respectively. Error represents standard deviation from triplicate samples.

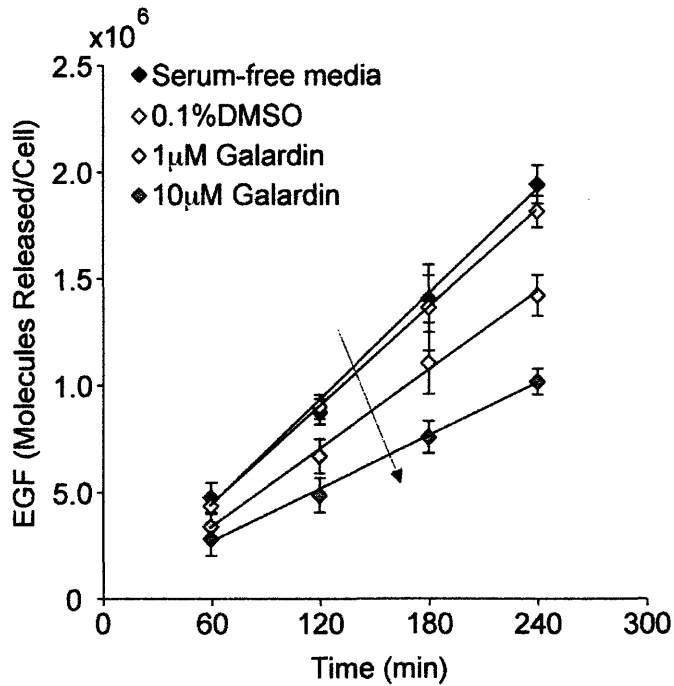


Figure 5.5.3. Broad spectrum metalloprotease inhibitor decreases TNGF release by 50%. TNGF cells were incubated in serum-free media, 0.1% DMSO as a carrier control, 1µM and 10µM of Galardin for 2 hours. Media was collected from triplicate wells, analyzed by EGF ELISA and normalized to cell number. Error represents standard deviation from triplicate samples. The linear release rate was decreased to 75% and 50% with 1µM and 10µM Galardin respectively.

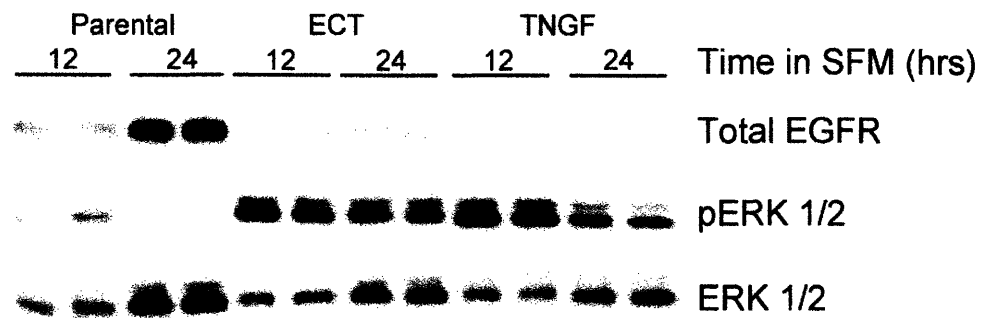


Figure 5.5.4. Autocrine stimulation leads to receptor downregulation and sustained ERK phosphorylation. Parental, ECT, and TNGF cells were starved in serum-free media (SFM) for 12 or 24 hours and lysed. Western blot analysis shows total EGFR levels, pERK 1/2, and then striped and re-probed for total ERK 1/2. Receptor levels are from a total cell lysate, compared to the quantitative surface counts shown below.

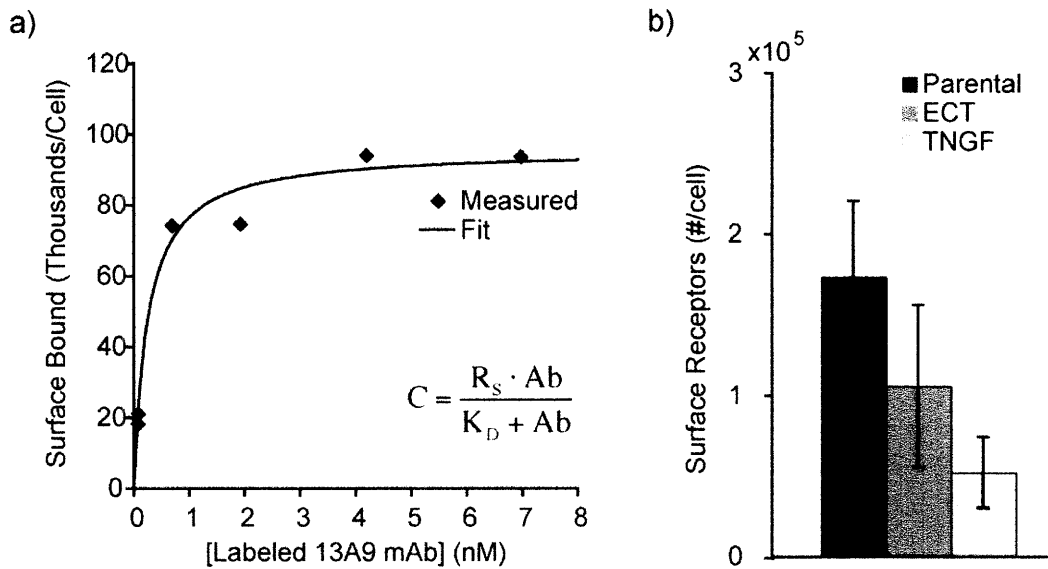


Figure 5.5.5. Quantitative measurements of surface EGF receptors on parental, ECT and TNGF cells. *a*, Surface EGFR levels were measured by incubating with increasing concentrations of ^{125}I labeled 13A9 mAb for 5 hours at 37C. Duplicate wells were then striped with an acid wash and counted. Data was fit to a binding equation to parse out the number of surface receptors, R_s . Values were normalized to an average cell count. *b*, Average surface receptor number for each cell type. Error represents standard deviation from the mean of experiments performed on different days.

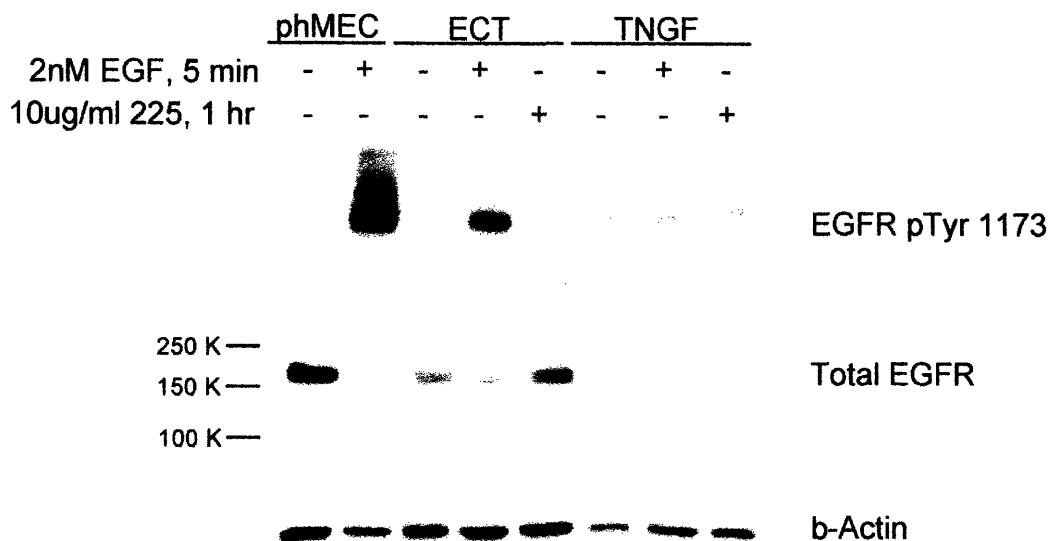
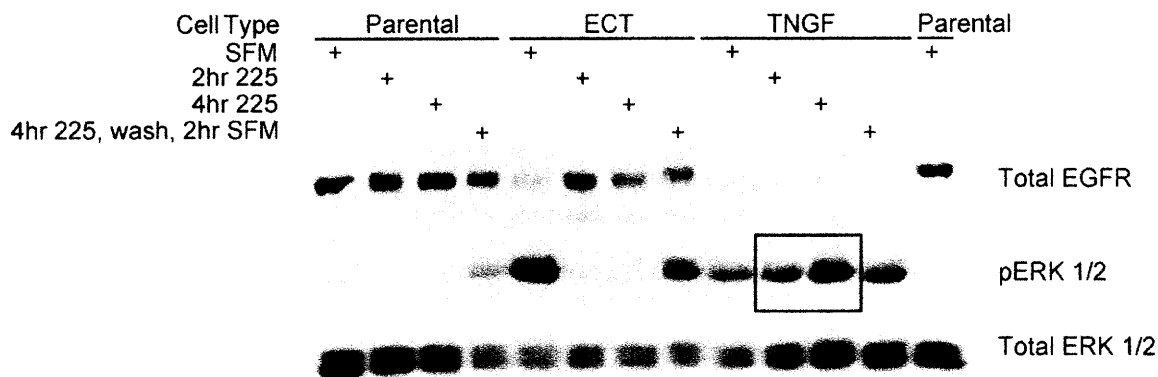


Figure 5.5.6. Exogenous EGF stimulates ECT but not TNGF EGFR phosphorylation. Parental, ECT and TNGF cells were starved overnight in serum-free media and then lysed, or stimulated for 5 minutes with 2nM of exogenous EGF, or inhibited for 1hr with 10ug/ml of 225. Western blots were probed for pTyr1173 EGFR and then stripped and re-probed for total EGFR and beta-Actin.

225-EGFR blocking Ab



PD153035-EGFR kinase inhibitor

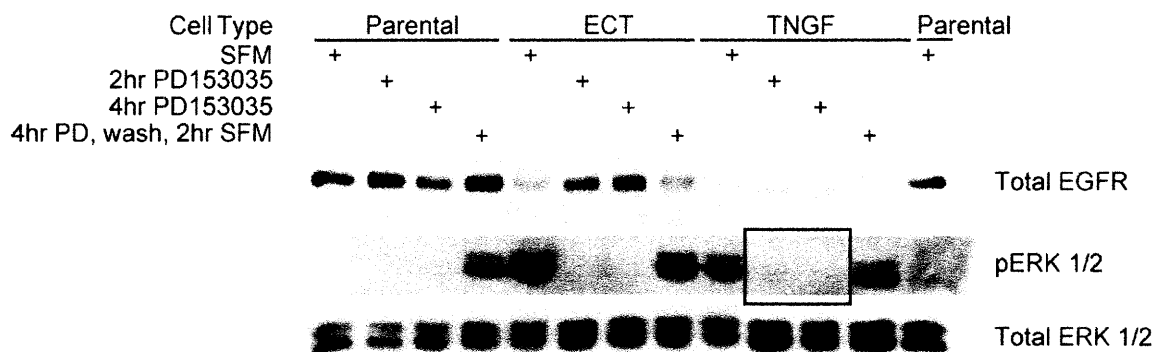


Figure 5.5.7. EGFR kinase inhibitor but not EGFR antibody blocks

TNGF ERK phosphorylation. Cells were incubated for 16 hrs in serum-free media and then either lysed, or incubated with either 10ug/ml of 225 mAb (top panel) or 1uM PD153035 (bottom panel) for 2 or 4 hrs. In addition, cells were also then washed and then incubated in fresh serum-free media for 2 hrs to see if signaling would resume. Western blots were probed for total EGFR and pERK 1/2, and then striped and reprobbed for total ERK 1/2.

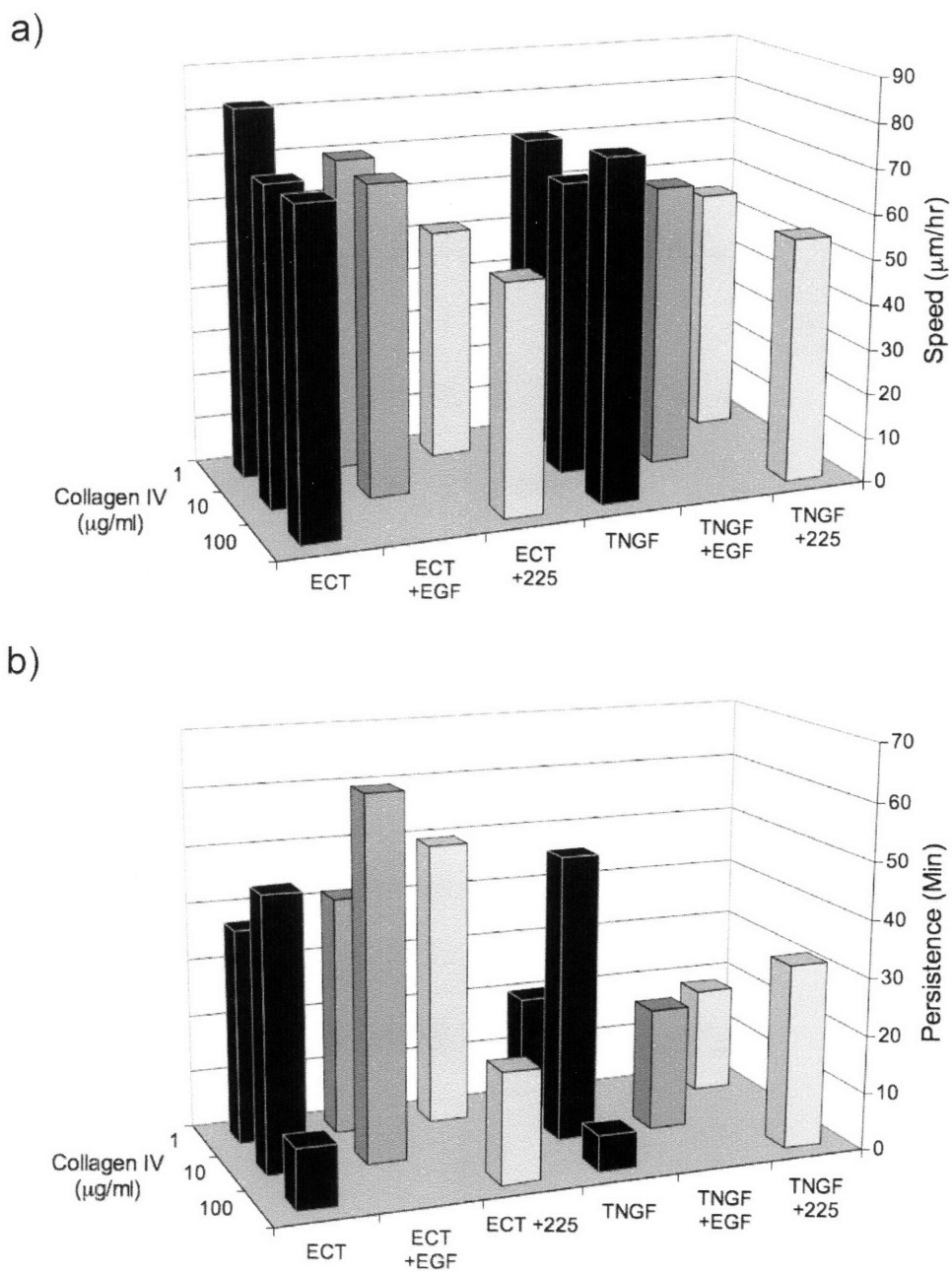


Figure 5.5.8. Cell migration speed and persistence as a function of ligand release and Collagen IV coating. Cells were plated on three different collagen IV coating levels and incubated in serum-free media overnight. Cell migration was measured using time-lapse video microscopy under serum-free media, 2nM EGF, or 10ug/ml of 225 mAb conditions. *a*, average cell speed. *b*, average cell persistence.

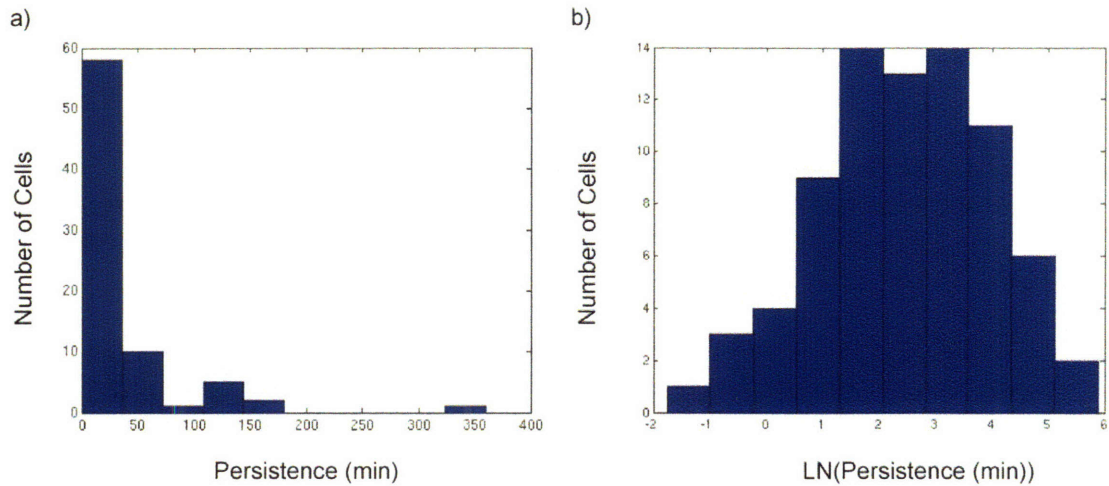


Figure 5.5.9. Log transformation of persistence values. Fit persistence values for each cell were log transformed to achieve a normal distribution. a) histogram of persistence values from a typical experiment. b) histogram of transformed values showing new distribution that is amenable to normal statistical analysis.

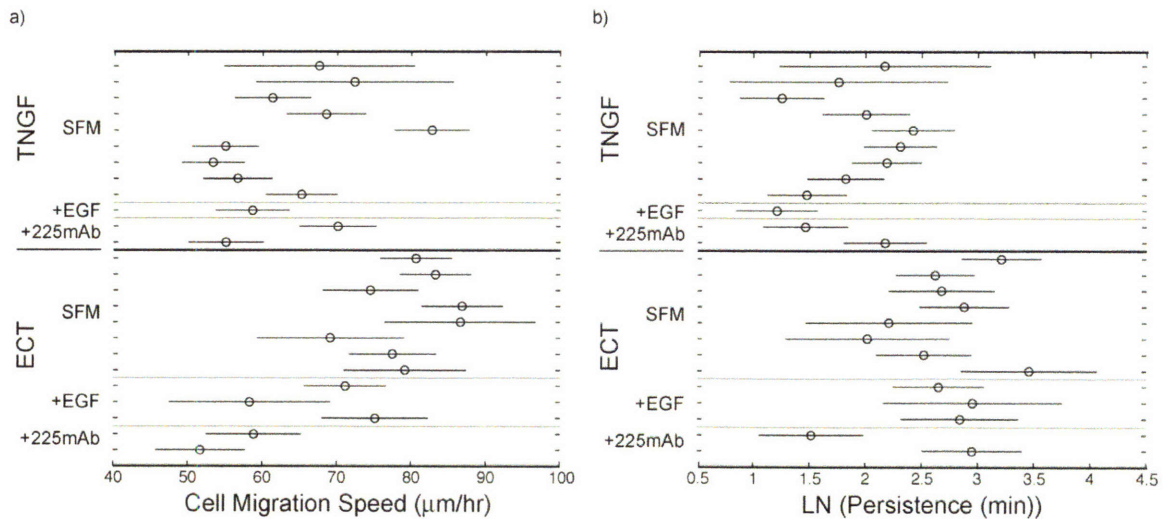


Figure 5.5.10. ANOVA analysis of cell migration speed and transformed persistence data. TNGF and ECT cells plated on 1µg/ml collagen IV coated dishes, under Serum-Free Media (SFM), 2nM EGF, and 10µg/ml 225 mAb conditions. Results from experiments on the same concentration of collagen conducted on different days are plotted separately to demonstrate the day-to-day variability. a, average cell speed \pm SEM, b, cell persistence values were log transformed and then plotted as the average \pm SEM.

5.6 References

- Arribas, J., F. Lopez-Casillas, and J. Massague. 1997. Role of the juxtamembrane domains of the transforming growth factor-alpha precursor and the beta-amyloid precursor protein in regulated ectodomain shedding. *J Biol Chem.* 272:17160-5.
- Band, V., and R. Sager. 1989. Distinctive traits of normal and tumor-derived human mammary epithelial cells expressed in a medium that supports long-term growth of both cell types. *Proc Natl Acad Sci U S A.* 86:1249-53.
- Bates, S.E., E.M. Valverius, B.W. Ennis, D.A. Bronzert, J.P. Sheridan, M.R. Stampfer, J. Mendelsohn, M.E. Lippman, and R.B. Dickson. 1990. Expression of the transforming growth factor-alpha/epidermal growth factor receptor pathway in normal human breast epithelial cells. *Endocrinology.* 126:596-607.
- Black, R.A., C.T. Rauch, C.J. Kozlosky, J.J. Peschon, J.L. Slack, M.F. Wolfson, B.J. Castner, K.L. Stocking, P. Reddy, S. Srinivasan, N. Nelson, N. Boiani, K.A. Schooley, M. Gerhart, R. Davis, J.N. Fitzner, R.S. Johnson, R.J. Paxton, C.J. March, and D.P. Cerretti. 1997. A metalloproteinase disintegrin that releases tumour-necrosis factor-alpha from cells. *Nature.* 385:729-33.
- Burke, P.M., and H.S. Wiley. 1999. Human mammary epithelial cells rapidly exchange empty EGFR between surface and intracellular pools. *J Cell Physiol.* 180:448-60.
- Chung, C.Y., S. Funamoto, and R.A. Firtel. 2001. Signaling pathways controlling cell polarity and chemotaxis. *Trends Biochem Sci.* 26:557-66.
- Condeelis, J.S., J.B. Wyckoff, M. Bailly, R. Pestell, D. Lawrence, J. Backer, and J.E. Segall. 2001. Lamellipodia in invasion. *Semin Cancer Biol.* 11:119-28.
- DeWitt, A.E., J.Y. Dong, H.S. Wiley, and D.A. Lauffenburger. 2001. Quantitative analysis of the EGF receptor autocrine system reveals cryptic regulation of cell response by ligand capture. *J Cell Sci.* 114:2301-13.
- Dunn, G.A., and A.F. Brown. 1987. A unified approach to analysing cell motility. *J Cell Sci Suppl.* 8:81-102.
- Feldner, J.C., and B.H. Brandt. 2002. Cancer cell motility--on the road from c-erbB-2 receptor steered signaling to actin reorganization. *Exp Cell Res.* 272:93-108.

- Firtel, R.A., and C.Y. Chung. 2000. The molecular genetics of chemotaxis: sensing and responding to chemoattractant gradients. *Bioessays*. 22:603-15.
- Gail, M.H., and C.W. Boone. 1970. The locomotion of mouse fibroblasts in tissue culture. *Biophys J*. 10:980-93.
- Gill, G.N., T. Kawamoto, C. Cochet, A. Le, J.D. Sato, H. Masui, C. McLeod, and J. Mendelsohn. 1984. Monoclonal anti-epidermal growth factor receptor antibodies which are inhibitors of epidermal growth factor binding and antagonists of epidermal growth factor binding and antagonists of epidermal growth factor-stimulated tyrosine protein kinase activity. *J Biol Chem*. 259:7755-60.
- Harris, R.C., E. Chung, and R.J. Coffey. 2003. EGF receptor ligands. *Exp Cell Res*. 284:2-13.
- Haugh, J.M., K. Schooler, A. Wells, H.S. Wiley, and D.A. Lauffenburger. 1999. Effect of epidermal growth factor receptor internalization on regulation of the phospholipase C-gamma1 signaling pathway. *J Biol Chem*. 274:8958-65.
- Hill, K., S. Welti, J. Yu, J.T. Murray, S.C. Yip, J.S. Condeelis, J.E. Segall, and J.M. Backer. 2000. Specific requirement for the p85-p110alpha phosphatidylinositol 3-kinase during epidermal growth factor-stimulated actin nucleation in breast cancer cells. *J Biol Chem*. 275:3741-4.
- Iijima, M., Y.E. Huang, and P. Devreotes. 2002. Temporal and spatial regulation of chemotaxis. *Dev Cell*. 3:469-78.
- Janes, K.A., J.G. Albeck, L.X. Peng, P.K. Sorger, D.A. Lauffenburger, and M.B. Yaffe. 2003. A high-throughput quantitative multiplex kinase assay for monitoring information flow in signaling networks: application to sepsis-apoptosis. *Mol Cell Proteomics*. 2:463-73.
- Levchenko, A., and P.A. Iglesias. 2002. Models of eukaryotic gradient sensing: application to chemotaxis of amoebae and neutrophils. *Biophys J*. 82:50-63.
- Li, S., G.D. Plowman, S.D. Buckley, and G.D. Shipley. 1992. Heparin inhibition of autonomous growth implicates amphiregulin as an autocrine growth factor for normal human mammary epithelial cells. *J Cell Physiol*. 153:103-11.
- Maheshwari, G., and D.A. Lauffenburger. 1998. Deconstructing (and reconstructing) cell migration. *Microsc Res Tech*. 43:358-68.

- Maheshwari, G., H.S. Wiley, and D.A. Lauffenburger. 2001. Autocrine epidermal growth factor signaling stimulates directionally persistent mammary epithelial cell migration. *J Cell Biol.* 155:1123-8.
- Piccolo, E., P.F. Innominato, M.A. Mariggio, T. Maffucci, S. Iacobelli, and M. Falasca. 2002. The mechanism involved in the regulation of phospholipase Cgamma1 activity in cell migration. *Oncogene.* 21:6520-9.
- Sahin, U., G. Weskamp, K. Kelly, H.M. Zhou, S. Higashiyama, J. Peschon, D. Hartmann, P. Saftig, and C.P. Blobel. 2004. Distinct roles for ADAM10 and ADAM17 in ectodomain shedding of six EGFR ligands. *J Cell Biol.* 164:769-79.
- Sawyer, C., J. Sturge, D.C. Bennett, M.J. O'Hare, W.E. Allen, J. Bain, G.E. Jones, and B. Vanhaesebroeck. 2003. Regulation of breast cancer cell chemotaxis by the phosphoinositide 3-kinase p110delta. *Cancer Res.* 63:1667-75.
- Segall, J.E., S. Tyrech, L. Boselli, S. Masseling, J. Helft, A. Chan, J. Jones, and J. Condeelis. 1996. EGF stimulates lamellipod extension in metastatic mammary adenocarcinoma cells by an actin-dependent mechanism. *Clin Exp Metastasis.* 14:61-72.
- Stampfer, M.R., A. Bodnar, J. Garbe, M. Wong, A. Pan, B. Villeponteau, and P. Yaswen. 1997. Gradual phenotypic conversion associated with immortalization of cultured human mammary epithelial cells. *Mol Biol Cell.* 8:2391-405.
- Stampfer, M.R., C.H. Pan, J. Hosoda, J. Bartholomew, J. Mendelsohn, and P. Yaswen. 1993. Blockage of EGF receptor signal transduction causes reversible arrest of normal and immortal human mammary epithelial cells with synchronous reentry into the cell cycle. *Exp Cell Res.* 208:175-88.
- Ware, M.F., A. Wells, and D.A. Lauffenburger. 1998. Epidermal growth factor alters fibroblast migration speed and directional persistence reciprocally and in a matrix-dependent manner. *J Cell Sci.* 111 (Pt 16):2423-32.
- Wells, A., M.F. Ware, F.D. Allen, and D.A. Lauffenburger. 1999. Shaping up for shipping out: PLCgamma signaling of morphology changes in EGF-stimulated fibroblast migration. *Cell Motil Cytoskeleton.* 44:227-33.
- Wiley, H.S., M.F. Woolf, L.K. Opresko, P.M. Burke, B. Will, J.R. Morgan, and D.A. Lauffenburger. 1998. Removal of the membrane-anchoring domain of epidermal growth factor leads to intracrine signaling and disruption of mammary epithelial cell organization. *J Cell Biol.* 143:1317-28.

- Winkler, M.E., L. O'Connor, M. Winget, and B. Fendly. 1989. Epidermal growth factor and transforming growth factor alpha bind differently to the epidermal growth factor receptor. *Biochemistry*. 28:6373-8.
- Wyckoff, J.B., L. Insel, K. Khazaie, R.B. Lichtner, J.S. Condeelis, and J.E. Segall. 1998. Suppression of ruffling by the EGF receptor in chemotactic cells. *Exp Cell Res*. 242:100-9.
- Xie, H., M.A. Pallero, K. Gupta, P. Chang, M.F. Ware, W. Witke, D.J. Kwiatkowski, D.A. Lauffenburger, J.E. Murphy-Ullrich, and A. Wells. 1998. EGF receptor regulation of cell motility: EGF induces disassembly of focal adhesions independently of the motility-associated PLCgamma signaling pathway. *J Cell Sci*. 111 (Pt 5):615-24.
- Yarden, Y. 2001. The EGFR family and its ligands in human cancer. signalling mechanisms and therapeutic opportunities. *Eur J Cancer*. 37 Suppl 4:S3-8.

Chapter 6: Conclusions and future directions

The goal of this thesis was to understand EGFR signaling and cell behavior in response to autocrine stimulation and the effects of varying the ligand release rate. We have shown that increased cell migration speed correlates linearly with ERK phosphorylation levels under both increasing autocrine release rates and exogenous stimulation. Autocrine presentation led to steady ERK phosphorylation that never reached exogenous stimulation levels. Exogenous EGF leads to an EGFR and ERK “overshoot” that was never seen under autocrine presentation. Even after blocking autocrine stimulation and subsequent removal of the inhibition, EGF receptor and ERK phosphorylation steadily increased towards previous levels. Interestingly, while autocrine induced ERK signaling is lower; cell migration speed was maximal under autocrine presentation. In addition, we investigated an EGFR-mediated positive feedback through ERK that stimulated a 4-fold increase in release rate of our TGF α based construct. The increased autocrine induced cell migration was dependent on ERK signaling, shown using a small molecule MEK inhibitor. MEK inhibition not

only inhibited ERK involvement in the biophysical processes underlying cell motility, but it also led to a decrease in ligand release rate. Therefore, the increased, autocrine induced cell speed is thought to be executed through steady ERK activity and positive feedback of ligand release (summarized in Figure 6.1.1).

As previously mentioned in Chapter 4, it is interesting to speculate that TGF α , and not EGF, is the most prominent EGFR ligand thought to be involved in EGF receptor activation in cancer progression and has been implicated as a potential biomarker for patient prognosis and response to therapy (Hsieh et al., 2000; Ishikawa et al., 2005; Seth et al., 1999; Yarden and Sliwkowski, 2001). While there may be several reasons why certain ligands are expressed in different tissues, the involvement of specific EGFR ligands in cancer development and progression may have arisen as a result of the type positive feedback of downstream signals on ligand shedding measured here. The positive feedback found specifically in TGF α shedding could play a key role in obtaining self-sufficiency in growth signals, a process known as a hallmark of cancer (Hanahan and Weinberg, 2000).

Many relevant and exciting results have been presented in this thesis that motivate future questions and research directions. The quantitative relationship between ERK phosphorylation and cell migration speed that demonstrates a disparity between autocrine versus exogenous presentation suggests future work on understanding the differences in network topology and the effects on cell behavior. Negative feedback, such as the transcriptional feedback of ZFP36 or

activation of dual-specificity phosphatases (DUSPs) that restrict the responsiveness of the cell to EGF stimuli described by Amit et al., could be differentially initiated in response to the large signaling activation “overshoot” during exogenous stimulation and potentially downregulate the subsequent cell migration processes (Amit et al., 2007). Future work is needed to develop a wider understanding of the network that could be divergently regulating cell migration processes under steady activation or dynamic peaks of activity. Although the work here focused on ERK activation, additional signaling pathways involved in cell migration, such as PI3K, PLC γ , and Rac, could also be probed under exogenous and autocrine stimulation (Wells, 2000). Alternatively, quantitative mass spec measurements could provide a systems level approach to understanding autocrine-induced signals (Wolf-Yadlin et al., 2007; Wolf-Yadlin et al., 2006; Zhang et al., 2005). Correlating these signaling states with quantitative measurements of cell adhesion, protrusion, and polarization could identify the key differences underlying the increase in autocrine-induced speed.

In addition to furthering our understanding of the signaling downstream of autocrine induced EGF receptor activation, we should investigate the subsequent cell motility in a 3D environment. While autocrine or paracrine presentation are thought to be more physiologically relevant modes of ligand presentation than exogenous stimulation, the high throughput assay developed in this work lacks the more realistic microstructure sterics, matrix mechanics, and adhesive properties achievable with 3D assays (Zaman et al., 2006). Work outlined in Chapter 5 also demonstrates the role of matrix interactions in governing cell

motility and suggests that autocrine induced cell migration may lead to different trends in a complex environment. While the initial steps were described in this work, future experiments could investigate the effects of ligand release on cell signaling and migration within a 3D matrix. In addition, under these experimental conditions it would be interesting to include ligand chimeras of low and high release containing a heparin-binding domain, thus adding an additional level of ligand regulation to gain further insight into the autocrine presentation of HB-EGF.

The experimental results in this thesis could also lead to the development of new computational models of autocrine stimulated EGF receptor signaling. Parameters such as the amount of ligand released per cell as a function of ERK phosphorylation under increasing concentrations of exogenous stimulation could help build models for positive feedback on ligand shedding. Steady EGF receptor and ERK phosphorylation levels under varying ligand release rates and after antibody removal could also validate models of autocrine induced signaling in the absence of exogenous stimulation. One question is whether the models and parameters used to fit the “overshoot” under exogenous stimulation will fail to model the lower, sustained levels of autocrine induced activation. Several published models describing EGF receptor signaling dynamics and autocrine regulation could facilitate the development of a new model to address these questions (Asthagiri and Lauffenburger, 2001; Hendriks et al., 2006; Maly et al., 2004; Miller et al., 2005; Schoeberl et al., 2002; Shvartsman et al., 2001). Initial work towards this effort, described in Appendix A, suggests that additional work

will be needed to recapitulate the sustained, low levels of ERK signaling measured under autocrine stimulation.

While EGF receptor dysregulation has received much attention and has been targeted in several cancer therapies, we believe that the work presented here showing increased cell speeds and positive feedback on ligand shedding provides further evidence that autocrine activation of the EGF receptor and ligand regulation may play a key roles in tumorigenesis (Bublil and Yarden, 2007; Ishikawa et al., 2005; Johnston et al., 2006; Kenny and Bissell, 2007; Normanno et al., 2006; Wells et al., 2002). Future work is necessary to further elucidate the mechanisms behind the enhanced autocrine driven migration and the translation of this *in vitro* work into 3D environments and *in vivo*.

6.1 Figures

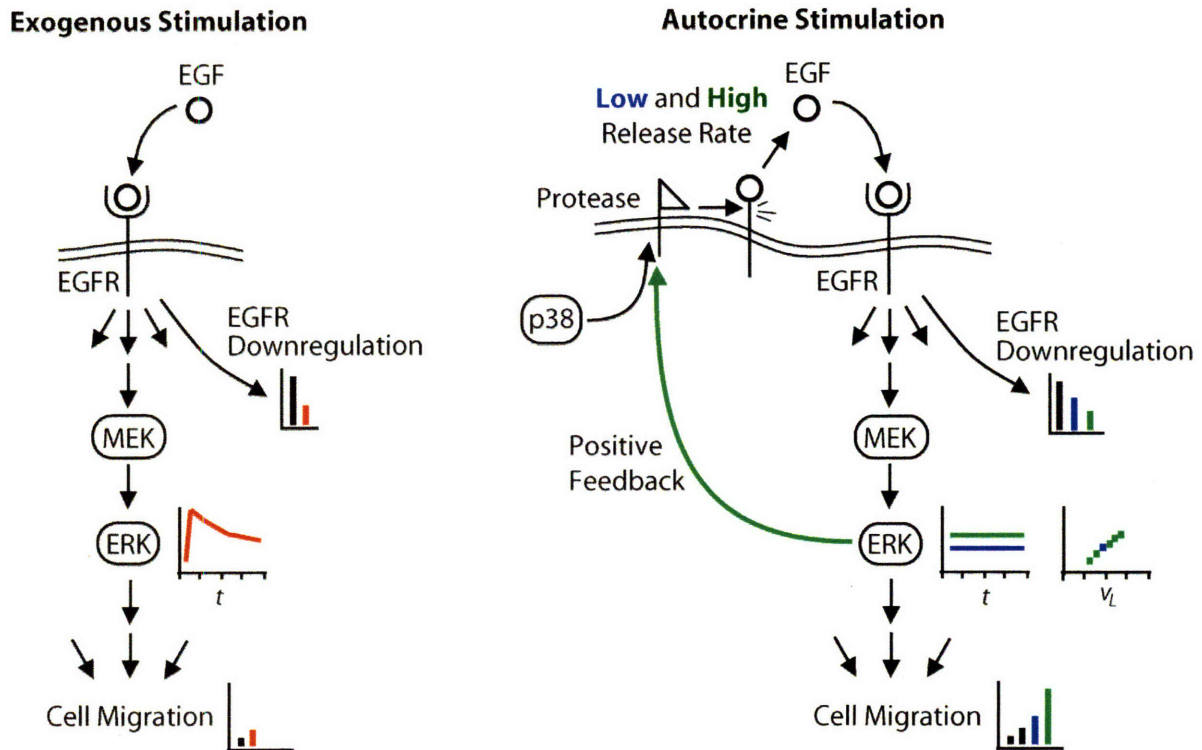


Figure 6.1.1. Schematic summarizing the results of this thesis.

Summarizing the effects of exogenous stimulation and autocrine presentation on receptor downregulation, ERK signaling dynamics, and cell migration speed. In addition, pERK measurements were shown to be a function of ligand release rate and positive feedback of pERK on the release of the TGF α based construct was investigated.

6.2 References

- Amit, I., A. Citri, T. Shay, Y. Lu, M. Katz, F. Zhang, G. Tarcic, D. Siwak, J. Lahad, J. Jacob-Hirsch, N. Amariglio, N. Vaisman, E. Segal, G. Rechavi, U. Alon, G.B. Mills, E. Domany, and Y. Yarden. 2007. A module of negative feedback regulators defines growth factor signaling. *Nat Genet.*
- Asthagiri, A.R., and D.A. Lauffenburger. 2001. A computational study of feedback effects on signal dynamics in a mitogen-activated protein kinase (MAPK) pathway model. *Biotechnol Prog.* 17:227-39.
- Bublil, E.M., and Y. Yarden. 2007. The EGF receptor family: spearheading a merger of signaling and therapeutics. *Curr Opin Cell Biol.* 19:124-34.
- Hanahan, D., and R.A. Weinberg. 2000. The hallmarks of cancer. *Cell.* 100:57-70.
- Hendriks, B.S., J. Cook, J.M. Burke, J.M. Beusmans, D.A. Lauffenburger, and D. de Graaf. 2006. Computational modelling of ErbB family phosphorylation dynamics in response to transforming growth factor alpha and heregulin indicates spatial compartmentation of phosphatase activity. *Syst Biol (Stevenage).* 153:22-33.
- Hsieh, E.T., F.A. Shepherd, and M.S. Tsao. 2000. Co-expression of epidermal growth factor receptor and transforming growth factor-alpha is independent of ras mutations in lung adenocarcinoma. *Lung Cancer.* 29:151-7.
- Ishikawa, N., Y. Daigo, A. Takano, M. Taniwaki, T. Kato, S. Hayama, H. Murakami, Y. Takeshima, K. Inai, H. Nishimura, E. Tsuchiya, N. Kohno, and Y. Nakamura. 2005. Increases of amphiregulin and transforming growth factor-alpha in serum as predictors of poor response to gefitinib among patients with advanced non-small cell lung cancers. *Cancer Res.* 65:9176-84.
- Johnston, J.B., S. Navaratnam, M.W. Pitz, J.M. Maniate, E. Wiechec, H. Baust, J. Gingerich, G.P. Skliris, L.C. Murphy, and M. Los. 2006. Targeting the EGFR pathway for cancer therapy. *Curr Med Chem.* 13:3483-92.
- Kenny, P.A., and M.J. Bissell. 2007. Targeting TACE-dependent EGFR ligand shedding in breast cancer. *J Clin Invest.* 117:337-45.
- Maly, I.V., H.S. Wiley, and D.A. Lauffenburger. 2004. Self-organization of polarized cell signaling via autocrine circuits: computational model analysis. *Biophys J.* 86:10-22.

- Miller, J.H., F. Zheng, S. Jin, L.K. Opresko, H.S. Wiley, and H. Resat. 2005. A model of cytokine shedding induced by low doses of gamma radiation. *Radiat Res.* 163:337-42.
- Normanno, N., A. De Luca, C. Bianco, L. Strizzi, M. Mancino, M.R. Maiello, A. Carotenuto, G. De Feo, F. Caponigro, and D.S. Salomon. 2006. Epidermal growth factor receptor (EGFR) signaling in cancer. *Gene.* 366:2-16.
- Schoeberl, B., C. Eichler-Jonsson, E.D. Gilles, and G. Muller. 2002. Computational modeling of the dynamics of the MAP kinase cascade activated by surface and internalized EGF receptors. *Nat Biotechnol.* 20:370-5.
- Seth, D., K. Shaw, J. Jazayeri, and P.J. Leedman. 1999. Complex post-transcriptional regulation of EGF-receptor expression by EGF and TGF-alpha in human prostate cancer cells. *Br J Cancer.* 80:657-69.
- Shvartsman, S.Y., H.S. Wiley, W.M. Deen, and D.A. Lauffenburger. 2001. Spatial range of autocrine signaling: modeling and computational analysis. *Biophys J.* 81:1854-67.
- Wells, A. 2000. Tumor invasion: role of growth factor-induced cell motility. *Adv Cancer Res.* 78:31-101.
- Wells, A., J. Kassis, J. Solava, T. Turner, and D.A. Lauffenburger. 2002. Growth factor-induced cell motility in tumor invasion. *Acta Oncol.* 41:124-30.
- Wolf-Yadlin, A., S. Hautaniemi, D.A. Lauffenburger, and F.M. White. 2007. Multiple reaction monitoring for robust quantitative proteomic analysis of cellular signaling networks. *Proc Natl Acad Sci U S A.* 104:5860-5.
- Wolf-Yadlin, A., N. Kumar, Y. Zhang, S. Hautaniemi, M. Zaman, H.D. Kim, V. Grantcharova, D.A. Lauffenburger, and F.M. White. 2006. Effects of HER2 overexpression on cell signaling networks governing proliferation and migration. *Mol Syst Biol.* 2:54.
- Yarden, Y., and M.X. Sliwkowski. 2001. Untangling the ErbB signalling network. *Nat Rev Mol Cell Biol.* 2:127-37.
- Zaman, M.H., L.M. Trapani, A.L. Sieminski, D. Mackellar, H. Gong, R.D. Kamm, A. Wells, D.A. Lauffenburger, and P. Matsudaira. 2006. Migration of tumor cells in 3D matrices is governed by matrix stiffness along with cell-matrix adhesion and proteolysis. *Proc Natl Acad Sci U S A.* 103:10889-94.
- Zhang, Y., A. Wolf-Yadlin, P.L. Ross, D.J. Pappin, J. Rush, D.A. Lauffenburger, and F.M. White. 2005. Time-resolved mass spectrometry of tyrosine phosphorylation sites in the epidermal growth factor receptor signaling network reveals dynamic modules. *Mol Cell Proteomics.* 4:1240-50.

Appendix A: Computational work

This appendix contains initial work on an autocrine EGFR model derived from the model by Hendriks et al. (Hendriks et al., 2006), and containing the ERK cascade previously described by Asthagiri et al. (Asthagiri and Lauffenburger, 2001). Figure A.1.1 shows a schematic of the various processes involved in the model. The model contains several compartments: bulk media, media within the cell boundary layer, cell membrane, cytoplasm, and endosome. The mathematical description of a diffusive flux between the bulk media and media within the cell boundary layer was based off of previous work by Oehrtman et al. (Oehrtman et al., 1998). Protease dynamics were adapted from Shvartsman et al. (Shvartsman et al., 2002). Ligand synthesis and protease activation were varied to achieve ligand release rates similar to those measured from ECT and TNGF cells. The concentration of EGF at the cell surface (within the boundary layer), surface receptor downregulation, and ERK activation were simulated under exogenous EGF (constant EGF in the bulk media) and ligand release conditions, in the absence or presence of the EGF receptor blocking 225 antibody.

This model consists of 93 ordinary differential equations, of which 44 describe the ERK cascade alone. From the base model, by Hendriks et al., describing only EGFR dynamics (excluding other HER family members) through ERK activation, 16 equations were added to include autocrine dynamics and antibody inhibition (Hendriks et al., 2006). All of the parameters used in the ligand and protease dynamics were unknown and therefore estimated. Initial work used ligand synthesis to vary the ultimate accumulation of EGF in the bulk media, see Figure A.1.2. However, the model was intended to describe differences in protease activity to achieve the different release rates. Optimization of the ligand and protease dynamics has yet to be completed, due to the large number of parameters still unknown. A simpler model could also be envisioned, that only includes a membrane bound ligand with variable shedding

kinetics. Additionally, the rate of ligand shedding could include dependence on simultaneous ERK activity to model results described in Chapter 4 of this thesis.

This appendix shows a simulation of EGFR and ERK signaling under varying EGF release rate and exogenous EGF stimulation conditions. The most significant result is the estimation of EGF concentration at the cell surface –a variable that is currently immeasurable. Low ligand release (~1,000 molecules of EGF released per cell per minute) leads to sub nanomolar concentrations of EGF while the high release (~10,000 molecules of EGF released per cell per min) results in a surface concentration of approximately 7 nM, see Figure A.1.3. The model also shows relevant levels of surface EGFR downregulation under the low and high autocrine conditions, comparable to those measured in both Chapter 3 and 5 for the ECT, TCT, and TNGF cells. Interestingly, this model overestimates the decrease in ERK activity over time. The autocrine and exogenously stimulated ERK activation levels decrease within an hour to a very low level, whereas experiments show a higher, steady level of activation. This model estimates receptor phosphatase activity with an exponential decay function attached to the ERK input. This time sensitive component of the model does not allow steady levels of ERK activation and therefore is not an appropriate way to handle receptor dephosphorylation under autocrine presentation. Future work could add receptor phosphatase species and additional reactions to better describe receptor deactivation. Additional concerns include the large number of equations and estimated parameters for a system with few measurable outputs. A simplified set of equations can be envisioned that decreases the number of species and allows some analytical analysis. Future work with computational autocrine models is promising, as these initial results of variable ligand accumulation in the media and receptor downregulation show strong resemblance to experimental results.

A.1 Figures

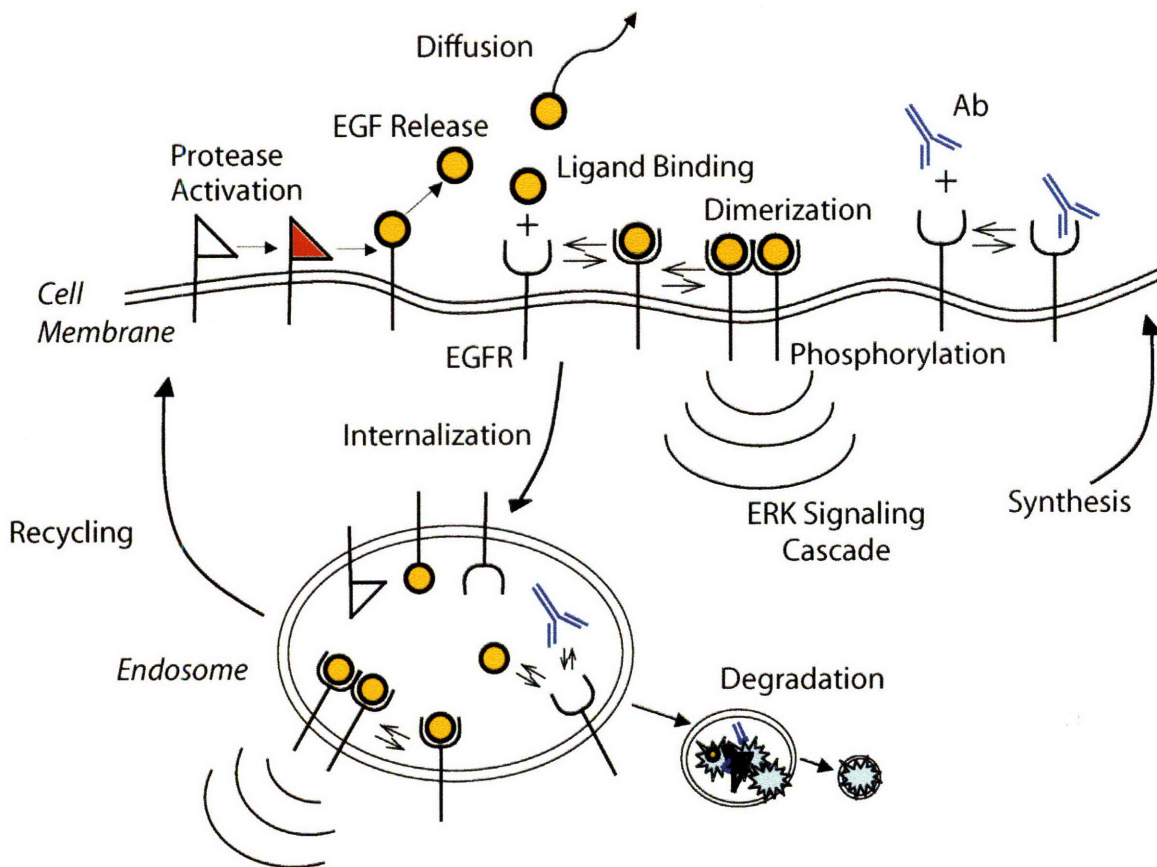


Figure A.1.1. Schematic of autocrine EGFR model components.

Schematic showing processes described in the ODE model, including synthesis (EGF, EGFR, and protease), protease activation, EGF release, EGF diffusion into bulk media from boundary layer, ligand binding, receptor dimerization, receptor phosphorylation, ERK signaling cascade, antibody binding, internalization of surface species, endosomal reactions, recycling and degradation.

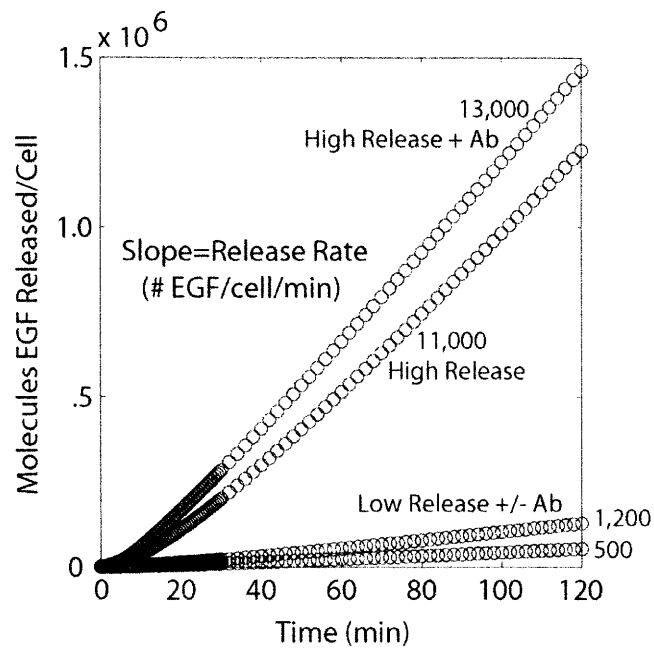


Figure A.1.2. Simulated ligand accumulation in bulk media. EGF accumulation in the bulk media is simulated for a 2 hour time course under low and high ligand synthesis conditions in the presence and absence of 10 ug/ml of 225 receptor blocking antibody. A linear fit to the slope of the line quantifies the ligand release rate. Adding 225 increases the accumulation of EGF under low and high release rate conditions.

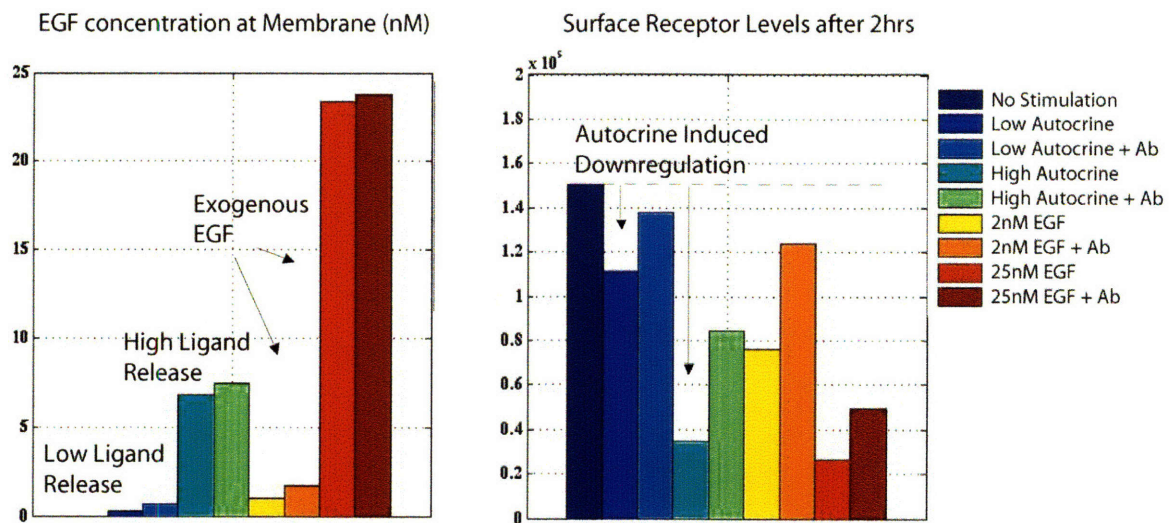


Figure A.1.3. Simulated surface EGF and EGFR levels. The final concentration of EGF at the cell membrane (within the boundary layer) and surface receptor numbers are shown under autocrine (low and high EGF release rates) and exogenous (2 or 25nM EGF in bulk media) EGF conditions after a 2-hour simulation. Autocrine induced receptor downregulation is shown in comparison to the 'No Stimulation' condition.

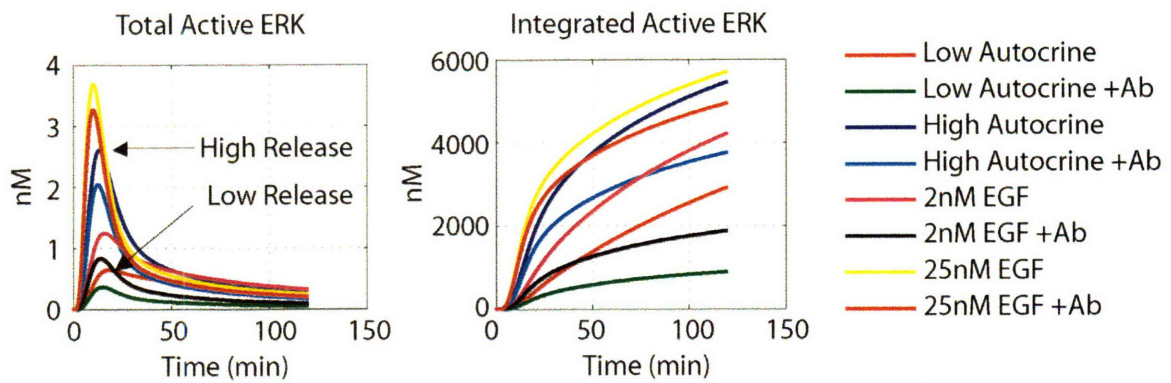


Figure A.1.4. Simulated ERK activity under autocrine and exogenous EGF. Total active ERK and integrated active ERK are shown as a function of time under low and high autocrine and exogenous EGF conditions in the presence and absence of 10 ug/ml 225 receptor blocking antibody.

A.2 References

Asthagiri, A.R., and D.A. Lauffenburger. 2001. A computational study of feedback effects on signal dynamics in a mitogen-activated protein kinase (MAPK) pathway model. *Biotechnol Prog.* 17:227-39.

Hendriks, B.S., J. Cook, J.M. Burke, J.M. Beusmans, D.A. Lauffenburger, and D. de Graaf. 2006. Computational modelling of ErbB family phosphorylation dynamics in response to transforming growth factor alpha and heregulin indicates spatial compartmentation of phosphatase activity. *Syst Biol (Stevenage)*. 153:22-33.

Oehrtman, G.T., H.S. Wiley, and D.A. Lauffenburger. 1998. Escape of autocrine ligands into extracellular medium: experimental test of theoretical model predictions. *Biotechnol Bioeng.* 57:571-82.

Shvartsman, S.Y., M.P. Hagan, A. Yacoub, P. Dent, H.S. Wiley, and D.A. Lauffenburger. 2002. Autocrine loops with positive feedback enable context-dependent cell signaling. *Am J Physiol Cell Physiol.* 282:C545-59.

A.3 Matlab Code

```
% Autocrine_comlist050706_2.m
%
% This code was developed using a Bart Hendriks' model building code
% This m-file creates plots of ligand release, receptor levels,
% EGF concentration at the cell membrane, and ERK activation levels
% To run this code, you will need the additional files, including:
% autocrine2_050608
% that define the species, parameters, and reaction fluxes, in addition to the files that
% solve the equations and make the plots. This code is what sets the conditions
% for the simulation that generates the plots below.
%
% 6/22/05
% Lisa Joslin
%
% This file varies the ligand synthesis to vary the ligand release rate
% Protease activation is constant in this case and could be used to introduce
% ligand specificity or variations in ligand release rate. As a first pass, ligand synthesis
% was varied to obtain ligand release rates of approx. 10,000 and 1,000 molecules/cell/min

clear all

% This file defines all of the compartments, species, parameters and reaction fluxes
autocrine2_050608

M = Model('Autocrine050706_2', Species, Parameter, Reaction, Compartment, CPL);

M = GenerateODEfile(M, 1);
```

```

% EGF Additions in soluble bulk media
EGF_doses = [0 2 25]; % nM

% Ab Conc in nM
X1_dose=10; %ug/ml
X1_dose=X1_dose*10^3*10^3/150000; %nM assuming 150,000 Da

%initial guess of kaP was 0.00833 1/s
kaP=[0.833 0.0833 0.00833 0.000833 0.0000833]; % 'Units', '1/s'
kpl=[1.00367 1.00367e-1 1.00367e-2 1.00367e-3 1.00367e-4]; % 'Units', '1/nM/sec'

%-----
%-----
% RUN 1: Get things set--Approach SS! No Autocrine production.

% HMEC (number per cell)
% Radius= 10um
ksyn_Ligand = 0; %this is an initial guess ****change later....
ksyn_Protease = 5; %this is an initial guess ****change later....
ksyn_R1 = 34;
% % convert synthesis rates to nM/sec:
ksyn_Ligand = ksyn_Ligand/PMCF*CPL;
ksyn_Protease = ksyn_Protease/PMCF*CPL;
ksyn_R1 = ksyn_R1/PMCF*CPL; % These are synthesis rates, now converted to nM/sec

tic;
% M = InitializeModelRun(M, 1, 'first try');
% tspan = [0:1:300 330:30:1800 2400:120:7200]; % timepoints for simulation (This is in SECONDS!)
% M = SolveModel(M, 1, tspan);

RunNumber = 0;

RunNumber = RunNumber + 1;
SS_Run = RunNumber;
RunName = 'Approach to SS';
ICfilename = "";
PVfilename = "";
M = InitializeModelRun(M, RunNumber, RunName, ICfilename, PVfilename, ...
    'ksyn_R1', ksyn_R1,...
    'ksyn_Protease', ksyn_Protease,...
    'ksyn_Ligand', ksyn_Ligand,...
    'EGF_BM', 0,...
    'kaP', kaP(3),...
    'kpl', kpl(3),...
    'X1_BM', 0);
M = SSReceptorGuesses(M, RunNumber);
tspan = [0:100000:1000000];
M= SolveModel(M, RunNumber, tspan);
toc;

%-----
%-----

%% RUN 2: Control--no stimulus

% HMEC (number per cell)
ksyn_Ligand = 0; %this is an initial guess
ksyn_Protease = 5; %this is an initial guess
ksyn_R1 = 34;

% % convert synthesis rates to nM/sec:
ksyn_Ligand = ksyn_Ligand/PMCF*CPL;
ksyn_Protease = ksyn_Protease/PMCF*CPL;
ksyn_R1 = ksyn_R1/PMCF*CPL; % These are synthesis rates, now converted to nM/sec

RunNumber = RunNumber + 1;
RunName = 'Autocrine timecourse';
M = InitializeModelRun(M, RunNumber, RunName, SS_Run, ...

```

```

'ksyn_R1', ksyn_R1,...
'ksyn_Protease', ksyn_Protease,...
'ksyn_Ligand', ksyn_Ligand,...
'EGF_BM', EGF_doses(1),...
'kaP',kaP(3),...
'kpl',kpl(3),...
'X1_BM', 0);
tspan = [0:1:300 330:30:1800 1920:120:7200]; % timepoints for simulation (This is in SECONDS!)
M = SolveModel(M, RunNumber, tspan);
toc;

%-----
% % RUN 3: vary ligand synthesis--low autocrine

% HMEC (number per cell)
ksyn_Ligand = 25; %this is an initial guess
ksyn_Protease = 5; %this is an initial guess
ksyn_R1 = 34;

% % convert synthesis rates to nM/sec:
ksyn_Ligand = ksyn_Ligand/PMCF*CPL;
ksyn_Protease = ksyn_Protease/PMCF*CPL;
ksyn_R1 = ksyn_R1/PMCF*CPL; % These are synthesis rates, now converted to nM/sec

RunNumber = RunNumber + 1;
RunName = 'Autocrine timecourse';
M = InitializeModelRun(M, RunNumber, RunName, SS_Run, ...
'ksyn_R1', ksyn_R1,...
'ksyn_Protease', ksyn_Protease,...
'ksyn_Ligand', ksyn_Ligand,...
'EGF_BM', EGF_doses(1),...
'kaP',kaP(3),...
'kpl',kpl(3),...
'X1_BM', 0);
tspan = [0:1:300 330:30:1800 1920:120:7200]; % timepoints for simulation (This is in SECONDS!)
M = SolveModel(M, RunNumber, tspan);
toc;

%-----
% % RUN 4: vary ligand synthesis--low autocrine +Ab

% HMEC (number per cell)
ksyn_Ligand = 25; %this is an initial guess
ksyn_Protease = 5; %this is an initial guess
ksyn_R1 = 34;

% % convert synthesis rates to nM/sec:
ksyn_Ligand = ksyn_Ligand/PMCF*CPL;
ksyn_Protease = ksyn_Protease/PMCF*CPL;
ksyn_R1 = ksyn_R1/PMCF*CPL; % These are synthesis rates, now converted to nM/sec

RunNumber = RunNumber + 1;
RunName = 'Autocrine timecourse';
M = InitializeModelRun(M, RunNumber, RunName, SS_Run, ...
'ksyn_R1', ksyn_R1,...
'ksyn_Protease', ksyn_Protease,...
'ksyn_Ligand', ksyn_Ligand,...
'EGF_BM', EGF_doses(1),...
'kaP',kaP(3),...
'kpl',kpl(3),...
'X1_BM', X1_dose);
tspan = [0:1:300 330:30:1800 1920:120:7200]; % timepoints for simulation (This is in SECONDS!)
M = SolveModel(M, RunNumber, tspan);
toc;

%-----
% % RUN 5: vary ligand synthesis--high autocrine

% HMEC (number per cell)
ksyn_Ligand = 250; %this is an initial guess

```

```

ksyn_Protease = 5; %this is an initial guess
ksyn_R1 = 34;

%% convert synthesis rates to nM/sec:
ksyn_Ligand = ksyn_Ligand/PMCF*CPL;
ksyn_Protease = ksyn_Protease/PMCF*CPL;
ksyn_R1 = ksyn_R1/PMCF*CPL; % These are synthesis rates, now converted to nM/sec

RunNumber = RunNumber + 1;
RunName = 'Autocrine timecourse';
M = InitializeModelRun(M, RunNumber, RunName, SS_Run, ...
    'ksyn_R1', ksyn_R1,...
    'ksyn_Protease', ksyn_Protease,...
    'ksyn_Ligand', ksyn_Ligand,...
    'EGF_BM', EGF_doses(1),...
    'kaP',kaP(3),...
    'kpl',kpl(3),...
    'X1_BM', 0);
tspan = [0:1:300 330:30:1800 1920:120:7200]; % timepoints for simulation (This is in SECONDS!)
M = SolveModel(M, RunNumber, tspan);
toc;

%-----
%% % RUN 6: vary ligand synthesis--high autocrine + Ab

% HMEC (number per cell)
ksyn_Ligand = 250; %this is an initial guess
ksyn_Protease = 5; %this is an initial guess
ksyn_R1 = 34;

%% convert synthesis rates to nM/sec:
ksyn_Ligand = ksyn_Ligand/PMCF*CPL;
ksyn_Protease = ksyn_Protease/PMCF*CPL;
ksyn_R1 = ksyn_R1/PMCF*CPL; % These are synthesis rates, now converted to nM/sec

RunNumber = RunNumber + 1;
RunName = 'Autocrine timecourse';
M = InitializeModelRun(M, RunNumber, RunName, SS_Run, ...
    'ksyn_R1', ksyn_R1,...
    'ksyn_Protease', ksyn_Protease,...
    'ksyn_Ligand', ksyn_Ligand,...
    'EGF_BM', EGF_doses(1),...
    'kaP',kaP(3),...
    'kpl',kpl(3),...
    'X1_BM', X1_dose);
tspan = [0:1:300 330:30:1800 1920:120:7200]; % timepoints for simulation (This is in SECONDS!)
M = SolveModel(M, RunNumber, tspan);
toc;

%-----
%% Run 7: exogenous EGF

% HMEC (number per cell)
ksyn_Ligand = 0; %this is an initial guess
ksyn_Protease = 5; %this is an initial guess
ksyn_R1 = 34;

%% convert synthesis rates to nM/sec:
ksyn_Ligand = ksyn_Ligand/PMCF*CPL;
ksyn_Protease = ksyn_Protease/PMCF*CPL;
ksyn_R1 = ksyn_R1/PMCF*CPL; % These are synthesis rates, now converted to nM/sec

RunNumber = RunNumber + 1;
RunName = 'Autocrine timecourse';
M = InitializeModelRun(M, RunNumber, RunName, SS_Run, ...
    'ksyn_R1', ksyn_R1,...
    'ksyn_Protease', ksyn_Protease,...
    'ksyn_Ligand', ksyn_Ligand,...
    'EGF_BM', EGF_doses(2),...
    'kaP',kaP(3),...

```

```

'kpl',kpl(3),...
'X1_BM', 0);
tspan = [0:1:300 330:30:1800 1920:120:7200]; % timepoints for simulation (This is in SECONDS!)
M = SolveModel(M, RunNumber, tspan);
toc;

%-----
%%% Run 8: exogenous EGF +Ab

% HMEC (number per cell)
ksyn_Ligand = 0; %this is an initial guess
ksyn_Protease = 5; %this is an initial guess
ksyn_R1 = 34;

% % convert synthesis rates to nM/sec:
ksyn_Ligand = ksyn_Ligand/PMCF*CPL;
ksyn_Protease = ksyn_Protease/PMCF*CPL;
ksyn_R1 = ksyn_R1/PMCF*CPL; % These are synthesis rates, now converted to nM/sec

RunNumber = RunNumber + 1;
RunName = 'Autocrine timecourse';
M = InitializeModelRun(M, RunNumber, RunName, SS_Run, ...
'ksyn_R1', ksyn_R1,...
'ksyn_Protease', ksyn_Protease,...
'ksyn_Ligand', ksyn_Ligand,...
'EGF_BM', EGF_doses(2),...
'kaP',kaP(3),...
'kpl',kpl(3),...
'X1_BM', X1_dose);
tspan = [0:1:300 330:30:1800 1920:120:7200]; % timepoints for simulation (This is in SECONDS!)
M = SolveModel(M, RunNumber, tspan);
toc;

%-----
%%% Run 9: exogenous EGF

% HMEC (number per cell)
ksyn_Ligand = 0; %this is an initial guess
ksyn_Protease = 5; %this is an initial guess
ksyn_R1 = 34;

% % convert synthesis rates to nM/sec:
ksyn_Ligand = ksyn_Ligand/PMCF*CPL;
ksyn_Protease = ksyn_Protease/PMCF*CPL;
ksyn_R1 = ksyn_R1/PMCF*CPL; % These are synthesis rates, now converted to nM/sec

RunNumber = RunNumber + 1;
RunName = 'Autocrine timecourse';
M = InitializeModelRun(M, RunNumber, RunName, SS_Run, ...
'ksyn_R1', ksyn_R1,...
'ksyn_Protease', ksyn_Protease,...
'ksyn_Ligand', ksyn_Ligand,...
'EGF_BM', EGF_doses(3),...
'kaP',kaP(3),...
'kpl',kpl(3),...
'X1_BM', 0);
tspan = [0:1:300 330:30:1800 1920:120:7200]; % timepoints for simulation (This is in SECONDS!)
M = SolveModel(M, RunNumber, tspan);
toc;

%-----
%%% Run 10: exogenous EGF +Ab

% HMEC (number per cell)
ksyn_Ligand = 0; %this is an initial guess
ksyn_Protease = 5; %this is an initial guess
ksyn_R1 = 34;

% % convert synthesis rates to nM/sec:
ksyn_Ligand = ksyn_Ligand/PMCF*CPL;

```

```

ksyn_Protease = ksyn_Protease/PMCF*CPL;
ksyn_R1 = ksyn_R1/PMCF*CPL; % These are synthesis rates, now converted to nM/sec

RunNumber = RunNumber + 1;
RunName = 'Autocrine timecourse';
M = InitializeModelRun(M, RunNumber, RunName, SS_Run, ...
    'ksyn_R1', ksyn_R1,...
    'ksyn_Protease', ksyn_Protease,...
    'ksyn_Ligand', ksyn_Ligand,...
    'EGF_BM', EGF_doses(3),...
    'kaP',kaP(3),...
    'kpl',kpl(3),...
    'X1_BM', X1_dose);
tspan = [0:1:300 330:30:1800 1920:120:7200]; % timepoints for simulation (This is in SECONDS!)
M = SolveModel(M, RunNumber, tspan);
toc;

save('Autocrine_050706_2', 'M', '-compress');

%-----PLOTS-----
% % Protease unactive and active and mem bound ligand
% Plots_multi(M,[2,3,4,5,6,7],[4,5,6], '#/cell')
%
% % Receptors total and total #P
% Plots_multi(M,[2,3],[39,40,41,42,43,44], '#/cell')
%
% % plots the number of total ErbB1 and the frxn #P for the [] run numbers
% PhosphoPlots_Lisa(M, [2,3])
%
% FrxnPlots(M, [2,3])
%
% % Soluble Ligand and Ab in the three compartments (bulk, media, endosomal
% % lumen)
% Plots_multi(M,[2,3],[1,2,3], 'nM')%17, 18, 19], 'nM')

input_legend=strvcat('No Stimulation','Low Autocrine','Low Autocrine +Ab','High Autocrine','High Autocrine +Ab','2nM
EGF','2nM EGF +Ab','25nM EGF','25nM EGF +Ab');

Plot_MOAOutputs(M,[2,3,4,5,6,7,8,9,10], BulkMedVol,input_legend, [3,4,5,6])

input_legend2=strvcat('Low Autocrine','Low Autocrine +Ab','High Autocrine','High Autocrine +Ab','2nM EGF','2nM EGF
+Ab','25nM EGF','25nM EGF +Ab');
Plots_multi(M,[3,4,5,6,7,8,9,10],[93,94], 'nM'), legend(input_legend2)

%
%
%
% % % VIEW EVERY SPECIES
% i=1;
% while i<length(M.Species)
% Plots_multi(M,[2,3,4,5,6,7,8,9,10],[i,i+1,i+2,i+3,i+4,i+5], 'nM')
% i=i+6;
% end
% %
% % % ERK plots
% Plots_multi(M,[2,3,4,5,6,7,8,9,10],[92,93,94], 'nM'), legend(input_legend)
% %

```